ON DECOUPLED QUASI-LINEARIZATION METHODS FOR SOLVING SYSTEMS OF NONLINEAR BOUNDARY VALUE PROBLEMS

A DISSERTATION SUBMITTED IN FULFILLMENT OF THE ACADEMIC REQUIREMENTS FOR THE DEGREE OF MASTER OF SCIENCE IN THE FACULTY OF SCIENCE AND AGRICULTURE

By

Olumuyiwa Otegbeye

School of Mathematical Sciences

University of KwaZulu Natal, Pietermaritzburg

2014

Dedication

To my lovely mum and my late father.

Acknowledgment

I am most grateful to God for giving me his grace to achieve all I have so far. My sincere gratitude goes to my supervisor Prof. S.S. Motsa for his guidance, help and support throughout the course of this dissertation and the foundation he lay during my Honours programme.

I extend special thanks to my mum for her strong belief in me, financial support and all her words of encouragement. To my brother and sisters, words alone can't express how grateful I am for all you did for me throughout my programme. A hearty thanks to Ntombifuthi for all your support and help even at inconvenient times.

I am also grateful to Christel, Faith, Shaun, my colleagues and the department members for all their contribution in making my dissertation a success.

Declaration

I hereby declare that this dissertation presents my original work and effort. It was carried out under the direct supervision of Prof. Sandile S. Motsa in the School of Mathematical Sciences, University of KwaZulu-Natal Pietermaritzburg.

It has not been submitted in any form to any University or institution for any degree or diploma. Where use has been made of the work of others it is duly acknowledged throughout in this work.

2014.

Student: _____ _____

Olumuyiwa Otegbeye Date

Supervisor: _____ _____

Prof. Sandile S. Motsa Date

Abstract

In this dissertation, a comparative study is carried out on three spectral based numerical methods which are the spectral quasilinearization method (SQLM), the spectral relaxation method (SRM) and the spectral local linearization method (SLLM). The study is carried out by applying the numerical methods on systems of differential equations modeling fluid flow problems. Residual error analysis is used in determining the speed of convergence, convergence rate and accuracy of the methods. In Chapter 1, all the terminologies and methods that are applied throughout the course of the study are introduced. In Chapter 2, the SRM, SLLM and SQLM are applied on an unsteady free convective heat and mass transfer on a stretching surface in a porous medium with suction/injection. In Chapter 3, the SRM, SLLM and SQLM are applied on an unsteady boundary layer flow due to a stretching surface in a rotating fluid. In Chapter 4, the SRM, SLLM and SQLM are used to solve an unsteady three-dimensional MHD boundary layer flow and heat transfer over an impulsively stretching plate. The purpose of this study is to assess the performance of the spectral based numerical methods when solving systems of differential equations. The performance of the methods are measured in terms of computational efficiency (in terms of time taken to generate solutions), accuracy and rate of convergence. The ease of development and implementation of the associated numerical algorithms are also considered.

Contents

List of Tables

List of Figures

Chapter 1

INTRODUCTION

Over the years, a number of computational methods have been developed to solve nonlinear equations. This has proven to be necessary especially for higher order systems that are difficult to solve analytically hence the need to obtain numerical approximations. Numerical methods are applied in different areas. According to Motsa et al. (2014), analytical solutions to engineering and science based problems can be obtained for some few problems hence the need to obtain numerical solutions. Systems of equations that model the problem of fluid flow such as boundary layer flow with heat and mass transfer are difficult to solve analytically (see Motsa (2013b);Liao (2006a)). Following Acton (1990), numerical methods are used to solve very complex geometrical problems but the accuracy of the methods are never exact unlike analytical methods though analytical methods are only applicable to some problems.

A number of methods (both analytical and numerical) have been used in solving complex fluid flow problems. Among such methods are classical methods based on finite differences, finite volume and finite element concepts. Other methods include Runge-Kutta method (Chamkha et al. (2010)), Keller-box method (Keller and Cebeci (1971)), Spectral methods (Gheorghiu, 2007; Van de Vosse and Minev, 1996), Homotopy Analysis method (Liao (2003)) and Perturbation methods (Simmonds and Mann (Simmonds and Mann)). More recently, spectral based numerical techniques have been developed such as the Spectral Quasilinearization Method (Motsa (2013a)), Spectral Relaxation Method (Motsa (2013b)), Spectral Local Linearization Method (Motsa (2013a)), Successive Linearization Method (Motsa and Sibanda,

2012; Makukula et al., 2010b) amongst other methods to try to improve on some of the limitations of the older methods.

The aim of this dissertation is to compare some of the numerical methods listed above specifically the Spectral relaxation method (SRM), Spectral local linearization method (SLLM) and Spectral quasilinearization method (SQLM). The comparison is done by investigating their convergence speed, rate of convergence and the accuracies of the converged solutions obtained using the methods. Most of the analysis performed in this dissertation is achieved by computing the norm of the residual error obtained using each of the methods on systems of equations modeling fluid flow problems. A summarized introduction to some of the processes involved throughout the course of this dissertation is provided as follows;

(i) Taylor series expansion,

(ii) Linearization of a univariate function,

(iii) Linearization of a multivariate function,

(iv) Condition for convergence,

(v) Gauss-Seidel Relaxation technique,

(vi) Spectral Methods,

(vii) Finite difference method,

(viii) Crank-Nicolson method,

(ix) Residual error.

1.1 Taylor series expansion

The Taylor series expansion is an expansion about any given point of a function, say x. As a general illustration, let $f(x) \in \Re$ be an infinitely differentiable function at a fixed point $x = z$. Then, the Taylor series expansion of the function is given by

$$f(x) \approx f(z) + f^{'}(z)(x-z) + \frac{f^{''}(z)}{2!}(x-z)^2 + \ldots + \frac{f^n(z)}{n!}(x-z)^n + \ldots. \tag{1.1}$$

1.2 Linearization of a univariate function

Consider a continuous and differentiable function $f(x) \in \Re$. The function is linearly approximated by applying Taylor series expansion to first order towards a fixed point $x = z$ in the form

$$f(x) \approx f(z) + f^{'}(z)(x - z). \tag{1.2}$$

1.3 Linearization of a multivariate function

Consider a nonlinear function $\mathbf{N}(f, u) = fu$. Linearization is achieved by applying Taylor series expansion to first order in the form

$$fu \approx f_r u_r + u_r \left(f_{r+1} - f_r\right) + f_r \left(u_{r+1} - u_r\right), \tag{1.3}$$

where r denotes previous iteration and $r + 1$ denotes current iteration.

1.4 Condition for convergence

To determine the convergence of an iteration scheme

$$Ax_{r+1} = Bx_r, \tag{1.4}$$

where x_r represents the solution at previous iterations and x_{r+1} represents the solution at the next iteration, convergence is indicated by

$$||Ax_{r+1} - Bx_r|| < \gamma, \tag{1.5}$$

where $||\cdot||$ is a vector norm and $\gamma \neq 0$ is very small. One of the most crucial expectations of a numerical method is the ability to converge to a fixed point. In the case where the method does not converge, divergence occurs and the iterative method is observed to be *unstable*.

1.5 Gauss-Seidel Method

This method is an iterative method in the sense that it starts with an initial solution/guess and it is used to obtain improved solutions recursively. Let $\mathbf{Ax} = \mathbf{b}$ be a system of l linear

equations of l variables such that

$$\begin{aligned} a_{11}x_1 + a_{12}x_2 + \cdots + a_{1(l-1)}x_{l-1} + a_{1l}x_l &= b_1, \\ a_{21}x_1 + a_{22}x_2 + \cdots + a_{2(l-1)}x_{l-1} + a_{2l}x_l &= b_2, \\ &\vdots \\ a_{l1}x_1 + a_{l2}x_2 + \cdots + a_{l(l-1)}x_{l-1} + a_{ll}x_l &= b_l. \end{aligned} \tag{1.6}$$

To obtain solutions $x_1\ , x_2, \ldots, x_l$, the system (1.6) is rewritten as:

$$x_1 = \frac{b_1}{a_{11}} - \frac{a_{12}}{a_{11}}x_2 + \cdots + \frac{a_{1(l-1)}}{a_{11}}x_{l-1} + \frac{a_{1l}}{a_{11}}x_l, \tag{1.7}$$

$$x_2 = \frac{b_2}{a_{22}} - \frac{a_{21}}{a_{22}}x_1 + \cdots + \frac{a_{2(l-1)}}{a_{22}}x_{l-1} + \frac{a_{2l}}{a_{22}}x_l, \tag{1.8}$$

$$\vdots$$

$$x_{l-1} = \frac{b_{l-1}}{a_{(l-1)(l-1)}} - \frac{a_{(l-1)1}}{a_{(l-1)(l-1)}}x_2 + \cdots + \frac{a_{(l-1)(l-2)}}{a_{(l-1)(l-1)}}x_{l-2} + \frac{a_{(l-1)l}}{a_{(l-1)(l-1)}}x_l, \tag{1.9}$$

$$x_l = \frac{b_l}{a_{ll}} - \frac{a_{l1}}{a_{ll}}x_1 + \frac{a_{l2}}{a_{ll}}x_2 + \cdots + \frac{a_{1(l-2)}}{a_{ll}}x_{l-2} + \frac{a_{l(l-1)}}{a_{ll}}x_{l-1}. \tag{1.10}$$

Initial approximations are given for each $x_1,\ x_2, \ldots, x_l$. The Gauss-Seidel method decouples the system (1.7) such that the solution obtained for x_1 in (1.7) is immediately substituted into (1.8) to solve for x_2 and so on. The process is shown below.

$$\begin{aligned} x_1^r &= \frac{b_1}{a_{11}} - \frac{a_{12}}{a_{11}}x_2^{r-1} + \cdots + \frac{a_{1(l-1)}}{a_{11}}x_{l-1}^{r-1} + \frac{a_{1l}}{a_{11}}x_l^{r-1}, \\ x_2^r &= \frac{b_2}{a_{22}} - \frac{a_{21}}{a_{22}}x_1^r + \cdots + \frac{a_{2(l-1)}}{a_{22}}x_{l-1}^{r-1} + \frac{a_{2l}}{a_{22}}x_l^{r-1}, \\ &\vdots \\ x_{l-1}^r &= \frac{b_{l-1}}{a_{(l-1)(l-1)}} - \frac{a_{(l-1)1}}{a_{(l-1)(l-1)}}x_1^r + \frac{a_{(l-1)2}}{a_{(l-1)(l-1)}}x_2^r + \cdots + \frac{a_{(l-1)l}}{a_{(l-1)(l-1)}}x_l^{r-1}, \\ x_l^r &= \frac{b_l}{a_{ll}} - \frac{a_{l1}}{a_{ll}}x_1^r + \frac{a_{l2}}{a_{ll}}x_2^r + \cdots + \frac{a_{l(l-1)}}{a_{ll}}x_{l-1}^r, \end{aligned} \tag{1.11}$$

where $r-1$ denotes previous approximations and r denotes current approximations. This process is continued until convergence to a fixed point is achieved.

1.6 Finite Difference methods

Finite difference methods are applied to differential equations to obtain approximate solutions. As reported by Anderson et al. (1995) and Trefethen (2000), partial differential

equations that depend on time make use of finite differences to obtain numerical solutions in the direction of time. Finite differences represent partial derivatives with finite difference approximations which are solved in place of the differential equations. Finite differences, as expressed by Mantzaris et al. (2001), make use of a high number of grid-points to obtain excellent accuracy. According to Anderson et al. (1995), the representation of derivatives using finite differences is based on Taylors series expansions. It was noted by Dlamini et al. (2013a) that they gave very accurate solutions using a large amount of grid points with better computational efficiency. There are a number of finite difference formulations. Below, three commonly used finite difference schemes are illustrated using the heat equation that models a one-dimensional temperature evolution expressed as:

$$u_t = \alpha u_{xx}, \qquad \alpha > 0, \tag{1.12}$$

where α is the thermal diffusivity. The explicit finite difference method which is forward in time t_n and central in space x_j is expressed as (Trefethen (2000))

$$\frac{u_j^{n+1} - u_j^n}{k} = \frac{u_{j+1}^n - 2u_j^n + u_{j-1}^n}{h^2}, \tag{1.13}$$

where $k = \Delta t$ and $h = \Delta x$. The implicit method which is backward in time t_n and central in space x_j expressed as

$$\frac{u_j^{n+1} - u_j^n}{k} = \frac{u_{j+1}^{n+1} - 2u_j^{n+1} + u_{j-1}^{n+1}}{h^2}. \tag{1.14}$$

Thirdly, the Crank-Nicolson approach which is central in time $t_{n+\frac{1}{2}}$ and central in space x_j (CTCS) is expressed as:

$$\frac{u_j^{n+1} - u_j^n}{k} = \frac{1}{2}\left(\frac{u_{j+1}^{n+1} - 2u_j^{n+1} + u_{j-1}^{n+1}}{h^2} + \frac{u_{j+1}^n - 2u_j^n + u_{j-1}^n}{h^2}\right). \tag{1.15}$$

It was Wang and Lin (1989) who noted that the implicit scheme requires more computational time than the explicit scheme but it is more accurate and stable than the explicit scheme.

1.7 Crank-Nicolson finite difference method

The Crank-Nicolson method has been proven to be numerically stable and is understood to have higher numerical accuracy when compared to the other finite difference methods (Hu

et al., 2008; Sun and Trueman, 2006). Chang et al. (1999) performed a comparative study by applying the linearized Crank-Nicolson finite difference method and 7 other numerical methods on three problems of the nonlinear generalized schrödinger equation and it was observed that the Crank-Nicolson finite difference method was very competent. Hu et al. (2008) obtained numerical solutions for the Rosenau-Burgers equation when proposing the Crank-Nicolson finite difference method to be an efficient method.

1.8 Spectral Methods

As reported by Gheorghiu (2007) and Van de Vosse and Minev (1996), spectral methods approximate functions using truncated series of orthogonal functions like the Chebyshev and Legendre polynomials. The spectral approximation transforms a function from a physical space to the spectral space. As observed by Gottlieb and Gottlieb (2009) and Trefethen (1996), spectral methods apply the concept of global representations in obtaining high order approximations. There are three types of spectral methods; namely the Tau spectral method, the Collocation spectral method and the Galerkin spectral method. According to Gottlieb and Gottlieb (2009), Baltensperger and Berrut (1999) and Ogundare (2009), the Tau and Galerkin spectral methods are weighted residual methods while the collocation spectral method is not. As reported by Babolian et al. (2007), the Tau and Galerkin methods are applied on expansion coefficients while the collocation methods are applied on physical space values of unknown functions. According to Gheorghiu (2007) and Boyd (2001), an important property of the spectral methods is the ability to transform self-adjoint differential problems into nonsymmetric discrete algebraic problems. Another property of spectral methods is their nondispersive nature. As noted by Mantzaris et al. (2001), they also exhibit exponential convergence/infinite-order accuracy.

The conditioning of differentiation matrices in spectral methods is explained in Cueto-Felgueroso and Juanes (2009) and Trefethen and Trummer (1987). As noted by Baltensperger and Berrut (1999), errors occur in the process of calculating the differentiation matrices for Chebyshev nodes. Trefethen and Trummer (1987) observed that the stability of spectral methods for problems associated with initial boundary value conditions was quite unknown.

Applications of spectral methods include periodic geometries (Trefethen (1996)). According to Boyd (2001), they are also applicable to flows with shock waves and fronts. Spectral methods have been applied successfully in multivariable cell population models by Mantzaris et al. (2001), in weather forecasting by Juang and Kanamitsu (1994) and in many other applications.

1.9 Residual Error

As defined by Yüzbaşi et al. (2014), an error that occurs as a result of computational estimation is regarded as a residual error. This comes about when discretization of differential equations occur. The residual error is calculated after obtaining approximate solutions to differential equations which is done by simply substituting the approximate solutions back into the differential equation. Because numerical analysis deals with approximate solutions and not exact, the residual error can be regarded to be that "extra bit" that is left after obtaining approximate solutions and inserting them back into the original differential equation. As an example, consider a differential equation of the form

$$Ax = b$$

with approximate solution y. The residual error in y is calculated as

$$\text{Res. error} = Ay - b.$$

From the example above, the residual error obtained is most certainly very small (except in the case where y is a poor approximation to x) but it is never zero because the solutions are approximations. It is essential to note that residual error does not tell the actual error of a solution (Cheng et al., 2003). It only indicates how close the approximate solution is to an analytic solution to an equation.

1.10 Quasilinearization Method (QLM)

The QLM, which is a generalization of the Newton-Rhapson method, was originally applied over half a century ago by Bellman and Kalaba (1965) to solve nonlinear ordinary and partial

differential equations. According to Mandelzweig and Tabakin (2001), it was constructed to address nonlinear areas of physical processes. It has been applied extensively to a lot of research areas. Bellman et al. (1967) extended the QLM on nonlinear multipoint boundary-value problems for systems of nonlinear ordinary differential equations. Shazad and Vatsala (1995) and Ahmad et al. (2001) applied the QLM on a second order ordinary nonlinear differential equation with Neumann boundary conditions while Nieto (1997) solved the 2^{nd} order nonlinear ODE with dirichlet boundary conditions with the QLM and Ahmad et al. (2002) extended the QLM to solve the same problem with mixed boundary conditions. Periodic boundary value problems were solved by Lakshmikantham et al. (1996) using the QLM. The QLM has been extended to convex functions by Lakshmikantham (1994). Jaddu (2002) applied the QLM on nonlinear optimal control problems with some constraints. The QLM has been applied in physics by Mandelzweig and Tabakin (2001) to the Lane-Emden, Thomas-Fermi, Duffing, and Blasius equations and in quantum physics by Krivec and Mandelzweig (2001).

1.11 Method Introduction

In this section, the steps taken to develop the algorithms for the spectral relaxation method (SRM), the spectral local linearization method (SLLM) and the spectral quasilinearization method (SQLM) are presented. For illustration purposes, a simple system of ordinary differential equations is used as a case study. More generalized description of the methods are given by Motsa (2013a) and Motsa (2013b).

1.11.1 Spectral Relaxation Method (SRM)

In this subsection, the development of the SRM algorithm is explained for a simple system of ordinary differential equations. The SRM is a relaxation method that uses the idea of the Gauss-Seidel relaxation technique to decouple a coupled system of differential equations and the spectral collocation method to integrate the decoupled system. Using the steps described for a general case by Motsa (2013b), a system of two ordinary differential equations is given

as:

$$\begin{aligned} f'''(\eta) + f(\eta)f''(\eta) + f'^2(\eta) + g(\eta) &= 0, \\ g''(\eta) + f(\eta)g(\eta) + g(\eta) &= 0, \end{aligned} \tag{1.16}$$

with corresponding boundary conditions:

$$f(0) = 1,\ f'(0) = 1,\ f'(\infty) = 0,\ g(0) = 1,\ g(\infty) = 0, \tag{1.17}$$

where prime ($'$) denotes differentiation with respect to η. In order to solve the system more efficiently, it is advisable to reduce the order of f''' in the first equation of the system (1.16) by introducing a new function, say u, where $u = f'$ and the new reduced system becomes:

$$f' = u, \tag{1.18}$$

$$u''(\eta) + f(\eta)u'(\eta) + u^2(\eta) + g(\eta) = 0, \tag{1.19}$$

$$g''(\eta) + f(\eta)g(\eta) + g(\eta) = 0,$$

with corresponding boundary conditions:

$$f(0) = 1,\ u(0) = 1,\ u(\infty) = 0,\ g(0) = 1,\ g(\infty) = 0. \tag{1.20}$$

Initial approximations are obtained so as to initiate the iterative process in obtaining numerical solutions till convergence is established. Initial approximation is obtained by establishing an initial guess that satisfies the given boundary condition (1.20). A suitable guess is

$$\begin{aligned} f_0 &= 1 - \exp^{-\eta}, \\ u_0 = g_0 &= \exp^{-\eta}. \end{aligned} \tag{1.21}$$

To decouple the system (1.18), the Gauss-Seidel relaxation method is applied to obtain a system of the form:

$$\begin{aligned} u''_{r+1}(\eta) + f_r(\eta)u'_{r+1}(\eta) &= -u_r^2(\eta) - g_r(\eta), \\ f'_{r+1} &= u_{r+1}, \\ g''_{r+1}(\eta) + f_{r+1}(\eta)g_{r+1}(\eta) + g_{r+1}(\eta) &= 0. \end{aligned} \tag{1.22}$$

The system (1.22) is a decoupled linear system of equations where the terms with $r-$subscripts are previous approximations and $(r+1)-$subscripts are current approximations.

To obtain numerical solutions from (1.22), Chebyshev spectral collocation method is applied on the system to integrate it. Full details on the application of spectral method is discussed in Trefethen (2000), Canuto et al. (1988) and in Chapter 2. It is necessary to transform the domain on which (1.22) is defined to the interval $[-1, 1]$. This process is carried out using the transformation

$$\eta = \frac{(b-a)(\tau+1)}{2}$$

to transform the interval $[a, b]$ to $[-1, 1]$. The spectral collocation method uses a differentiation matrix D to approximate the derivatives of unknown variables (terms with $(r+1)$) in (1.22) at each collocation point. Higher order derivatives are obtained as powers of $\mathbf{D}$ in the form

$$\begin{aligned} \mathbf{D}^2\mathbf{u}_{r+1} + \mathbf{f}_r(\mathbf{D}\mathbf{u}_{r+1}) &= -\mathbf{u}_r^2 - \mathbf{g}_r, \\ \mathbf{D}\mathbf{f}_{r+1} &= \mathbf{u}_{r+1}, \\ \mathbf{D}^2\mathbf{g}_{r+1} + \mathbf{f}_{r+1}\mathbf{g}_{r+1} + \mathbf{g}_{r+1} &= 0, \end{aligned} \tag{1.23}$$

where $\mathbf{u}_{r+1} = [u_{r+1}(\tau_0)\, u_{r+1}(\tau_1) \cdots u_{r+1}(\tau_{\bar{\mathrm{N}}})]^T$, $\mathbf{f}_{r+1} = [f_{r+1}(\tau_0)\, f_{r+1}(\tau_1) \cdots f_{r+1}(\tau_{\bar{\mathrm{N}}})]^T$, $\mathbf{g}_{r+1} = [g_{r+1}(\tau_0)\, g_{r+1}(\tau_1) \cdots g_{r+1}(\tau_{\bar{\mathrm{N}}})]^T$ are vector functions and $\mathbf{D} = 2D/(b-a)$. The system (1.23) is written in a compact form as

$$\begin{aligned} \mathbf{A}_1\mathbf{f}_{r+1} = \mathbf{B}_1, &\quad f_{r+1}(\tau_{\bar{\mathrm{N}}}) = 1, \\ \mathbf{A}_2\mathbf{u}_{r+1} = \mathbf{B}_2, &\quad u_{r+1}(\tau_{\bar{\mathrm{N}}}) = 1, \quad u_{r+1}(\tau_0) = 0, \\ \mathbf{A}_3\mathbf{g}_{r+1} = \mathbf{B}_3, &\quad g_{r+1}(\tau_{\bar{\mathrm{N}}}) = 1, \quad g_{r+1}(\tau_0) = 0, \end{aligned} \tag{1.24}$$

where

$$\begin{aligned} \mathbf{A}_1 = \mathbf{D}, &\quad \mathbf{B}_1 = \mathbf{g}_r, \\ \mathbf{A}_2 = \mathbf{D}^2 + \mathbf{diag}\,[\mathbf{f}_r]\,\mathbf{D}, &\quad \mathbf{B}_1 = -\mathbf{u}_r^2 - \mathbf{g}_r, \\ \mathbf{A}_3 = \mathbf{D}^2 + \mathbf{diag}\,[\mathbf{f}_{r+1}] + \mathbf{I}, &\quad \mathbf{B}_3 = \mathbf{0}, \end{aligned} \tag{1.25}$$

where $\mathbf{diag}\,[\mathbf{f}_r]$ represents a diagonal matrix of vectors and $\mathbf{0}$ is a $(\bar{\mathrm{N}}+1) \times 1$ vector.

To illustrate how the boundary conditions are implemented on the system, the following is given:

$$\begin{aligned} \mathbf{M}_1\mathbf{P}_1 &= \mathbf{Q}_1, \\ \mathbf{M}_2\mathbf{P}_2 &= \mathbf{Q}_2, \\ \mathbf{M}_3\mathbf{P}_3 &= \mathbf{Q}_3, \end{aligned}$$

where

$$\mathbf{M}_1 = \left[\begin{array}{c} \\ \mathbf{A}_1 \\ \\ \hline 0 \quad 0 \quad \cdots \quad 0 \quad 1 \end{array}\right], \qquad \mathbf{P}_1 = \left[\begin{array}{c} f_{r+1,0} \\ f_{r+1,1} \\ \vdots \\ \vdots \\ \hline f_{r+1,N} \end{array}\right], \qquad \mathbf{Q}_1 = \left[\begin{array}{c} \\ \mathbf{B}_1 \\ \\ \hline 1 \end{array}\right],$$

$$\mathbf{M}_2 = \left[\begin{array}{c} 1 \quad 0 \quad \cdots \quad 0 \quad 0 \\ \hline \\ \mathbf{A}_2 \\ \\ \hline 0 \quad 0 \quad \cdots \quad 0 \quad 1 \end{array}\right], \qquad \mathbf{P}_2 = \left[\begin{array}{c} u_{r+1,0} \\ u_{r+1,1} \\ \vdots \\ \vdots \\ \hline u_{r+1,N} \end{array}\right], \qquad \mathbf{Q}_2 = \left[\begin{array}{c} 0 \\ \hline \\ \mathbf{B}_2 \\ \\ \hline 1 \end{array}\right],$$

$$\mathbf{M}_3 = \left[\begin{array}{c} 1 \quad 0 \quad \cdots \quad 0 \quad 0 \\ \hline \\ \mathbf{A}_3 \\ \\ \hline 0 \quad 0 \quad \cdots \quad 0 \quad 1 \end{array}\right], \qquad \mathbf{P}_3 = \left[\begin{array}{c} g_{r+1,0} \\ \hline g_{r+1,1} \\ \vdots \\ \vdots \\ \hline g_{r+1,N} \end{array}\right], \qquad \mathbf{Q}_3 = \left[\begin{array}{c} 0 \\ \hline \\ \mathbf{B}_3 \\ \\ \hline 1 \end{array}\right].$$

1.11.2 Spectral Local Linearization Method (SLLM)

In this subsection, the steps taken to develop the algorithm for solving the same system of ODEs (1.16) using the SLLM are shown. It is of great significance to note that the only difference between the SRM and the SLLM is in the initial stage of developing the algorithm. In the previous section, it was shown that Gauss-Seidel relaxation method was applied immediately on the reduced system (1.18). In this case however, as reported for a general case by Motsa (2013a), the SLLM applies Taylor series expansion on a univariate nonlinear term.

In the reduced system (1.18), the nonlinear term is u^2 and is linearized by applying Taylor series expansion on it in the form shown below.

$$\begin{aligned} u^2 &= u_r^2 + 2u_r\left(u_{r+1} - u_r\right) \\ &= 2u_r u_{r+1} - u_r^2. \end{aligned} \tag{1.26}$$

The result obtained in (1.26) is substituted back into (1.18) and the Gauss-Seidel relaxation method is applied to decouple the system to obtain:

$$\begin{aligned} u_{r+1}^{''}(\eta) + f_r(\eta)u_{r+1}^{'}(\eta) + 2u_r(\eta)u_{r+1}(\eta) &= u_r^2(\eta) - g_r(\eta), \\ f_{r+1}^{'} &= u_{r+1}, \\ g_{r+1}^{''}(\eta) + f_{r+1}(\eta)g_{r+1}(\eta) + g_{r+1}(\eta) &= 0. \end{aligned} \tag{1.27}$$

The system (1.27) is a decoupled linear system of equations where the terms containing $r-$subscripts are previous approximations and $(r+1)-$subscripts are current approximations.

The Chebyshev spectral collocation method is applied to the system (1.27) to obtain approximate solutions using the differentiation matrix $\mathbf{D} = 2D/(b-a)$. The order of the derivatives of the functions determines the power of the differentiation matrix $\mathbf{D}$ such that (1.27) becomes:

$$\begin{aligned} \mathbf{D}^2\mathbf{u}_{r+1} + \mathbf{f}_r\mathbf{D}\mathbf{u}_{r+1} + \mathbf{u}_r\mathbf{u}_{r+1} &= \mathbf{u}_r^2 - \mathbf{g}_r, \\ \mathbf{D}\mathbf{f}_{r+1} &= \mathbf{u}_{r+1}, \\ \mathbf{D}^2\mathbf{g}_{r+1} + \mathbf{f}_{r+1}\mathbf{g}_{r+1} + \mathbf{g}_{r+1} &= \mathbf{0}. \end{aligned} \tag{1.28}$$

This is written in a compact form as

$$\begin{aligned} \mathbf{A}_1\mathbf{f}_{r+1} = \mathbf{B}_1, \quad & f_{r+1}\left(\tau_{\bar{\mathrm{N}}}\right) = 1, \\ \mathbf{A}_2\mathbf{u}_{r+1} = \mathbf{B}_2, \quad & u_{r+1}\left(\tau_{\bar{\mathrm{N}}}\right) = 1, \quad u_{r+1}\left(\tau_0\right) = 0, \\ \mathbf{A}_3\mathbf{g}_{r+1} = \mathbf{B}_3, \quad & g_{r+1}\left(\tau_{\bar{\mathrm{N}}}\right) = 1, \quad g_{r+1}\left(\tau_0\right) = 0, \end{aligned} \tag{1.29}$$

where

$$\begin{aligned} \mathbf{A}_1 = \mathbf{D}, \quad & \mathbf{B}_1 = \mathbf{g}_r, \\ \mathbf{A}_2 = \mathbf{D}^2 + \mathbf{diag}\left[\mathbf{f}_r\right]\mathbf{D} + \mathbf{diag}\left[\mathbf{u}_r\right], \quad & \mathbf{B}_1 = -\mathbf{u}_r^2 - \mathbf{g}_r, \\ \mathbf{A}_3 = \mathbf{D}^2 + \mathbf{diag}\mathbf{f}_{r+1} + \mathbf{I}, \quad & \mathbf{B}_3 = \mathbf{0}, \end{aligned} \tag{1.30}$$

where $\mathbf{diag}\left[\mathbf{f}_r\right]$ represents a diagonal matrix of vectors, $\mathbf{I}$ an identity matrix of size $(\bar{\mathrm{N}}+1)\times(\bar{\mathrm{N}}+1)$ and $\mathbf{0}$ is a $(\bar{\mathrm{N}}+1)\times 1$ vector.

The boundary conditions are implemented on the system as shown:

$$\begin{aligned}\mathbf{M}_1\mathbf{P}_1 &= \mathbf{Q}_1,\\ \mathbf{M}_2\mathbf{P}_2 &= \mathbf{Q}_2,\\ \mathbf{M}_3\mathbf{P}_3 &= \mathbf{Q}_3,\end{aligned}$$

where

$$\mathbf{M}_1 = \begin{bmatrix} & & & & \\ & & \mathbf{A}_1 & & \\ & & & & \\ \hline 0 & 0 & \cdots & 0 & 1 \end{bmatrix}, \quad \mathbf{P}_1 = \begin{bmatrix} f_{r+1,0} \\ f_{r+1,1} \\ \vdots \\ \vdots \\ \hline f_{r+1,N} \end{bmatrix}, \quad \mathbf{Q}_1 = \begin{bmatrix} \\ \mathbf{B}_1 \\ \\ \hline 1 \end{bmatrix},$$

$$\mathbf{M}_2 = \begin{bmatrix} 1 & 0 & \cdots & 0 & 0 \\ \hline & & & & \\ & & \mathbf{A}_2 & & \\ & & & & \\ \hline 0 & 0 & \cdots & 0 & 1 \end{bmatrix}, \quad \mathbf{P}_2 = \begin{bmatrix} u_{r+1,0} \\ u_{r+1,1} \\ \vdots \\ \vdots \\ \hline u_{r+1,N} \end{bmatrix}, \quad \mathbf{Q}_2 = \begin{bmatrix} 0 \\ \hline \\ \mathbf{B}_2 \\ \\ \hline 1 \end{bmatrix},$$

$$\mathbf{M}_3 = \begin{bmatrix} 1 & 0 & \cdots & 0 & 0 \\ \hline & & & & \\ & & \mathbf{A}_3 & & \\ & & & & \\ \hline 0 & 0 & \cdots & 0 & 1 \end{bmatrix}, \quad \mathbf{P}_3 = \begin{bmatrix} g_{r+1,0} \\ \hline g_{r+1,1} \\ \vdots \\ \vdots \\ \hline g_{r+1,N} \end{bmatrix}, \quad \mathbf{Q}_3 = \begin{bmatrix} 0 \\ \hline \\ \mathbf{B}_3 \\ \\ \hline 1 \end{bmatrix}.$$

1.11.3 Spectral Quasilinearization Method (SQLM)

In this subsection, the steps taken to apply the SQLM on the given system of ODEs (1.16) are shown. Following the general description provided by Motsa (2013a), the SQLM, an extension of the QLM (a Newton-Rhapson method that was originally used by Bellman and Kalaba (1965) for solving functional equations), identifies all univariate and multivariate nonlinear

terms in the system (1.16) and linearization is performed by applying Taylor series expansion. The resulting linearized system is solved as a coupled system.

Consider the system (1.16). The nonlinear terms are $f(\eta)f^{''}(\eta),\ f^{'2}(\eta)$ and $f(\eta)g(\eta)$. They are linearized using the Taylor series expansion as shown below.

$$\begin{aligned} ff^{''} &= f_r f_r^{''} + f_r^{''}\left(f_{r+1} - f_r\right) + f_r\left(f_{r+1}^{''} - f_r^{''}\right) \\ &= f_r^{''} f_{r+1} + f_r f_{r+1}^{''} - f_r f_r^{''}. \end{aligned} \tag{1.31}$$

$$\begin{aligned} f^{'2} &= f_r^{'2} + 2f_r^{'}\left(f_{r+1}^{'} - f_r^{'}\right) \\ &= 2f_r^{'} f_{r+1}^{'} - f_r^{'2}. \end{aligned} \tag{1.32}$$

$$\begin{aligned} fg &= f_r g_r + g_r\left(f_{r+1} - f_r\right) + f_r\left(g_{r+1} - g_r\right) \\ &= g_r f_{r+1} + f_r g_{r+1} - f_r g_r. \end{aligned} \tag{1.33}$$

The solutions obtained in $(1.31 - 1.33)$ are substituted back into (1.16) and the coupled linear system is obtained:

$$\begin{aligned} f_{r+1}^{'''} + f_r^{''} f_{r+1} + f_r f_{r+1}^{''} + 2f_r^{'} f_{r+1}^{'} + g_{r+1} &= f_r f_r^{''} + f_r^{'2}, \\ g_{r+1}^{''} + g_r f_{r+1} + f_r g_{r+1} + g_{r+1} &= f_r g_r, \end{aligned} \tag{1.34}$$

with corresponding boundary conditions:

$$f(0) = 1,\ f^{'}(0) = 1,\ f^{'}(\infty) = 0,\ h(0) = 1,\ h(\infty) = 0, \tag{1.35}$$

The system (1.34) is a coupled linear system of equations where the $r-$terms are initial (previous) approximations and $(r+1)-$terms are next (current) approximations.

Chebyshev spectral collocation method is applied on the system (1.34) to obtain approximate solutions. The main idea behind the spectral collocation method is the use of the differentiation matrix $\mathbf{D} = 2D/(b-a)$ to approximate derivatives of unknown variables (terms at $(r+1)$). The order of the derivatives of the functions determines the power of the differentiation matrix $\mathbf{D}$ so that (1.34) becomes:

$$\begin{aligned} \mathbf{D}^3\mathbf{f}_{r+1} + \mathbf{f}_r^{''}\mathbf{f}_{r+1} + \mathbf{f}_r\mathbf{D}^2\mathbf{f}_{r+1} + 2\mathbf{f}_r^{'}\mathbf{D}\mathbf{f}_{r+1} + \mathbf{g}_{r+1} &= \mathbf{f}_r\mathbf{f}_r^{''} + \mathbf{f}_r^{'2}, \\ \mathbf{D}^2\mathbf{g}_{r+1} + \mathbf{g}_r\mathbf{f}_{r+1} + \mathbf{f}_r\mathbf{g}_{r+1} + \mathbf{g}_{r+1} &= \mathbf{f}_r\mathbf{g}_r. \end{aligned} \tag{1.36}$$

This is written in a compact form as

$$\begin{aligned} \mathbf{A}_{11}\mathbf{f}_{r+1} + \mathbf{A}_{12}\mathbf{g}_{r+1} = \mathbf{B}_1, \quad f_{r+1}\left(\tau_{\bar{\mathrm{N}}}\right) = 1,\ f_{r+1}\left(\tau_{\bar{\mathrm{N}}-1}\right) = 1,\ f_{r+1}\left(\tau_{\bar{0}}\right) = 0, \\ \mathbf{A}_{21}\mathbf{f}_{r+1} + \mathbf{A}_{22}\mathbf{g}_{r+1} = \mathbf{B}_2, \quad g_{r+1}\left(\tau_{\bar{\mathrm{N}}}\right) = 1, \quad g_{r+1}\left(\tau_{\bar{0}}\right) = 0, \end{aligned} \tag{1.37}$$

where

$$\begin{aligned} \mathbf{A}_{11} = \mathbf{D}^3 + \mathbf{diag}\left[\mathbf{f}_r\right]\mathbf{D}^2 + \mathbf{diag}\left[\mathbf{f}_r^{'}\right]\mathbf{D} + \mathbf{diag}\left[\mathbf{f}_r^{''}\right],\ \mathbf{A}_{12} = \mathbf{I}, \quad \mathbf{B}_1 = \mathbf{f}_r\mathbf{f}_r^{''} + \mathbf{f}_r^{'2}, \\ \mathbf{A}_{21} = \mathbf{diag}\left[\mathbf{g}_r\right], \quad \mathbf{A}_{22} = \mathbf{D}^2 + \mathbf{diag}\left[\mathbf{f}_r\right] + \mathbf{I}, \quad \mathbf{B}_2 = \mathbf{f}_r\mathbf{g}_r, \end{aligned} \tag{1.38}$$

where $\mathbf{diag}\left[\cdots\right]$ represents a diagonal matrix of vectors and $\mathbf{I}$ an identity matrix of size $(\bar{\mathrm{N}}+1)\times(\bar{\mathrm{N}}+1)$. The system (1.37) is represented in matrix form as shown:

$$\begin{bmatrix} \mathbf{A}_{11} & \mathbf{A}_{12} \\ \mathbf{A}_{21} & \mathbf{A}_{22} \end{bmatrix} \begin{bmatrix} \mathbf{f}_{r+1} \\ \mathbf{g}_{r+1} \end{bmatrix} = \begin{bmatrix} \mathbf{B}_1 \\ \mathbf{B}_2 \end{bmatrix},$$

where all the entries in the matrix are all matrices and boundary conditions are imposed on them in the forms shown below.

$$\mathbf{A}_{11} = \begin{bmatrix} \mathbf{D}_{0,0} & \mathbf{D}_{0,1} & \cdots & \mathbf{D}_{0,N-1} & \mathbf{D}_{0,N} \\ \hline & & \mathbf{A}_{11} & & \\ \hline \mathbf{D}_{N,0} & \mathbf{D}_{N,1} & \cdots & \mathbf{D}_{N,N-1} & \mathbf{D}_{N,N} \\ \hline 0 & 0 & \cdots & 0 & 1 \end{bmatrix}, \quad \mathbf{A}_{12} = \begin{bmatrix} 0 & 0 & \cdots & 0 & 0 \\ \hline & & \mathbf{A}_{12} & & \\ \hline 0 & 0 & \cdots & 0 & 0 \\ \hline 0 & 0 & \cdots & 0 & 0 \end{bmatrix},$$

$$\mathbf{A}_{21} = \begin{bmatrix} 0 & 0 & \cdots & 0 & 0 \\ \hline & & \mathbf{A}_{21} & & \\ \hline 0 & 0 & \cdots & 0 & 0 \end{bmatrix}, \quad \mathbf{A}_{22} = \begin{bmatrix} 1 & 0 & \cdots & 0 & 0 \\ \hline & & \mathbf{A}_{22} & & \\ \hline 0 & 0 & \cdots & 0 & 1 \end{bmatrix}, \quad \mathbf{f}_{r+1} = \begin{bmatrix} f_{r+1,0} \\ \hline \\ \vdots \\ \\ \hline f_{r+1,N-1} \\ \hline f_{r+1,N} \end{bmatrix}, \quad \mathbf{g}_{r+1} = \begin{bmatrix} g_{r+1,0} \\ \hline \\ \vdots \\ \\ \hline g_{r+1,N-1} \\ \hline g_{r+1,N} \end{bmatrix},$$

$$\mathbf{B}_1 = \begin{bmatrix} 0 \\ \hline \\ \mathbf{B}_1 \\ \\ \hline 1 \\ \hline 1 \end{bmatrix}, \quad \mathbf{B}_2 = \begin{bmatrix} 0 \\ \hline \\ \mathbf{B}_2 \\ \\ \hline 1 \end{bmatrix}.$$

1.12 Structure of Dissertation

The remaining part of this dissertation is outlined as follows:

* Comparative study of the SRM, SLLM and SQLM is carried out in solving the unsteady free convective heat and mass transfer on a stretching surface in a porous medium with suction/injection in Chapter 2.

* In Chapter 3, the comparative study of the SRM, SLLM and SQLM is given via the solution of the unsteady boundary layer flow due to a stretching surface in a rotating fluid.

* The unsteady three-dimensional MHD boundary layer flow and heat transfer over an impulsively stretching plate is solved using the SRM, SLLM and SQLM to conclude the comparative study in Chapter 4.

* In Chapter 5, a general conclusion is given.

Chapter 2

Unsteady free convective heat and mass transfer on a stretching surface in a porous medium with suction/injection

2.1 Introduction

Studies have shown that fluid dynamics and transfer of heat problems due to a stretching sheet are important in aerodynamic extrusion processes, production of paper, spinning of metal, glass blowing, drawing plastic films, cooling of an infinite metallic plate in a cooling bath, the boundary layer along material handling conveyers and in many other applications. The quality of the final product depends on the rate of heat transfer at the stretching surface (Chamkha et al. (2010), Nazar et al. (2004a), Nazar et al. (2008), Kumari and Nath (2009), Ishak et al. (2006), and Liao (2006b)).

The past fifty years have seen increasingly rapid advances in the field of fluid flow. Sakiadis (1961) pioneered the study of flow due to a surface moving at constant velocity in a quiescent fluid. Tsou et al. (1967) investigated the effect of transfer of heat at the boundary on a continuously moving surface with a constant velocity and experimentally agreed with the

measured profiles numerically obtained by Sakiadis (1961). The effect of parameters such as heat and mass transfer, suction/injection, linear/nonlinear stretching of surface, uniform/non-uniform wall temperature/heat flux on the study of fluid flow have been considered by, among many others, Erickson et al. (1966), Chamkha et al. (2010), Gupta and Gupta (1977) to mention a few. The unsteady free convective heat and mass transfer on a stretching surface in a porous medium with suction/injection was examined by Chamkha et al. (2010) using a fourth-order Runge-Kutta scheme with the shooting method. The same problem was studied by Motsa and Shateyi (2012c) using the successive linearization method (SLM). Motsa (2013b) analyzed the same problem during the introduction of the spectral relaxation method (SRM). The same problem was again investigated by Dlamini et al. (2013b) using the spectral relaxation method (SRM), the compact finite difference relaxation method (CFD-RM), the spectral quasilinearization method (SQLM) and the compact finite difference quasilinearization method (CFD-QLM) where it was observed that the CFD-QLM and the CFD-RM needed a large number of grid-points for very good accuracy to be achieved. Motsa (2013a) examined the same problem using the spectral local linearization method (SLLM) and the spectral quasilinearization method (SQLM) and concluded that the accuracy of the SQLM decreased as the number of collocation points used were increased. Pop and Na (1996) investigated the unsteady flow over a stretching surface with the wall impulsively stretched at time $t = 0$ with a velocity varying linearly with a distance x along the surface. Xu and Liao (2005) obtained series solution using the homotopy analysis method to an unsteady magnetohydrodynamic (MHD) viscous flows of non-Newtonian fluids caused by an impulsively stretching plate. Elbashbeshy and Bazid (2003) investigated the effect of internal heat generation on the heat transfer over an unsteady stretching surface moving with a power law velocity by obtaining numerical solutions using the fourth-order Runge-Kutta integration scheme with the Newton Raphson shooting method. Ali et al. (2010) studied the problem of unsteady laminar boundary layer flow caused by an impulsively stretching surface with constant viscous flow until the flow arrives at the final steady state ($\xi = 1$) using the Keller-Box method for numerical simulations. Ariel (2003) and Wang (1984) studied the steady three-dimensional flow due to the stretching surface. Mehmood and Ali (2006) investigated the effects of some parameters on the flow of a viscous fluid over a stretching plate with heat transfer analysis in the presence of viscous dissipation by applying the homotopy analysis method. Liao (2006a)

solved the unsteady boundary-layer flows caused by an impulsively stretching flat to obtain an analytic solution using the homotopy analysis method. Elbashbeshy and Bazid (2004) applied the fourth order Runge-Kutta-Merson to obtain similarity solution for momentum and heat transfer in an unsteady flow in which the motion is brought about as a result of linear stretching of a horizontal stretching surface.

The problem of an unsteady three-dimensional boundary layer flow and heat transfer induced by an impulsively stretched plane surface in two lateral directions in the presence of a magnetic field considered in this chapter was investigated by Kumari and Nath (2009) using the homotopy analysis method to obtain analytical solutions and finite-difference method with quasilinearization approach to obtain numerical solutions. Kumari et al. (1996) investigated the unsteady free convection flow over a continuous moving vertical surface in an ambient fluid. Pop and Na (1996) investigated an unsteady flow past a stretching sheet by applying the Shanks transformation. The Keller-Box method was used for a numerical study of an unsteady mixed convection boundary layer flow near the stagnation point on a vertical surface in a porous medium by Nazar et al. (2004b). The study of an unsteady boundary layer flow due to a stretching surface in a rotating fluid was considered by Nazar et al. (2004a) who applied the Keller-Box method for numerical solutions, a method that was also used in investigation carried out by Ishak et al. (2006) in observing the behavior of an unsteady mixed convection boundary layer flow due to a stretching vertical surface. Liao (2006b) studied the unsteady boundary-layer flows over an impermeable stretching plate and obtained series solutions using the homotopy analysis method (HAM). The method was later used by Hang and Pop (2007) to obtain series solutions to an unsteady three-dimensional magnetohydrodynamic (MHD) boundary layer flows with heat transfer over an impulsively stretching plate. By applying an implicit finite-difference scheme, Seshadri and Nath (2002) studied an unsteady mixed convection flow in the stagnation region of a heated vertical plate due to impulsive motion. Nazar et al. (2008) investigated an unsteady boundary layer flow over a stretching sheet in a micropolar fluid using the Keller-Box method.

The aim of this study was to compare three numerical methods (the spectral relaxation method (SRM), the spectral local linearization method (SLLM) and the spectral quasilin-

earization method (SQLM)) that were shown by others to be easy to implement, converged quite fast and to very accurate results. This was done in a bid to validate earlier observations of (Motsa, 2013a) and (Motsa, 2013b) on the numerical techniques. After validation, the methods were compared against one another so as to further ascertain the claims of their reliability for solving systems of differential equations. The spectral relaxation method (SRM), spectral local linearization method (SLLM) and the spectral quasilinearization method (SQLM) were applied on an unsteady free convective heat and mass transfer on a stretching surface in a porous medium with suction/injection. These are spectral based methods that were introduced by Motsa (2013a) and Motsa (2013b). The reason was to compare the three numerical techniques against one another to discover how well they perform in terms of convergence and accuracy when applied on a system of ordinary differential equations. This comparison was performed by investigating the effect of number of iterations, effect of number of collocation points and effect of the domain truncation on the accuracy of the solution. This study, however, was not done in a bid to replace other known methods. Rather, it was done to include the methods in the list of reliable methods already in existence. A considerable amount of research has been carried out using these numerical methods (SRM, SLLM and SQLM) with very good observations being made concerning their accuracies and ease of application.

As reported in Motsa (2013b), the motivation behind the Spectral relaxation method (SRM) is to decouple a nonlinear system of differential equations using the idea of the Gauss-Seidel approach and then apply Chebyshev pseudospectral collocation technique on the decoupled system. The systems are solved by starting from an initial approximation (or guess that satisfies all boundary conditions) which is used to generate subsequent approximations iteratively until convergence is obtained at some point. Shateyi and Makinde (2013) used the SRM to study the steady stagnation-point flow and heat transfer of an electrically conducted incompressible viscous fluid with the disk surface convectively heated and radially stretching. The accuracy of the method was validated by comparing with the result obtained using the MATLAB inbuilt bvp4c and was observed to be a perfect match. The convergence of the SRM was seen to be faster than the bvp4c in terms of both the time taken for convergence and number of iterations taken to achieve convergence. Shateyi and Marewo (2013) applied the SRM on MHD boundary layer flow with heat and mass transfer of an incompressible upper-

convected Maxwell fluid over a stretching sheet in the presence of viscous dissipation and thermal radiation as well as chemical reaction where the accuracy of the SRM was observed to be accurate after comparing with the bvp4c (a MATLAB inbuilt routine). Makukula et al. (2012b) examined the steady von Kármán flow of a Reiner-Rivlin fluid flow with Joule heating, viscous dissipation using the SRM for numerical simulations. Successive Over-relaxation (SOR) was used to accelerate the convergence of the SRM and it was noted that the method gives very accurate solutions when compared to other methods. Motsa (2013b) solved the MHD boundary layer flow over a shrinking sheet, similarity variable boundary layer flow in the presence of Hall effects and an unsteady free convective heat and mass transfer on a stretching surface in a porous medium with suction/injection using the SRM noting that the method was very straightforward as linearization wasn't required and the method gave very accurate results with few few grid points. Kameswaran et al. (2013) used the spectral relaxation method (SRM) in studying the effect of fluid and physical parameters on the flow and heat transfer characteristics of three different water-based nanofluids containing copper oxide CuO, aluminium oxide Al_2O_3 and titanium dioxide TiO_2 nanoparticles. The successive over-relaxation (SOR) technique was applied to improve the accuracy and efficiency of the SRM. The results obtained were shown to be in good agreement with results obtained using bvp4c and other results from published literature. In Shateyi and Prakash (2014), the SRM was applied on the problem of MHD flow of a nano-fluid past a stretching sheet in the presence of thermal radiation and the result obtained was validated by comparing with result obtained from known literature and bvp4c where it was observed that all three results were in good agreement. Motsa et al. (2014) studied the unsteady heat transfer in a nanofluid over a permeable stretching or shrinking surface using the SRM and the SQLM for numerical simulations where it was observed that the SRM was more accurate than the SQLM. Makukula et al. (2014) investigated the reactions of thermal transesterification in the production of biodiesel from vegetable oils using the SRM. Kameswaran et al. (2014) introduced a new algorithm for modeling internal heat generation in nanofluid flow in the presence of a stretching sheet in a porous medium applying the SRM for numerical solutions. Motsa et al. (2013) modified the SRM to a multistage SRM (MSRM) to obtain numerical solutions of hyperchaotic systems.

Chapter 2 – Unsteady free convective heat and mass transfer on a stretching surface in a porous medium with suction/injection

As shown in Motsa (2013a), the spectral local linearization method's (SLLM) scheme decouples the reduced nonlinear system of equations, identifies the nonlinear singular terms and then linearizes them using the single term Taylor series expansion to obtain a decoupled linear system of differential equations. Chebyshev pseudospectral collocation method is applied on the linear systems. And the systems are solved by having an initial approximation(or guess) which will be used to generate subsequent approximations iteratively until convergence is obtained at some point. Motsa (2013a) used the SLLM and the SQLM to solve the Blasius boundary layer equation and the Unsteady Free Convective Heat and Mass Transfer on a Stretching Surface in a Porous Medium with Suction/Injection. It was noted that the convergence rate of the SLLM could be improved by applying Successive Over-relaxation (SOR) and that the SQLM converged very fast with a small amount of collocation points to some accurate result but an increase in collocation points led to a decline in accuracy of the numerical solution obtained. Motsa et al. (2013) examined, using the SLLM, the natural convection boundary layer flow that arises in glass-fibre production process and noted that the SLLM was easy to implement and produced accurate results at very good rate of convergence. Dlamini et al. (2013b) studied the MHD boundary layer flow over a shrinking sheet and an unsteady free convective heat and mass transfer on a stretching surface in a porous medium with suction/injection using the compact finite difference relaxation method (CFD-RM), compact finite difference quasilinearization method (CFD-QLM), spectral relaxation method (SRM) and the spectral quasilinearization method (SQLM). The spectral based methods were observed to be much better than the compact finite difference methods in terms of both computational speed and accuracy.

The quasilinearization method (QLM) is a generalization of the Newton-Rhapson method that was originally used by Bellman and Kalaba (1965) for solving functional equations. Motsa (2013a) furthered the application of the QLM by applying spectral collocation method to solve the linearized equation. Reduction of order of equations is not necessary when the spectral quasilinearization method (SQLM) is applied. Rather, nonlinear terms are identified in the system of equations and linearized using the Taylor series expansion for multiple variables to obtain a linear coupled system of equations. Chebyshev pseudospectral collocation method is applied to solve the linear systems. The systems are solved starting with an

initial approximation (or guess that satisfies all boundary conditions) which is used to generate subsequent approximations iteratively until convergence is obtained at some point. The concept of the SQLM is similar to that of the successive linearisation method (SLM) which is another Newton-Rhapson based method. The SLM (Motsa and Sibanda, 2012; Makukula et al., 2010b) has been applied extensively in a number of published studies (Awad et al., 2011; Motsa et al., 2011; Shateyi and Motsa, 2011a; Makukula et al., 2010a,c; Sibanda et al., 2012; Motsa et al., 2012; Shateyi and Motsa, 2011b; Motsa, 2011; Motsa and Shateyi, 2012b, 2011; Makukula et al., 2012a). Makukula et al. (2011) investigated an MHD boundary layer past a porous shrinking sheet with a chemical reaction and suction using the SLM to obtain numerical solutions. The effects of chemical reaction parameter, hall and ion-slip currents on an MHD micropolar fluid flow with thermal diffusivity was studied by Motsa and Shateyi (2012a) with the aid of the SLM. Motsa and Shateyi (2012d) observed the effects of partial slip, thermal diffusion and diffusion-thermo on steady MHD convective flow due to a rotating disk by obtaining numerical solutions with the SLM. Motsa and Sibanda (2013) studied the Falkner-Skan boundary layer equations by applying the quasilinearization method embedded in the spectral homotopy analysis method (SHAM) to obtain a sequence of integration schemes with arbitrary higher order convergence. Motsa et al. (2014) investigated the unsteady heat transfer in a nanofluid over a permeable stretching or shrinking surface using the SRM and the SQLM for numerical simulations and it was observed that the SQLM converged faster than the SRM and the SQLM could yield multiple solutions while the SRM was limited to one solution.

When applying the three methods, it was observed that their algorithms were easy to set up and gave very accurate results with few grid points. The convergence rate of the methods were observed to be high and their accuracies were very impressive. The SRM is straightforward as linearization is not done. However, successive over-relaxation (SOR) was applied to speed up convergence which implies in some cases, the convergence of the methods might not be quick enough. When the number of collocation points became very large, the accuracy of the SQLM declined.

In this chapter, a system of nonlinear ordinary differential equations modeling an unsteady free convective heat and mass transfer on a stretching surface in a porous medium with suction/injection was investigated using the SRM, SLLM and SQLM to obtain numerical solutions. The aim of this study was to compare the SRM, SLLM and SQLM to observe how efficient they were in solving systems of ordinary differential equations. To achieve this, certain objectives had to be accomplished. Firstly, the ease of implementing the SRM, SLLM and SQLM on the system of ordinary differential equations was investigated to note how straightforward/cumbersome it was in developing their respective algorithms. The effect of collocation (grid) points on the accuracy of the solutions obtained was studied to understand if an increase in the number of collocation points affected the accuracy of solutions obtained. The domain truncation used was also considered as a key factor to be observed with the purpose of determining the effect of the size of the domain on the accuracy of solutions obtained. It is essential to note that the system of ODEs are solved on a semi-infinite domain which, for numerical application purposes, is approximated by domain truncation. And finally, iterations were used to determine which method converged the fastest.

This chapter begins with a formulation of the mathematical equations which model the unsteady free convective heat and mass transfer on a stretching surface in a porous medium with suction/injection. A description of how the different methods have been applied on the equations is then. Finally, the solutions are examined critically in graphical and tabular forms.

2.2 Mathematical formulation

In this section, the formulation of the mathematical equations that govern an unsteady free convective heat and mass transfer on a stretching surface in a porous medium with suction/injection are presented.

As described by Chamkha et al. (2010), we consider an unsteady boundary layer flow that occurs as a result of a stretching permeable surface fitted into a uniform medium which is porous. At an initial time $t = 0$, the sheet is stretched impulsively with the velocity variable $U_w(x, t)$. The fluid properties are assumed as constants, and a first-order homogeneous

chemical reaction is assumed to take place in the flow. Using these assumptions alongside the Boussinesq approximation, the governing boundary-layer equations that are based on the balance laws of mass, linear momentum, energy and concentration species for this investigation can be expressed as:

$$\frac{\partial u}{\partial x}+\frac{\partial \upsilon}{\partial y} = 0, \tag{2.1}$$

$$\frac{\partial u}{\partial t}+u\frac{\partial u}{\partial x}+\upsilon\frac{\partial u}{\partial y} = \upsilon\frac{\partial^2 u}{\partial y^2}+g\beta_T(T-T_\infty)+g\beta_C(C-C_\infty)-\frac{\upsilon}{k_1}u, \tag{2.2}$$

$$\frac{\partial T}{\partial t}+u\frac{\partial T}{\partial x}+\upsilon\frac{\partial T}{\partial y} = \alpha\frac{\partial^2 T}{\partial y^2}, \tag{2.3}$$

$$\frac{\partial C}{\partial t}+u\frac{\partial C}{\partial x}+\upsilon\frac{\partial C}{\partial y} = D\frac{\partial^2 C}{\partial y^2}-k_c(C-C_\infty), \tag{2.4}$$

where x and y are the cartesian coordinates, t is the time, v and u are the velocity components along the x and y directions respectively, $\upsilon=\frac{\mu}{\rho}$ is the kinematic viscosity, μ is the constant viscosity of the fluid in the boundary layer region, ρ is the effective thermal diffusivity, k_c is the rate of chemical reaction, g is the acceleration due to gravity, β_T is the volumetric coefficient of thermal expansion, β_C is the volumetric coefficient of concentration expansion, k_1 and D are permeability of porous media and coefficient of mass diffusivity, respectively, while T_∞ and C_∞ are the free stream temperature and concentration, respectively.

The boundary conditions of (2.1)-(2.4) are expressed as;

$$\begin{aligned} u=U_w, \qquad \upsilon=\Upsilon_w, \quad T=T_w, \qquad C=C_w \;\; at\; y=0,\\ u=0, \qquad T=T_\infty, \qquad C=C_\infty \; as \; y \;\rightarrow\; \infty. \end{aligned} \tag{2.5}$$

The stretching velocity $U_w(x,t)$, the surface temperature $T_w(x,t)$ and the surface concentration $C_w(x,t)$ are assumed to be of the form;

$$U_w(x,t)=\frac{ax}{1-ct}, \;\; T_w(x,t)=T_\infty+\frac{bx}{1-ct}, \;\; C_w(x,t)=C_\infty+\frac{bx}{1-ct}, \tag{2.6}$$

where a,b and c are said to be constants with $ct<1$, and both a and c have dimension time^{-1}, Υ_w is the suction/injection parameter. $\Upsilon_w<0$ denotes suction while $\Upsilon_w>0$ denotes an injection parameter.

The following self-similar transformation are introduced(see Ishak et al. (2006), Ishak et al. (2008) and Ishak et al. (2009));

$$\eta = \left(\frac{U_w}{\upsilon x}\right)^{\frac{1}{2}},\ \psi = (\upsilon x U_w)^{\frac{1}{2}} f(\eta),\ \theta(\eta) = \frac{T - T_\infty}{T_w - T_\infty},\ \phi(\eta) = \frac{C - C_\infty}{C_w - C_\infty}, \tag{2.7}$$

where $\psi(x, y, t)$ is a stream function related to the components of the velocity fields. The stream function $\psi(x, y, t)$ is defined in terms of the velocity components as $u = \frac{\partial \psi}{\partial y}$ and $\upsilon = -\frac{\partial \psi}{\partial x}$; it can be verified easily that the continuity equation (2.1) is identically satisfied. Introducing the relations (2.7) into equations (2.2)-(2.4), the following dimensionless ordinary differential equations and dimensionless boundary conditions are obtained:

$$f''' + ff'' - (f')^2 - A(f' + \frac{\eta}{2}f'') + Gr\theta + Gc\phi = 0, \tag{2.8}$$

$$\frac{1}{Pr}\theta'' - f'\theta + f\theta' - A(\theta + \frac{1}{2}\eta\theta') = 0, \tag{2.9}$$

$$\frac{1}{Sc}\phi'' - f'\phi + f\phi' - A(\phi + \frac{1}{2}\eta\phi') - \gamma\phi = 0, \tag{2.10}$$

with corresponding boundary conditions:

$$\begin{aligned} f(0) = f_w,\ f'(0) = 1,\ \theta(0) = 1,\ \phi(0) = 1, \\ f'(\infty) = 0,\ \theta(\infty) = 0,\ \phi(\infty) = 0\ as\ \eta \to \infty, \end{aligned} \tag{2.11}$$

where a prime denotes differentiation with respect to η, f_w is the suction parameter when $f_w > 0$ and the injection parameter when $f_w < 0$, γ is the chemical reaction constant, $Pr = \frac{\upsilon}{\alpha}$ is the Prandtl number, $Sc = \frac{\upsilon}{D}$ is the Schmidt number, $A = \frac{c}{a}$ is a parameter that measures flow unsteadiness, $K = \frac{\upsilon x}{k_1 U_w}$ is the permeability parameter, $Gr = g\beta_T \frac{(T_w - T_\infty)x}{U_w^2}$ is the Grashof number, $Gc = g\beta_C \frac{(C_w - C_\infty)x}{U_w^2}$ is the modified Grashof number.

The quantities of physical interest are the local skin-friction coefficients C_f, local Nusselt number Nu_x, and the local Sherwood Sh_x, which are defined as follows:

$$\begin{aligned} \tau_w = \mu \left(\frac{\partial u}{\partial y}\right)_{y=0},\ C_f = \frac{\tau_w}{\rho U_w^2/2}, \quad & \frac{1}{2} C_f Re_x^{1/2} = -f''(0), \\ q_w = -k \left.\frac{\partial T}{\partial y}\right|_{y=0},\ Nu_x = \frac{q_w}{(T_w - T_\infty)}\left(\frac{x}{k}\right), \quad & Nu_x Re_x^{-1/2} = \theta'(0), \\ m_w = -\rho D \left.\frac{\partial C}{\partial y}\right|_{y=0},\ Sh_x = \frac{m_w}{(C_w - C_\infty)}\left(\frac{x}{\rho D}\right), \quad & Sh_x Re_x^{-1/2} = -\phi'(0). \end{aligned} \tag{2.12}$$

In this chapter as stated earlier, the system of equations (2.8 - 2.11) are solved using the spectral relaxation method (SRM), the spectral local linearization method (SLLM) and the spectral quasilinearization method (SQLM) for the purpose of determining if the methods are comparable over a couple of varied parameters. At the end of this, the objective is to validate that the methods are indeed efficient, easy to implement and give good accuracy.

2.3 Problem Solution Techniques

In this section, the spectral relaxation method (SRM), the spectral local linearization method (SLLM) and the spectral quasi-linearization method (SQLM) are all employed in obtaining solution to the system of equations (2.8 - 2.11). In the following subsections, a detailed description of the steps taken in coming up with their respective algorithms is given.

2.3.1 Spectral Relaxation Method (SRM)

In this subsection, the application of the SRM to the system of equations (2.8 - 2.11) is presented.

The main idea behind this approach is decoupling system (2.8 - 2.11) and applying chebychev pseudo-spectral collocation method to integrate the decoupled system obtained.
To apply the SRM on (2.8 - 2.10), we let $f^{'}(\eta) = g(\eta)$ to reduce the order of equation (2.8) and the nonlinear coupled system of equations becomes;

$$\begin{aligned} f^{'} &= g, \\ g^{''} + fg^{'} - g^2 - Kg - A\left(g + \frac{\eta}{2}g^{'}\right) + Gr\theta + Gc\phi &= 0, \\ \frac{1}{Pr}\theta^{''} - g\theta + f\theta^{'} - A\left(\theta + \frac{\eta}{2}\theta^{'}\right) &= 0, \\ \frac{1}{Sc}\phi^{''} - g\phi + f\phi^{'} - A\left(\phi + \frac{\eta}{2}\phi^{'}\right) - \gamma\phi &= 0. \end{aligned} \tag{2.13}$$

On (2.13), the concept of the Gauss-Seidel relaxation technique is applied to decouple the reduced system to obtain:

$$f^{'}_{r+1} = g_r, \tag{2.14}$$

$$g_{r+1}^{''} + f_r g_{r+1}^{'} - (A+K)\, g_{r+1} + \frac{\eta}{2} g_{r+1}^{'} = g_r^2 - Gr\theta_r - Gc\phi_r, \tag{2.15}$$

$$\frac{1}{Pr}\theta_{r+1}^{''} - g_{r+1}\theta_{r+1} + f_{r+1}\theta_{r+1}^{'} - A\left(\theta_{r+1} + \frac{\eta}{2}\theta_{r+1}^{'}\right) = 0, \tag{2.16}$$

$$\frac{1}{Sc}\phi_{r+1}^{''} - g_{r+1}\phi_{r+1} + f_{r+1}\phi_{r+1}^{'} - (A+\gamma)\,\phi_{r+1} - A\frac{\eta}{2}\phi_{r+1}^{'} = 0, \tag{2.17}$$

with boundary conditions;

$$\begin{aligned} f_{r+1}(0) = fw,\ g_{r+1}(0) = 1,\ g_{r+1}(\infty) = 0,\ \theta_{r+1}(0) = 1, \\ \theta_{r+1}(\infty) = 0,\ \phi_{r+1}(0) = 1,\ \phi_{r+1}(\infty) = 0, \end{aligned} \tag{2.18}$$

where terms containing $r+1-$subscripts denote current approximations while terms containing $r-$subscripts denote previous approximations.

A compact form of (2.14-2.17) is written as

$$\begin{aligned} f_{r+1}^{'} = g_r, \qquad f_{r+1} = f_w, \\ g_{r+1}^{''} + a_{1,r} g_{r+1}^{'} - a_{2,r} g_{r+1} &= a_{3,r}, \\ \left(\frac{1}{Pr}\right)\theta_{r+1}^{''} + b_{1,r}\theta_{r+1}^{'} - b_{2,r}\theta_{r+1} - b_{3,r}\theta_{r+1} &= 0, \\ \left(\frac{1}{Sc}\right)\phi_{r+1}^{''} + c_{1,r}\phi_{r+1}^{'} - c_{2,r}\phi_{r+1} - c_{3,r}\phi_{r+1} &= 0, \end{aligned} \tag{2.19}$$

where

$$\begin{aligned} a_{1,r} = f_r - \frac{A\eta}{2}, \quad a_{2,r} = K + A, \quad a_{3,r} = g_r^2 - Gr\theta_r - Gc\phi_r \\ b_{1,r} = f_r - \frac{A\eta}{2}, \quad b_{2,r} = g_r, \quad b_{3,r} = A \\ c_{1,r} = f_r - \frac{A\eta}{2}, \quad c_{2,r} = g_r, \quad c_{3,r} = A + \gamma. \end{aligned} \tag{2.20}$$

At this point, the Chebyshev pseudo-spectral collocation technique is employed to integrate system (2.19). The pseudo-spectral collocation technique (described in Hussaini and Zang (1987), Trefethen (2000)) is based on Chebyshev polynomials that are defined on the domain $[-1, 1]$ in the $x-$direction in the form:

$$T_k(x) = \cos\left[k\cos^{-1}(x)\right]. \tag{2.21}$$

The grid (collocation) points are based on Chebyshev-Gauss-Lobatto points that are defined by:

$$x_j = cos\left(\frac{\pi j}{N_x}\right), \quad -1 \le x \le 1, \quad j = 0, 1, 2, 3, \ldots, N_x. \tag{2.22}$$

.

For the spectral method to be applied successfully, the physical domain on which the governing system of equations (2.8 - 2.11) is defined $[0, \infty)$ is transformed to $[-1, 1]$ using the transformation

$$x = \frac{2\eta}{L} - 1, \quad -1 \leq x \leq 1, \tag{2.23}$$

where the interval $[0, \infty)$ is replaced by $[0, L]$ and L is a scaling parameter assumed to be large.

As described by Trefethen (2000), the basic idea of the spectral method is to approximate unknown functions in system (2.19) (the functions at $r + 1$)in the full domain using an interpolating higher order Lagrange polynomial at the given collocation points. Functions are approximated using the Lagrange interpolating polynomials in the form shown below.

$$f(x) \approx \sum_{k=0}^{N_x} f_k L_k(x), \tag{2.24}$$

where L_k are the Lagrange interpolating polynomials,

$$l_k(x_j) = \begin{cases} 1, & k = j, \\ 0, & k \neq j. \end{cases} \tag{2.25}$$

Interpolating functions are differentiated to approximate derivatives of the function $f(x)$ as shown below.

$$\begin{aligned} f^{'}(x) &= \sum_{k=0}^{N_x} f_k L_k^{'}(x), \\ f^{''}(x) &= \sum_{k=0}^{N_x} f_k L_k^{''}(x), \\ &\vdots \\ f^{n}(x) &= \sum_{k=0}^{N_x} f_k L_k^{n}(x), \quad n = 1, 2, \cdots . \end{aligned} \tag{2.26}$$

Functions and their derivatives are evaluated by collocating at selected grid (collocation)

points in the forms shown below.

$$\begin{aligned} f^{'}(x_j) &= \sum_{k=0}^{N_x} f_k L_k^{'}(x) = \sum_{k=0}^{N_x} D_{jk} f_k, \\ f^{''}(x_j) &= \sum_{k=0}^{N_x} f_k L_k^{''}(x) = \sum_{k=0}^{N_x} D_{jk}^2 f_k, \\ &\vdots \\ f^{n}(x_j) &= \sum_{k=0}^{N_x} f_k L_k^{n}(x) = \sum_{k=0}^{N_x} D_{jk}^n f_k, \quad n = 1, 2, \cdots, \end{aligned} \tag{2.27}$$

where

$$D_{jk} f_k = L_k^{'}(x_j),\ D_{jk}^2 f_k = L_k^{''}(x_j),\ D_{jk}^n f_k = L_k^{n}(x_j), \quad n = 1, 2, \cdots. \tag{2.28}$$

D is the differentiation matrix of size $(N_x + 1) \times (N_x + 1)$. The entries of matrix D are computed as described below. Chebyshev differentiation matrix: For each $N_x \geq 1$, let row and columns of the Chebyshev differentiation matrix D be indexed from 0 to N_x. As described by Trefethen (2000), the entries are of the forms:

$$\begin{aligned} (D)_{00} &= \frac{2N_x^2 + 1}{6}, \quad (D)_{N_x N_x} = -\frac{2N_x^2 + 1}{6}, \\ (D)_{jj} &= -\frac{x_j}{2\left(1 - x_j^2\right)}, \quad j = 1, 2, \ldots N_x - 1, \\ (D)_{ij} &= -\frac{c_i\,(-1)^{i+j}}{c_j\,(x_i - x_j)}, \quad i \neq j \quad i, j = 1, 2, \ldots N_x - 1, \end{aligned} \tag{2.29}$$

where

$$c_i = \begin{cases} 2 & r = 0 \text{ or } N_x, \\ 1 & \textit{otherwise.} \end{cases} \tag{2.30}$$

The differentiation matrix $\mathbf{D} = \frac{2D}{L}$ is used to approximate derivatives of unknown variables in our system (2.19) and the new system is obtained:

$$\mathbf{D}\mathbf{F}_{r+1} = \mathbf{g}_r, \tag{2.31}$$

$$\left[\mathbf{D}^2 + \mathbf{diag}\left[\mathbf{a}_{1,r}\right]\mathbf{D} - \mathbf{a}_{2,r}\mathbf{I}\right]\mathbf{G}_{r+1} = \mathbf{a}_{3,r}, \tag{2.32}$$

$$\left[\frac{1}{Pr}\mathbf{D}^2 + \mathbf{diag}\left[\mathbf{b}_{1,r}\right]\mathbf{D} - \mathbf{diag}\left[\mathbf{b}_{2,r}\right] - \mathbf{b}_{3,r}\mathbf{I}\right]\mathbf{\Theta_{r+1}} = 0, \tag{2.33}$$

$$\left[\frac{1}{Sc}\mathbf{D}^2 + \mathbf{diag}\left[\mathbf{c}_{1,r}\right]\mathbf{D} - \mathbf{diag}\left[\mathbf{c}_{2,r}\right] - \mathbf{c}_{3,r}\mathbf{I}\right]\mathbf{\Phi}_{r+1} = 0, \tag{2.34}$$

with boundary conditions

$$f_{r+1}(x_{N_x}) = fw,\ g_{r+1}(x_{N_x}) = 1,\quad g_{r+1}(x_0) = 0,\quad \Theta_{r+1}(x_{N_x}) = 1,\quad \Theta_{r+1}(x_0) = 0,\quad \Phi_{r+1}(x_{N_x}) = 1,\quad \Phi_{r+1}(x_0) = 0. \tag{2.35}$$

The system (2.31 − 2.34) can be represented in a compact form as:

$$\mathbf{A}_1\mathbf{F}_{r+1} = \mathbf{B}_1, \tag{2.36}$$

$$\mathbf{A}_2\mathbf{G}_{r+1} = \mathbf{B}_2, \tag{2.37}$$

$$\mathbf{A}_3\mathbf{\Theta}_{r+1} = \mathbf{B}_3, \tag{2.38}$$

$$\mathbf{A}_4\mathbf{\Phi}_{r+1} = \mathbf{B}_4, \tag{2.39}$$

where

$$\mathbf{A}_1 = \mathbf{D},\ \mathbf{B}_1 = \mathbf{g}_r, \tag{2.40}$$

$$\mathbf{A}_2 = \mathbf{D}^2 + \mathbf{diag}\left[\mathbf{a}_{1,r}\right]\mathbf{D} - \mathbf{a}_{2,r}\mathbf{I},\ \mathbf{B}_2 = \mathbf{a}_{3,r}, \tag{2.41}$$

$$\mathbf{A}_3 = \frac{1}{Pr}\mathbf{D}^2 + \mathbf{diag}\left[\mathbf{b}_{1,r}\right]\mathbf{D} - \mathbf{diag}\left[\mathbf{b}_{2,r}\right] - \mathbf{b}_{3,r}\mathbf{I},\ \mathbf{B}_3 = \mathbf{0}, \tag{2.42}$$

$$\mathbf{A}_4 = \frac{1}{Sc}\mathbf{D}^2 + \mathbf{diag}\left[\mathbf{c}_{1,r}\right]\mathbf{D} - \mathbf{diag}\left[\mathbf{c}_{2,r}\right] - \mathbf{c}_{3,r}\mathbf{I},\ \mathbf{B}_4 = \mathbf{0}, \tag{2.43}$$

$$\mathbf{diag}[\mathbf{a}_{1,r}] = \begin{bmatrix} a_{1,r}(x_0) & & & \\ & a_{1,r}(x_1) & & \\ & & \ddots & \\ & & & a_{1,r}(x_{N_x}) \end{bmatrix},\quad \mathbf{diag}[\mathbf{b}_{1,r}] = \begin{bmatrix} b_{1,r}(x_0) & & & \\ & b_{1,r}(x_1) & & \\ & & \ddots & \\ & & & b_{1,r}(x_{N_x}) \end{bmatrix},$$

$$\mathbf{diag}[\mathbf{c}_{1,r}] = \begin{bmatrix} c_{1,r}(x_0) & & & \\ & c_{1,r}(x_1) & & \\ & & \ddots & \\ & & & c_{1,r}(x_{N_x}) \end{bmatrix},\quad \mathbf{diag}[\mathbf{b}_{2,r}] = \begin{bmatrix} b_{2,r}(x_0) & & & \\ & b_{2,r}(x_1) & & \\ & & \ddots & \\ & & & b_{2,r}(x_{N_x}) \end{bmatrix},$$

$$\mathbf{diag}[\mathbf{c}_{2,r}] = \begin{bmatrix} c_{2,r}(x_0) & & & \\ & c_{2,r}(x_1) & & \\ & & \ddots & \\ & & & c_{2,r}(x_{N_x}) \end{bmatrix},\quad \mathbf{a}_{2,r}\mathbf{I} = \begin{bmatrix} a_{2,r}(x_0) & & & \\ & a_{2,r}(x_1) & & \\ & & \ddots & \\ & & & a_{2,r}(x_{N_x}) \end{bmatrix},$$

$$\mathbf{b}_{3,r}\mathbf{I} = \begin{bmatrix} b_{3,r}(x_0) & & & \\ & b_{3,r}(x_1) & & \\ & & \ddots & \\ & & & b_{3,r}(x_{N_x}) \end{bmatrix},\quad \mathbf{c}_{3,r}\mathbf{I} = \begin{bmatrix} c_{3,r}(x_0) & & & \\ & c_{3,r}(x_1) & & \\ & & \ddots & \\ & & & c_{3,r}(x_{N_x}) \end{bmatrix}.$$

$\mathbf{F}_{r+1} = [f(x_0), f(x_1), \ldots, f(x_{N_x}),]^T$, $\mathbf{G}_{r+1} = [g(g_0), g(x_1), \ldots, g(x_{N_x})]^T$, $\mathbf{\Theta}_{r+1} = [\theta(x_0), \theta(x_1), \ldots, \theta(x_{N_x})),^T$ and $\mathbf{\Phi}_{r+1} = [\phi(x_0), \phi(x_1), \ldots, \phi(x_{N_x})),^T$ are vectors of sizes $(N_x+1)\times 1$. $\mathbf{0}$ is a vector of size $(N_x+1)\times 1$ and $\mathbf{I}$ is an identity matrix of size $(N_x+1)\times(N_x+1)$.

To illustrate how the boundary conditions are implemented on the system, the following is given:

$$\begin{aligned}\mathbf{M}_1\mathbf{P}_1 &= \mathbf{Q}_1,\\ \mathbf{M}_2\mathbf{P}_2 &= \mathbf{Q}_2,\\ \mathbf{M}_3\mathbf{P}_3 &= \mathbf{Q}_3,\\ \mathbf{M}_4\mathbf{P}_4 &= \mathbf{Q}_4,\end{aligned}$$

where

$$\mathbf{M}_1=\begin{bmatrix}\\ \mathbf{A}_1\\ \\ \hline 0 & 0 & \cdots & 0 & 1\end{bmatrix},\quad \mathbf{P}_1=\begin{bmatrix}f_{r+1,0}\\ f_{r+1,1}\\ \vdots\\ \vdots\\ \hline f_{r+1,N}\end{bmatrix},\quad \mathbf{Q}_1=\begin{bmatrix}\\ \mathbf{B}_1\\ \\ \hline fw\end{bmatrix},$$

$$\mathbf{M}_2=\begin{bmatrix}1 & 0 & \cdots & 0 & 0\\ \hline \\ \mathbf{A}_2\\ \\ \hline 0 & 0 & \cdots & 0 & 1\end{bmatrix},\quad \mathbf{P}_2=\begin{bmatrix}g_{r+1,0}\\ g_{r+1,1}\\ \vdots\\ \vdots\\ \hline g_{r+1,N}\end{bmatrix},\quad \mathbf{Q}_2=\begin{bmatrix}0\\ \hline \\ \mathbf{B}_2\\ \\ \hline 1\end{bmatrix},$$

$$\mathbf{M}_3=\begin{bmatrix}1 & 0 & \cdots & 0 & 0\\ \hline \\ \mathbf{A}_3\\ \\ \hline 0 & 0 & \cdots & 0 & 1\end{bmatrix},\quad \mathbf{P}_3=\begin{bmatrix}\theta_{r+1,0}\\ \hline \theta_{r+1,1}\\ \vdots\\ \vdots\\ \hline \theta_{r+1,N}\end{bmatrix},\quad \mathbf{Q}_3=\begin{bmatrix}0\\ \hline \\ \mathbf{B}_3\\ \\ \hline 1\end{bmatrix},$$

$$\mathbf{M}_4=\begin{bmatrix} 1 & 0 & \cdots & 0 & 0 \\ \hline & & & & \\ & & \mathbf{A}_4 & & \\ & & & & \\ \hline 0 & 0 & \cdots & 0 & 1 \end{bmatrix}, \qquad \mathbf{P}_4=\begin{bmatrix} \phi_{r+1,0} \\ \hline \phi_{r+1,1} \\ \vdots \\ \vdots \\ \hline \phi_{r+1,N} \end{bmatrix}, \qquad \mathbf{Q}_4=\begin{bmatrix} 0 \\ \hline \\ \mathbf{B}_4 \\ \\ \hline 1 \end{bmatrix}.$$

2.3.2 Spectral Local Linearization Method

In this subsection, the application of the SLLM on the system of equations (2.8 - 2.11) is shown.

The main idea behind this approach is identifying nonlinear terms of the same function and its derivative in each of the equations of the system (2.8 - 2.11), linearizing and decoupling the system (2.8 - 2.11) and applying chebychev pseudo-spectral collocation method to integrate the decoupled system obtained.
To apply the SLLM on (2.8 - 2.10), set $f^{'}(\eta) = g(\eta)$ to reduce the order of equation (2.8) and the nonlinear coupled system of equations becomes;

$$\begin{aligned} f^{'} &= g, \\ g^{''} + fg^{'} - g^2 - Kg - A\left(g + \frac{\eta}{2}g^{'}\right) + Gr\theta + Gc\phi &= 0, \\ \frac{1}{Pr}\theta^{''} - g\theta + f\theta^{'} - A(\theta + \frac{\eta}{2}\theta^{'}) &= 0, \\ \frac{1}{Sc}\phi^{''} - g\phi + f\phi^{'} - A(\phi + \frac{\eta}{2}\phi^{'}) - \gamma\phi &= 0. \end{aligned} \tag{2.44}$$

The nonlinear term in the system (2.44) is g^2 and it is linearized using Taylor series expansion as shown below

$$\begin{aligned} g_{r+1}^2 &= g_r^2 + 2g_r\left(g_{r+1} - g_r\right) \\ &= 2g_r g_{r+1}^2 - g_r^2, \end{aligned} \tag{2.45}$$

where the terms containing $r+1-$subscripts denote current approximations and terms containing $r-$subscripts denote previous approximations. Equation (2.45) is substituted into

(2.44) and the nonlinear system is decoupled using the concept of the Gauss-Seidel relaxation method to obtain:

$$f'_{r+1} = g_{r+1}, \tag{2.46}$$

$$g''_{r+1} + f_r g'_{r+1} - (A+K)g_{r+1} + \frac{A\eta}{2}g'_{r+1} - 2g_r g_{r+1} = -g_r^2 - Gr\theta_r - Gc\phi_r, \tag{2.47}$$

$$\frac{1}{Pr}\theta''_{r+1} - g_r\theta_{r+1} + f_r\theta'_{r+1} - A(\theta_{r+1} + \frac{\eta}{2}\theta'_{r+1}) = 0, \tag{2.48}$$

$$\frac{1}{Sc}\phi''_{r+1} - g_r\phi_{r+1} + f_r\phi'_{r+1} - (A+\gamma)\phi_{r+1} - A\frac{\eta}{2}\phi'_{r+1} = 0, \tag{2.49}$$

with boundary conditions:

$$\begin{aligned} f_{r+1} = fw, \quad g_{r+1}(0) = 1, \quad g_{r+1}(\infty) = 0, \quad \theta_{r+1}(0) = 1, \\ \theta_{r+1}(\infty) = 0, \quad \phi_{r+1}(0) = 1, \quad \phi_{r+1}(\infty) = 0, \end{aligned} \tag{2.50}$$

where the terms at r denote terms known from previous iteration while the terms at $r+1$ denote unknown terms at current iteration.

A compact form of (2.46 - 2.49) is written as:

$$\begin{aligned} f'_{r+1} &= g_r, \\ g''_{r+1} + a_{1,r}g'_{r+1} - a_{2,r}g_{r+1} - a_{3,r}g_{r+1} &= a_{4,r}, \\ \left(\frac{1}{Pr}\right)\theta''_{r+1} + b_{1,r}\theta'_{r+1} - b_{2,r}\theta_{r+1} - b_{3,r}\theta_{r+1} &= 0, \\ \left(\frac{1}{Sc}\right)\phi''_{r+1} + c_{1,r}\phi'_{r+1} - c_{2,r}\phi_{r+1} - c_{3,r}\phi_{r+1} &= 0, \end{aligned} \tag{2.51}$$

where

$$\begin{aligned} a_{1,r} = f_r - \frac{A\eta}{2}, \quad a_{2,r} = K + A, \quad a_{4,r} = -g_r^2 - Gr\theta_r - Gc\phi_r, \\ a_{3,r} = 2g_r, \quad b_{1,r} = f_r - \frac{A\eta}{2}, \quad b_{2,r} = g_r, \quad b_{3,r} = A, \\ c_{1,r} = f_r - \frac{A\eta}{2}, \quad c_{2,r} = g_r, \quad c_{3,r} = A + \gamma. \end{aligned} \tag{2.52}$$

As was discussed earlier, Chebyshev spectral collocation method is applied on the system (2.51) where the differentiation matrix $\mathbf{D}$ (where $\mathbf{D} = \frac{2D}{L}$) is used to approximate derivatives of unknown variables in the system (2.51) and a new system is obtained:

$$\mathbf{DF}_{r+1} = \mathbf{g}_r, \tag{2.53}$$

$$\left[\mathbf{D}^2 + \mathbf{diag}\left[\mathbf{a}_{1,r}\right]\mathbf{D} - \mathbf{a}_{2,r}\mathbf{I} - \mathbf{diag}\left[\mathbf{a}_{3,r}\right]\right]\mathbf{G}_{r+1} = \mathbf{a}_{3,r}, \tag{2.54}$$

$$\left[\frac{1}{Pr}\mathbf{D}^2 + \mathbf{diag}\left[\mathbf{b}_{1,r}\right]\mathbf{D} - \mathbf{diag}\left[\mathbf{b}_{2,r}\right] - \mathbf{b}_{3,r}\mathbf{I}\right]\mathbf{\Theta}_{r+1} = \mathbf{0}, \tag{2.55}$$

$$\left[\frac{1}{Sc}\mathbf{D}^2 + \mathbf{diag}\left[\mathbf{c}_{1,r}\right]\mathbf{D} - \mathbf{diag}\left[\mathbf{c}_{2,r}\right] - \mathbf{c}_{3,r}\mathbf{I}\right]\mathbf{\Phi}_{r+1} = \mathbf{0}, \tag{2.56}$$

with corresponding boundary conditions

$$\begin{aligned} g_{r+1}\left(x_{N_x}\right) = 1, \quad g_{r+1}\left(x_0\right) = 0, \quad \theta_{r+1}\left(x_{N_x}\right) = 1, \quad \theta_{r+1}\left(x_0\right) = 0, \\ \phi_{r+1}\left(x_{N_x}\right) = 1, \quad \phi_{r+1}\left(x_0\right) = 0, \quad f_{r+1}\left(x_{N_x}\right). \end{aligned} \tag{2.57}$$

The system (2.53 - 2.56) can be represented in a more simplified form as:

$$\begin{aligned} \mathbf{A}_1\mathbf{F}_{r+1} &= \mathbf{B}_1, \\ \mathbf{A}_2\mathbf{G}_{r+1} &= \mathbf{B}_2, \\ \mathbf{A}_3\mathbf{\Theta}_{r+1} &= \mathbf{B}_3, \\ \mathbf{A}_4\mathbf{\Phi}_{r+1} &= \mathbf{B}_4, \end{aligned} \tag{2.58}$$

where

$$\begin{aligned} \mathbf{A}_1 &= \mathbf{D}, \mathbf{B}_1 = \mathbf{g}_r, \\ \mathbf{A}_2 &= \mathbf{D}^2 + \mathbf{diag}\left[\mathbf{a}_{1,r}\right]\mathbf{D} - \mathbf{a}_{2,r}\mathbf{I} - \mathbf{diag}\left[\mathbf{a}_{3,r}\right], \mathbf{B}_2 = \mathbf{a}_{4,r}, \\ \mathbf{A}_3 &= \frac{1}{Pr}\mathbf{D}^2 + \mathbf{diag}\left[\mathbf{b}_{1,r}\right]\mathbf{D} - \mathbf{diag}\left[\mathbf{b}_{2,r}\right] - \mathbf{b}_{3,r}\mathbf{I}, \mathbf{B}_3 = \mathbf{0}, \\ \mathbf{A}_4 &= \frac{1}{Sc}\mathbf{D}^2 + \mathbf{diag}\left[\mathbf{c}_{1,r}\right]\mathbf{D} - \mathbf{diag}\left[\mathbf{c}_{2,r}\right] - \mathbf{c}_{3,r}\mathbf{I}, \mathbf{B}_4 = \mathbf{0}. \end{aligned}$$

The boundary conditions are implemented on the system in the same procedure as shown in the previous subsection.

2.3.3 Spectral Quasi-linearization Method

In this subsection, the SQLM iteration scheme for (2.8 - 2.11) is developed.

The main idea behind this approach is identifying multiple nonlinear terms from the system (2.8 - 2.11), linearizing the terms and applying Chebychev pseudo-spectral collocation method

to integrate the coupled system obtained.

To apply the SQLM to (2.8 - 2.10), the univariate and multivariate nonlinear terms are identified in the system which are $f^{'2}$, $ff^{'}$, $f^{'}\theta$, $f\theta^{'}$, $f^{'}\phi$ and $f\phi^{'}$. Apart from the observation that the SQLM solves a system as coupled while the SLLM solves as decoupled, the SLLM only linearizes nonlinear terms that contain the dominant function and its' derivatives in a particular equation (for example g^2) while the SQLM linearizes both univariate and multivariate nonlinear terms. The linearization of the multivariate terms are shown below in the forms:

$$\begin{aligned} f^{'2} &= f_r^{'2} + 2f_r^{'}\left(f_{r+1}^{'} - f_r^{'}\right) \\ &= 2f_r^{'}f_{r+1}^{'2} - f_r^{'2}. \end{aligned} \tag{2.59}$$

,

$$\begin{aligned} ff^{'} &= f_r f_r^{'} + f_r\left(f_{r+1}^{'} - f_r^{'}\right) + f_r^{'}\left(f_{r+1} - f_r\right) \\ &= f_r f_{r+1}^{'} + f_r^{'} f_{r+1} - f_r f_r^{'}. \end{aligned} \tag{2.60}$$

,

$$\begin{aligned} f\theta^{'} &= f_r\theta_r^{'} + \theta_r^{'}\left(f_{r+1} - f_r\right) + f_r\left(\theta_{r+1} - \theta_r\right) \\ &= f_r\theta_{r+1}^{'} + \theta_r^{'} f_{r+1} - f_r\theta_r^{'}. \end{aligned} \tag{2.61}$$

$$\begin{aligned} f\phi^{'} &= f_r\phi_r^{'} + \phi_r^{'}\left(f_{r+1} - f_r\right) + f_r\left(\phi_{r+1}^{'} - \phi_r^{'}\right) \\ &= f_r\phi_{r+1}^{'} + \phi_r^{'} f_{r+1} - f_r\phi_r^{'}. \end{aligned} \tag{2.62}$$

$$\begin{aligned} f^{'}\phi &= f_r^{'}\phi_r + \phi_r\left(f_{r+1}^{'} - f_r^{'}\right) + f_r^{'}\left(\phi_{r+1} - \phi_r\right) \\ &= f_r^{'}\phi_{r+1} + \phi_r f_{r+1}^{'} - f_r^{'}\phi_r. \end{aligned} \tag{2.63}$$

$$\begin{aligned} f^{'}\theta &= f_r^{'}\theta_r + \theta_r\left(f_{r+1}^{'} - f_r^{'}\right) + f_r^{'}\left(\theta_{r+1} - \theta_r\right) \\ &= f_r^{'}\theta_{r+1} + \theta_r f_{r+1}^{'} - f_r^{'}\theta_r. \end{aligned} \tag{2.64}$$

Solutions obtained in (2.59 - 2.64) are inserted into (2.8 - 2.10) and the following linear coupled system is obtained:

$$f_{r+1}^{'''} + \left(f_r - A\frac{\eta}{2}\right) f_r^{''} - \left(2f_r^{'} + A + K\right) f_{r+1}^{'} + f_r^{''} f_{r+1} + Gr\theta_{r+1} + Gc\phi_{r+1} = f_r f_r^{''} - f_r^{'2}, \tag{2.65}$$

$$\frac{1}{Pr}\theta^{''}_{r+1} + \left(f_r - A\frac{\eta}{2}\right)\theta^{'}_{r+1} - \left(f^{'}_r + A\right)\theta_{r+1} - f^{'}_{r+1}\theta_r + f_{r+1}\theta^{'}_r = f_r\theta^{'}_r - f^{'}_{r+1}\theta_r, \tag{2.66}$$

$$\frac{1}{Sc}\phi^{''}_{r+1} + \left(f_r - A\frac{\eta}{2}\right)\phi^{'}_{r+1} - \left(f^{'}_r + A + \gamma\right)\phi_{r+1} - f^{'}_{r+1}\phi_r + f_{r+1}\phi^{'}_r = f_r\phi^{'}_r - f^{'}_{r+1}\phi_r, \tag{2.67}$$

with boundary conditions;

$$f_{r+1}(0) = 1, f^{'}_{r+1}(0) = 1, f^{'}_{r+1}(\infty) = 0, \theta_{r+1}(0) = 1, \theta_{r+1}(\infty) = 0, \phi_{r+1}(0) = 1, \phi_{r+1}(\infty) = 0. \tag{2.68}$$

The system (2.65 - 2.67) is expressed in a compact form as:

$$\begin{aligned} f^{''''}_{r+1} + a_{1,r}f^{'''}_{r+1} - a_{2,r}f^{''}_{r+1} + a_{3,r}f^{'}_{r+1} + a_{4,r}f_{r+1} + Gr\theta_{r+1} + Gc\phi_{r+1} &= a_{5,r}, \\ \frac{1}{Pr}\theta^{''}_{r+1} + b_{1,r}\theta^{'}_{r+1} - b_{2,r}\theta_{r+1} - \theta^{'}f_{r+1} + \theta^{'}f_{r+1} &= b_{3,r}, \\ \frac{1}{Sc}\phi^{''}_{r+1} + c_{1,r}\phi^{'}_{r+1} - c_{2,r}\phi_{r+1} - \phi^{'}f_{r+1} + \phi^{'}f_{r+1} &= c_{3,r}. \end{aligned} \tag{2.69}$$

where

$$\begin{aligned} a_{1,r} = f_r + \frac{A\eta}{2}, \quad a_{2,r} = 2f^{'}_r + A, \quad a_{3,r} = f^{''}_r \\ a_{4,r} = f_r f^{''}_r - f^{'2}_r, \quad b_{1,r} = f_r + \frac{A\eta}{2}, \quad b_{2,r} = f^{'}_r + A \\ b_{3,r} = f_r\theta^{'}_r - f^{'}_r\theta_r \quad c_{1,r} = f_r + \frac{A\eta}{2}, \quad c_{2,r} = f^{'}_r + A + \gamma \\ c_{3,r} = f_r\phi^{'}_r - f^{'}_r\phi_r \end{aligned} \tag{2.70}$$

Spectral collocation is applied at this point using the differentiation matrix $\mathbf{D}$ to approximate derivatives of unknown variables in the system (2.69) and the new system of equations are obtained:

$$\begin{aligned} \mathbf{A}_{11}\mathbf{F}_{r+1} + \mathbf{A}_{12}\mathbf{\Theta}_{r+1} + \mathbf{A}_{13}\mathbf{\Phi}_{r+1} &= \mathbf{B}_1, \\ \mathbf{A}_{21}\mathbf{F}_{r+1} + \mathbf{A}_{22}\mathbf{\Theta}_{r+1} + \mathbf{A}_{23}\mathbf{\Phi}_{r+1} &= \mathbf{B}_2, \\ \mathbf{A}_{31}\mathbf{F}_{r+1} + \mathbf{A}_{32}\mathbf{\Theta}_{r+1} + \mathbf{A}_{33}\mathbf{\Phi}_{r+1} &= \mathbf{B}_3, \end{aligned} \tag{2.71}$$

where

$$\mathbf{A}_{11} = \mathbf{D}^3 + \mathbf{diag}\left(\mathbf{a}_{1,r}\right)\mathbf{D}^2 - \mathbf{diag}\left(2\mathbf{f}^{'}_r\right)\mathbf{D} - (K + A)\mathbf{D} + \mathbf{diag}\left(f^{''}_r\right), \tag{2.72}$$

$$\mathbf{A}_{12} = Gr\mathbf{I}, \quad \mathbf{A}_{13} = Gc\mathbf{I}, \tag{2.73}$$

$$\mathbf{A}_{22} = \frac{1}{Pr}\mathbf{D}^2 + \mathbf{diag}\left(\mathbf{b}_{1,r}\right)\mathbf{D} - \mathbf{diag}\left(\mathbf{f}^{'}_r\right) - A\mathbf{I}, \tag{2.74}$$

$$\mathbf{A}_{21} = \mathbf{diag}\left(\theta_r^{'}\right) - \mathbf{diag}\left(\theta_r\right)\mathbf{D}, \quad \mathbf{A}_{23} = \mathbf{0}, \tag{2.75}$$

$$\mathbf{A}_{33} = \frac{1}{Sc}\mathbf{D}^2 + \mathbf{diag}\left(\mathbf{c}_{1,r}\right)\mathbf{D} - \mathbf{diag}\left(\mathbf{f}_r^{'}\right) - (A+\gamma)\mathbf{I} \tag{2.76}$$

$$\mathbf{A}_{31} = \mathbf{diag}\left(\phi_r^{'}\right) - \mathbf{diag}\left(\phi_r\right)\mathbf{D}, \quad \mathbf{A}_{32} = \mathbf{0}. \tag{2.77}$$

$$\mathbf{B}_1 = \mathbf{c}_{1,r}, \quad \mathbf{B}_2 = \mathbf{c}_{2,r}, \quad \mathbf{B}_3 = \mathbf{c}_{3,r}. \tag{2.78}$$

with corresponding boundary conditions

$$\begin{aligned} f(x_{N_x-1}) = 1,\ f(x_{N_x}) = 1,\ f(x_0) = 0,\ \theta(x_{N_x}) = 1, \\ \theta(x_0) = 0,\ \phi(x_{N_x}) = 1,\ \phi(x_0) = 0. \end{aligned} \tag{2.79}$$

The system (2.71) is solved as a coupled matrix system as shown below.

$$\begin{bmatrix} \mathbf{A}_{11} & \mathbf{A}_{12} & \mathbf{A}_{13} \\ \mathbf{A}_{21} & \mathbf{A}_{22} & \mathbf{A}_{23} \\ \mathbf{A}_{31} & \mathbf{A}_{32} & \mathbf{A}_{33} \end{bmatrix} \times \begin{bmatrix} \mathbf{F}_{r+1} \\ \mathbf{\Theta}_{r+1} \\ \mathbf{\Phi}_{r+1} \end{bmatrix} = \begin{bmatrix} \mathbf{B}_1 \\ \mathbf{B}_2 \\ \mathbf{B}_3 \end{bmatrix},$$

The boundary conditions are imposed on the individual matrices as follows:

$$\mathbf{A}_{11} = \begin{bmatrix} \mathbf{D}_{0,0} & \mathbf{D}_{0,1} & \cdots & \mathbf{D}_{0,N-1} & \mathbf{D}_{0,N} \\ & & \mathbf{A}_{11} & & \\ \mathbf{D}_{N,0} & \mathbf{D}_{N,1} & \cdots & \mathbf{D}_{N,N-1} & \mathbf{D}_{N,N} \\ 0 & 0 & \cdots & 0 & 1 \end{bmatrix}, \quad \mathbf{A}_{12} = \begin{bmatrix} 0 & 0 & \cdots & 0 & 0 \\ & & \mathbf{A}_{12} & & \\ 0 & 0 & \cdots & 0 & 0 \\ 0 & 0 & \cdots & 0 & 0 \end{bmatrix},$$

$$\mathbf{A}_{13} = \begin{bmatrix} 0 & 0 & \cdots & 0 & 0 \\ & & \mathbf{A}_{13} & & \\ 0 & 0 & \cdots & 0 & 0 \\ 0 & 0 & \cdots & 0 & 0 \end{bmatrix},$$

$$\mathbf{A}_{21} = \begin{bmatrix} 0 & 0 & \cdots & 0 & 0 \\ & & \mathbf{A}_{21} & & \\ 0 & 0 & \cdots & 0 & 0 \end{bmatrix}, \quad \mathbf{A}_{22} = \begin{bmatrix} 1 & 0 & \cdots & 0 & 0 \\ & & \mathbf{A}_{22} & & \\ 0 & 0 & \cdots & 0 & 1 \end{bmatrix}, \quad \mathbf{A}_{23} = \begin{bmatrix} 0 & 0 & \cdots & 0 & 0 \\ & & \mathbf{A}_{23} & & \\ 0 & 0 & \cdots & 0 & 0 \end{bmatrix},$$

$$\mathbf{A}_{31}=\begin{bmatrix} 0 & 0 & \cdots & 0 & 0 \\ \hline & & \mathbf{A}_{31} & & \\ \hline 0 & 0 & \cdots & 0 & 0 \end{bmatrix}, \quad \mathbf{A}_{32}=\begin{bmatrix} 0 & 0 & \cdots & 0 & 0 \\ \hline & & \mathbf{A}_{32} & & \\ \hline 0 & 0 & \cdots & 0 & 0 \end{bmatrix}, \quad \mathbf{A}_{33}=\begin{bmatrix} 1 & 0 & \cdots & 0 & 0 \\ \hline & & \mathbf{A}_{33} & & \\ \hline 0 & 0 & \cdots & 0 & 1 \end{bmatrix},$$

$$\mathbf{F}_{r+1}=\begin{bmatrix} f_{r+1,0} \\ \hline \vdots \\ \hline f_{r+1,N-1} \\ \hline f_{r+1,N} \end{bmatrix}, \quad \mathbf{\Theta}_{r+1}=\begin{bmatrix} \theta_{r+1,0} \\ \hline \vdots \\ \vdots \\ \hline \theta_{r+1,N} \end{bmatrix}, \quad \mathbf{\Phi}_{r+1}=\begin{bmatrix} \phi_{r+1,0} \\ \hline \vdots \\ \vdots \\ \hline \phi_{r+1,N} \end{bmatrix}, \quad \mathbf{B}_1=\begin{bmatrix} 0 \\ \hline \mathbf{B}_1 \\ \hline 1 \\ \hline fw \end{bmatrix}, \quad \mathbf{B}_2=\begin{bmatrix} 0 \\ \hline \mathbf{B}_2 \\ \hline 1 \end{bmatrix},$$

$$\mathbf{B}_3=\begin{bmatrix} 0 \\ \hline \mathbf{B}_3 \\ \hline 1 \end{bmatrix}.$$

2.4 Results and Discussion

In this section, the numerical results obtained from (2.8, 2.9, 2.10 and 2.11) using the spectral relaxation method (SRM), the spectral local linearization method (SLLM) and the spectral quasilinearization method (SQLM) are presented. Results for the velocity, temperature and concentration profiles are displayed together with the local skin-friction coefficients C_f, local Nusselt number Nu_x, and the local Sherwood number Sh_x. The solutions obtained using the three techniques (SRM, SLLM & SQLM) were examined and compared to see if they converged to the same result. In the case where the three methods converged to the same result, the aim was to ascertain how well they compared against one other. To achieve this, the following variations were put into consideration;

(i) Number of iterations taken to achieve convergence,

(ii) Effect of increasing the number of collocation points (N),

(iii) Effect of increasing the number of iterations,

(iv) Effect of increasing the domain truncation (L).

For the purpose of this study, parameters used in the system of ordinary differential equations (2.8-2.11) were assigned specific values except where stated otherwise. The value of the Prandtl number used is the value assigned to water which is $Pr = 1$. The Schmidt number chosen which is close to the value assigned to Carbon dioxide (Sc=0.94) is $Sc = 1$. The unsteadiness parameter is set to be A = 1. The chemical parameter is set to $\gamma = 1$. The Grashof number and the modified Grashof number are both fixed at $Gr = Gc = 1$. The suction parameter is set to be $fw = 1$. The permeability parameter is fixed at $K = 2$. Unless where varied, the value of the number of collocation points used was $N = 100$ and the domain truncation $L = 20$. All results presented in tabular and graphical forms were obtained at these values unless where specified.

All the three methods (SRM, SLLM & SQLM) were used in generating solutions by starting with an initial approximation. The initial approximation was chosen as a function that satisfied all the given boundary conditions (2.11). This approximation is referred to as an initial guess. The initial guess was used to generate the next iteration and the process carried on iteratively. The initial approximation that satisfied all the boundary conditions (2.11) were:

$$f_0 = f_w + 1 - \exp^{-\eta}, \quad g_0 = \theta_0 = \phi_0 = \exp^{-\eta}. \tag{2.80}$$

Tables 2.1, 2.2 and 2.3 presents the convergence of the solutions obtained for the skin friction, Nusselt number and Sherwood number when applying the SRM, SLLM and the SQLM, respectively. The aim of these tables showing convergence of the three numerical methods was to show the number of iterations it took for the solutions to converge to results that are consistent to at least 8 decimal digits. The results displayed are the results of the Skin friction $f''(0)$, the Nusselt number $\theta'(0)$ and the Sherwood number $\phi'(0)$.

Table 2.1: Convergence of solutions obtained using the SRM, SLLM and SQLM for the skin friction $-f''(0)$

	SQLM	SRM	SLLM
iterations	-f''(0)	-f''(0)	-f''(0)
1	1.87637592	2.06242210	1.93278339
2	1.90741596	1.87885708	1.90543381
3	1.90764678	1.91323759	1.90784674
4	1.90764682	1.90655959	1.90762866
5	1.90764681	1.90785868	1.90764846
6	1.90764681	1.90760552	1.90764666
7	1.90764681	1.90765486	1.90764683
8	1.90764681	1.90764524	1.90764681
9	1.90764681	1.90764712	1.90764681
10	1.90764681	1.90764675	1.90764681
11	1.90764681	1.90764683	1.90764681
12	1.90764681	1.90764681	1.90764681
⋮			⋮
20	1.90764681	1.90764681	1.90764681

Table 2.2: Convergence of solutions obtained using the SRM, SLLM and SQLM for the Nusselt number $-\theta^{'}(0)$

	SQLM	SRM	SLLM
iterations	$-\theta^{'}(0)$	$-\theta^{'}(0)$	$-\theta^{'}(0)$
1	1.84077855	2.06242210	1.93278339
2	1.87122388	1.84975171	1.86699928
3	1.87149678	1.87551005	1.87191349
4	1.87149682	1.87070813	1.87145908
5	1.87149682	1.87165023	1.87150025
6	1.87149682	1.87146691	1.87149651
7	1.87149682	1.87150265	1.87149685
8	1.87149682	1.87149568	1.87149682
9	1.87149682	1.87149704	1.87149682
10	1.87149682	1.87149678	1.87149682
11	1.87149682	1.87149683	1.87149682
12	1.87149682	1.87149682	1.87149682
⋮			⋮
20	1.87149682	1.87149682	1.87149682

Table 2.3: Convergence of solutions obtained using the SRM, SLLM and SQLM for the Sherwood number $-\phi^{'}(0)$

	SQLM	SRM	SLLM
iterations	-$\phi^{'}(0)$	-$\phi^{'}(0)$	-$\phi^{'}(0)$
1	2.19726299	2.29029241	2.29029241
2	2.22652292	2.21242179	2.22388003
3	2.22665592	2.22929246	2.22691117
4	2.22665592	2.22613916	2.22663283
5	2.22665592	2.22675644	2.22665802
6	2.22665592	2.22663633	2.22665573
7	2.22665592	2.22665974	2.22665594
8	2.22665592	2.22665518	2.22665592
9	2.22665592	2.22665607	2.22665592
10	2.22665592	2.22665590	2.22665592
11	2.22665592	2.22665593	2.22665592
12	2.22665592	2.22665592	2.22665592
⋮			⋮
20	2.22665592	2.22665592	2.22665592

Table 2.4: Computational time used by the SRM, SLLM and SQLM in obtaining the skin friction $-f^{''}(0)$, the Nusselt number $-\theta^{'}(0)$ and the Sherwood number $-\phi^{'}(0)$ after 20 iterations

	SQLM	SRM	SLLM
Time (Sec)	0.823061	0.56341	0.713155

It can be observed from the data in Table 2.1 and Table 2.2 that the SQLM converges fastest after 4 iterations while it takes 8 iterations for the SLLM and 12 iterations for the SRM to converge to a consistent solution.

As shown in Table 2.3, the SQLM converges very quickly at the 2^{nd} iteration while the SLLM converges after 8 iterations and the SRM converges after 12 iterations. Clearly, what this means is that an increase in the number of iterations used improves the accuracy until convergence is attained. That point is said to be a "saturation" point where an increase in number of iterations will only increase computational time and not make any positive significance in the accuracy of the solution. When convergence is attained for each method, it can be seen that the results are in excellent agreement with each other. Table 2.4 gives the computational time in generating the numerical solutions presented in Tables 2.1, 2.2 and 2.3. It is observed that the three methods are computationally efficient (in terms of speed) as the three methods take less than a second to generate solutions.

To further verify the results obtained using these methods, the solutions obtained using the SRM, SLLM and SQLM are validated against solutions obtained by other known numerical methods. Chamkha et al. (2010) applied a fourth-order Runge-Kutta scheme with the shooting method to obtain solutions presented in Table 2.5. The influences of the parameters on the dimensionless system are studied in that research as well. Sharidan et al. (2006) studied the same problem but without the concentration profile using the Keller-box method. Table 2.5 shows solution of Skin friction coefficient $-f''(0)$ obtained when $fw = Gr = Gc = K = 0$ and A at 0.8 and 1.2. In this chapter, the SRM, SLLM, and SQLM were applied and the obtained solutions were found to match the solutions obtained by Chamkha et al. (2010) and Sharidan et al. (2006).

Table 2.5: Comparison of $-f''(0)$ with those reported by Chamkha et al. (2010) and Sharidan et al. (2006)

A	Chamkha et al. (2010)	Sharidan et al. (2006)	Present work
0.8	1.261512	1.261042	1.26104261
1.2	1.378052	1.377722	1.37772391

As shown in Table 2.5, it is observed that the three solutions are in good agreement to three decimal places while the result obtained in this study and that of Sharidan et al. (2006) agree to the six decimal places shown in their reported result. This gives confidence that the SRM,

SLLM and SQLM results are valid.

Figures 2.1 – 2.9 show the effect of the number of collocation points, different values of domain truncation and number of iterations on the accuracy of the solution. Accuracy here is determined using the infinity norm of the residual error. The residual error is calculated by inserting approximate solution obtained back into the original system of equations (2.8 - 2.10). The residual error for the SRM, SLLM and the SQLM is hence represented as:

$$\begin{aligned} Res(\mathbf{f}) &= \mathbf{f}''' + \mathbf{f}\mathbf{f}'' - \left(\mathbf{f}''\right)^2 - A\left(\mathbf{f}' + \frac{\eta}{2}\mathbf{f}''\right) + Gr\theta + Gc\phi, \\ Res(\theta) &= \frac{1}{Pr}\theta'' - \mathbf{f}'\theta + \mathbf{f}\theta' - A(\theta + \frac{1}{2}\eta\theta'), \\ Res(\phi) &= \frac{1}{Sc}\phi'' - \mathbf{f}'\phi + \mathbf{f}\phi' - A\left(\phi + \frac{1}{2}\eta\phi'\right) - \gamma\phi, \end{aligned} \tag{2.81}$$

where the system of equations (2.81) is made up of approximate solutions obtained using the SRM, SLLM and the SQLM. The infinity norms of (2.81) defined as

$$\begin{aligned} IN_r(f) &= ||Res(\mathbf{f})||_\infty, \\ IN_r(\theta) &= ||Res(\theta)||_\infty, \\ IN_r(\phi) &= ||Res(\phi)||_\infty, \end{aligned} \tag{2.82}$$

were used to identify the extent by which approximate solution of (2.81) deviates from real solution. At the minimum point where the residual error can no longer improve, *optimal residual* is said to be attained and that is the point that was used in determining the convergence and accuracy of the solutions obtained with the SRM, SLLM and SQLM.

Table 2.6: Convergence of $||Res(\mathbf{f})||_\infty$ obtained using the SRM, SLLM and SQLM

	SQLM	SRM	SLLM
iterations	$\|\|Res(\mathbf{f})\|\|_\infty$	$\|\|Res(\mathbf{f})\|\|_\infty$	$\|\|Res(\mathbf{f})\|\|_\infty$
1	4.7×10^{-2}	7.1×10^{-3}	3.13×10^{-1}
2	4.4×10^{-4}	2.6×10^{-3}	5.6×10^{-2}
3	3.1×10^{-7}	2.3×10^{-4}	1.1×10^{-2}
4	4.6×10^{-7}	2.1×10^{-5}	2.1×10^{-3}
5	2.5×10^{-7}	1.9×10^{-6}	4.1×10^{-4}
6	2.1×10^{-7}	1.7×10^{-7}	8.1×10^{-5}
7	2.0×10^{-7}	1.6×10^{-8}	1.6×10^{-5}
8	5.5×10^{-7}	1.4×10^{-9}	3.1×10^{-6}
9	1.03×10^{-7}	1.3×10^{-10}	6.0×10^{-7}
10	7.2×10^{-8}	1.2×10^{-11}	1.7×10^{-7}
11	3.4×10^{-7}	7.0×10^{-12}	2.3×10^{-8}
12	4.8×10^{-7}	6.0×10^{-12}	4.4×10^{-9}
13	3.5×10^{-7}	4.0×10^{-12}	8.7×10^{-10}
14	8.8×10^{-8}	2.1×10^{-11}	1.7×10^{-10}
15	3.3×10^{-7}	1.1×10^{-11}	3.3×10^{-11}

Table 2.7: Convergence of $||Res(\theta)||_\infty$ obtained using the SRM, SLLM and SQLM

	SQLM	SLLM	SRM
iterations	$\|\|Res(\theta)\|\|_\infty$	$\|\|Res(\theta)\|\|_\infty$	$\|\|Res(\theta)\|\|_\infty$
1	4.5×10^{-2}	1.4×10^{-1}	1.6×10^{-1}
2	4.3×10^{-4}	6.1×10^{-3}	3.5×10^{-2}
3	1.05×10^{-7}	5.6×10^{-4}	6.5×10^{-3}
4	1.3×10^{-10}	5.1×10^{-5}	1.3×10^{-3}
5	6.8×10^{-11}	4.6×10^{-6}	2.5×10^{-4}
6	5.3×10^{-11}	4.2×10^{-7}	4.8×10^{-5}
7	1.4×10^{-10}	3.8×10^{-8}	9.4×10^{-6}
8	2.2×10^{-11}	3.5×10^{-9}	1.8×10^{-6}
9	4.8×10^{-11}	3.2×10^{-10}	3.6×10^{-7}
10	1.1×10^{-10}	2.9×10^{-11}	6.9×10^{-8}
11	5.4×10^{-11}	2.4×10^{-11}	1.4×10^{-8}
12	8.1×10^{-11}	1.9×10^{-11}	2.7×10^{-9}
13	1.4×10^{-10}	5.0×10^{-12}	5.2×10^{-10}
14	3.5×10^{-11}	7.0×10^{-12}	1.0×10^{-10}
15	3.4×10^{-11}	1.1×10^{-11}	2.0×10^{-11}

Table 2.8: Convergence of $||Res(\phi)||_\infty$ obtained using the SRM, SLLM and SQLM

iterations	SQLM $\|\|Res(\phi)\|\|_\infty$	SLLM $\|\|Res(\phi)\|\|_\infty$	SRM $\|\|Res(\phi)\|\|_\infty$
1	6.1×10^{-2}	1.3×10^{-1}	1.5×10^{-1}
2	4.2×10^{-4}	5.4×10^{-3}	3.2×10^{-2}
3	5.4×10^{-8}	5.0×10^{-4}	5.9×10^{-3}
4	2.6×10^{-11}	4.5×10^{-5}	1.2×10^{-3}
5	2.4×10^{-11}	4.1×10^{-6}	2.3×10^{-4}
6	5.7×10^{-11}	3.7×10^{-7}	4.4×10^{-5}
7	3.0×10^{-11}	3.3×10^{-8}	8.6×10^{-6}
8	7.5×10^{-11}	3.0×10^{-9}	1.7×10^{-6}
9	2.9×10^{-11}	2.8×10^{-10}	3.3×10^{-7}
10	2.0×10^{-11}	2.5×10^{-11}	6.3×10^{-8}
11	1.5×10^{-11}	1.3×10^{-11}	1.2×10^{-8}
12	2.2×10^{-11}	5.0×10^{-12}	2.4×10^{-9}
13	9.0×10^{-11}	1.0×10^{-11}	4.7×10^{-10}
14	4.2×10^{-11}	2.1×10^{-11}	9.2×10^{-11}
15	3.9×10^{-11}	1.0×10^{-12}	1.8×10^{-11}

Table 2.9: Computational time used by the SRM, SLLM and SQLM in obtaining $||Res(\mathbf{f})||_\infty$, $||Res(\theta)||_\infty$ and $||Res(\phi)||_\infty$ after 20 iterations

	SQLM	SRM	SLLM
Time (Sec)	0.783428	1.322560	1.07730

Tables 2.6, 2.7 and 2.8 display the residual error norm of the solutions for the system of equations (2.8 - 2.10) obtained using the SRM, SLLM and the SQLM. It can be observed from the tables that as the number of iterations increase, the norm of the residual decreases which means that the approximate solutions obtained using the three methods get more accurate as the iterative process continues. The norm of the residual decreases to a point where convergence is achieved and that convergence point shows the level of accuracy of

the methods. It can be seen in Table 2.6 that the SQLM converges fastest after just three iterations while it takes the SRM ten iterations and the SLLM thirteen iterations to converge. Furthermore, it is also observed that the SQLM converges to a larger residual error norm than the SRM and SLLM which shows that the SQLM is less accurate than the other two methods.

Table 2.7 gives a comparison of the residual error norms of the three methods for the energy equation. It is observed that the SQLM takes 4 iterations to converge while it takes the SLLM 8 iterations and the SRM 12 iterations which indicates that the SQLM converges faster. The three methods in this case can be seen to be comparable in terms of accuracy. From Table 2.8, it can be seen that the SQLM converges fastest after 4 iterations while the SLLM converges after 9 iterations and the SRM converges after 13 iterations. The three methods converge to similar residual error norms which implies that the accuracy of the methods on the concentration equation are comparable. Table 2.9 gives the computational time taken in generating the norm of the residual error of the three methods. It is observed that all three methods generate the norms very quickly which shows that the three methods are computationally efficient in terms of speed. It can be seen that the SQLM is the fastest as it took 0.78 seconds to generate the norms followed by the SLLM that took 1.08 seconds and the SRM with 1.32 seconds.

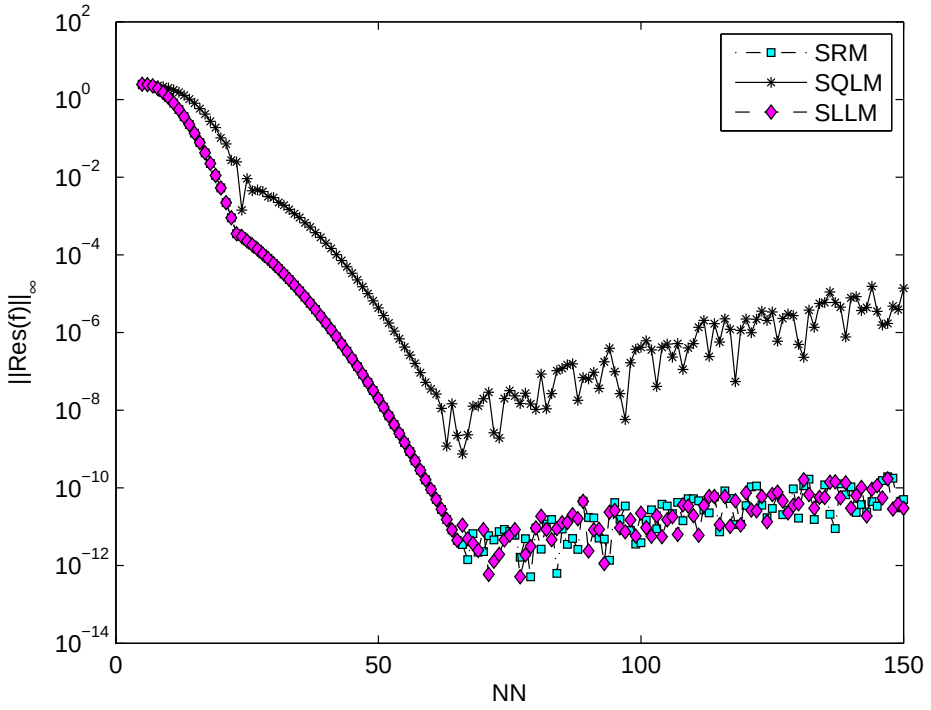

Figure 2.1: Effect of collocation points on $||Res(f)||_\infty$

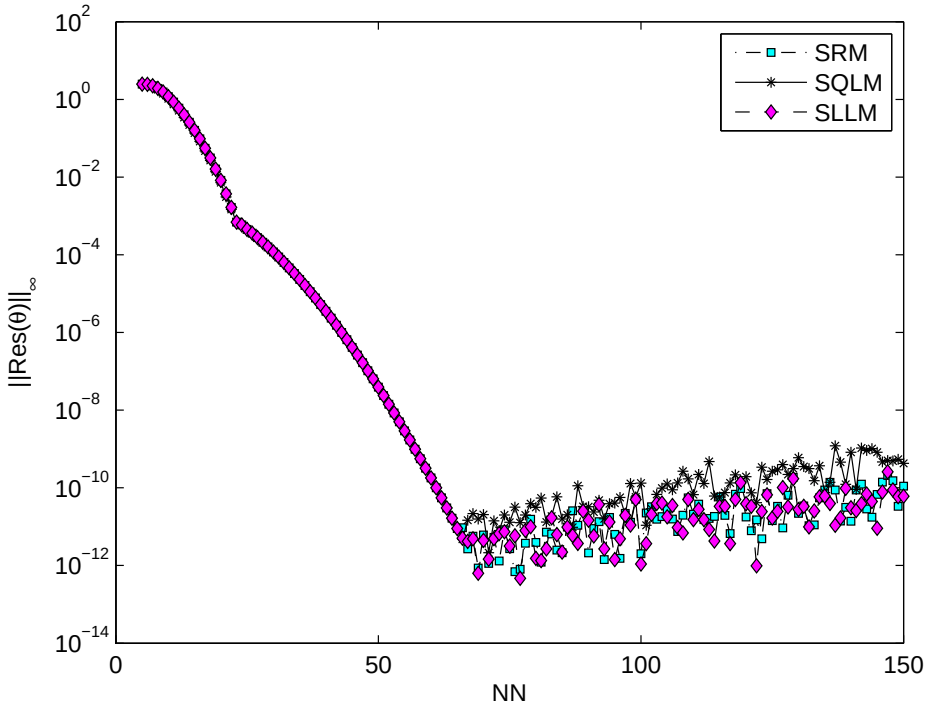

Figure 2.2: Effect of collocation points on $||Res(\theta)||_\infty$

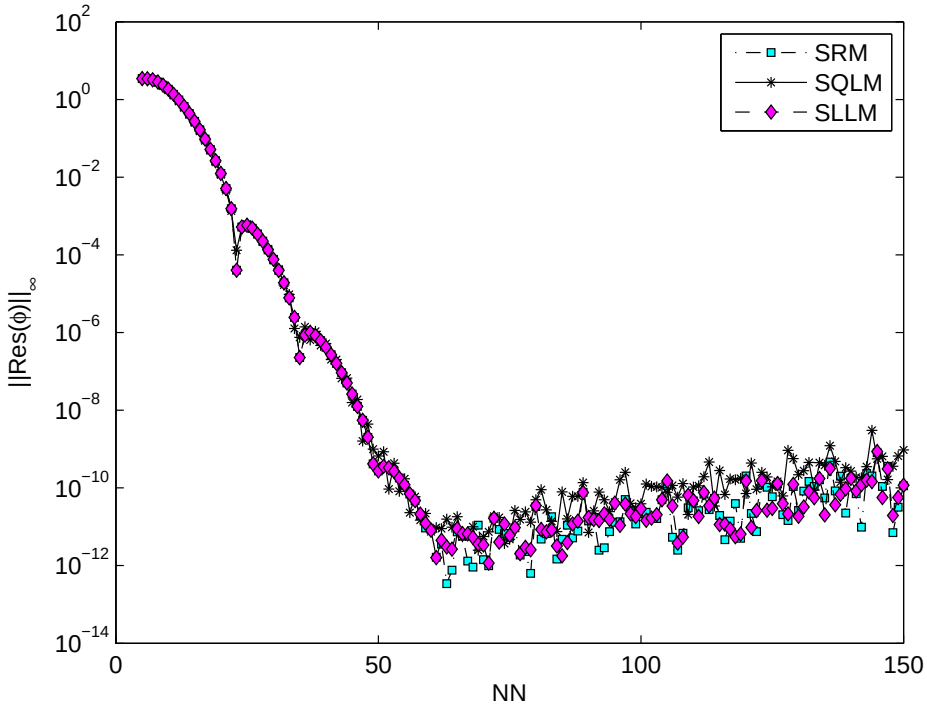

Figure 2.3: Effect of collocation points on $||Res(\phi)||_\infty$

Figures 2.1-2.3 documents the effect of increasing the number of collocation points on the accuracy of the solutions obtained by the SRM, SLLM and SQLM. Motsa (2013a) noted that the SQLM converged quickly with few collocation points while Motsa (2013b) observed that the SRM gave very accurate results with few collocation points.

In Fig. 2.1, it is observed that an increase in the number of collocation points reduces the residual error very quickly to a point where the "optimal residual" is achieved (that is, the minimum residual error attainable). It can be observed that the optimal residual of the SQLM is about 10^{-9} while the optimal residuals of the SRM and the SLLM are about 10^{-12}. When the behavior of the SQLM is studied closely, observation can be made that accuracy is best when the number of collocation points used range between 60 and 70 and then the accuracy slowly declines. This implies that very large amount of collocation points used will cause lesser accuracy to be attained and this observation is supported by Motsa (2013a). The conclusion can be drawn here that the SQLM is less accurate than the other methods while the SRM and the SLLM are comparable. Figure 2.2 shows that the residual error reduces as

collocation points increase. But the optimal residual of the three methods are about the same at 10^{-12}. It is observed that the accuracy of the three methods declines as the number of collocation points get very large but that of the SQLM is more pronounced than those of the SRM and SLLM. If the number of collocation points are restricted in Fig. 2.2, conclusion can be made that the accuracies of the three methods are very much comparable as their minimum residual are about the same. Figure 2.3 shows that the residual error decreases as the number of collocation points increases until optimal residual is achieved at 10^{-12}. Again, the trend of the SQLM getting less accurate increasingly as number of collocation points gets larger is observed. But the three numerical methods are comparable within a range of collocation points.

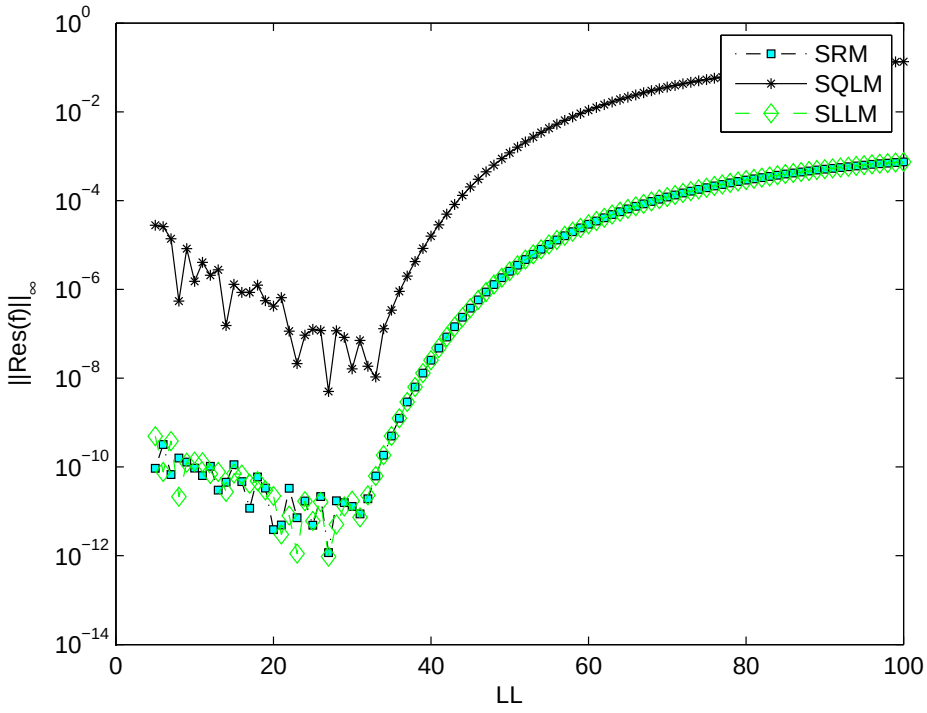

Figure 2.4: Effect of domain truncation on $||Res(f)||_\infty$

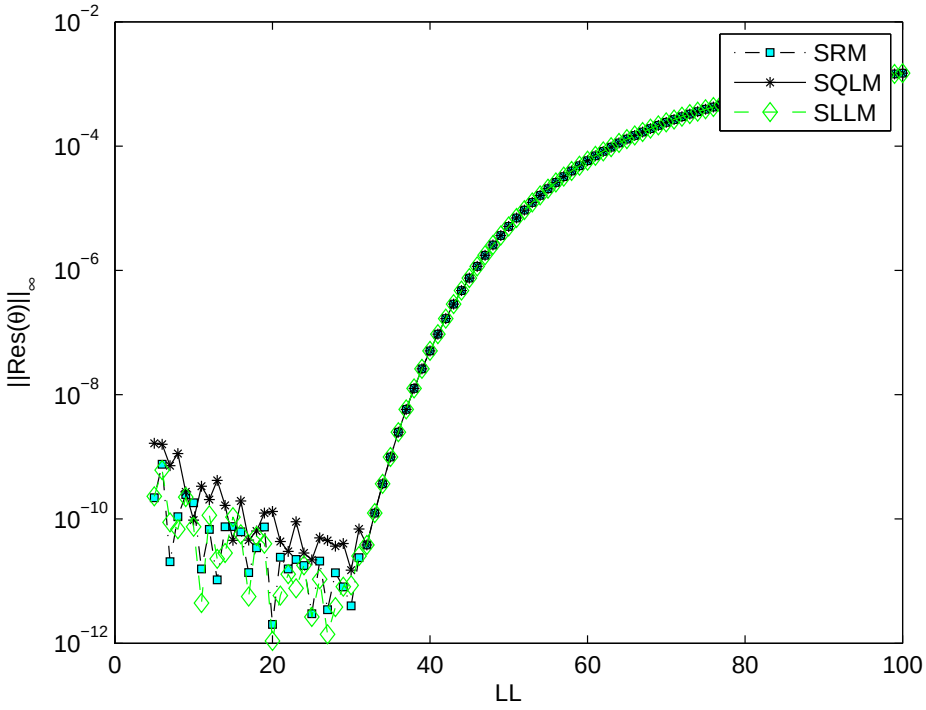

Figure 2.5: Effect of domain truncation on $||Res(\theta)||_\infty$

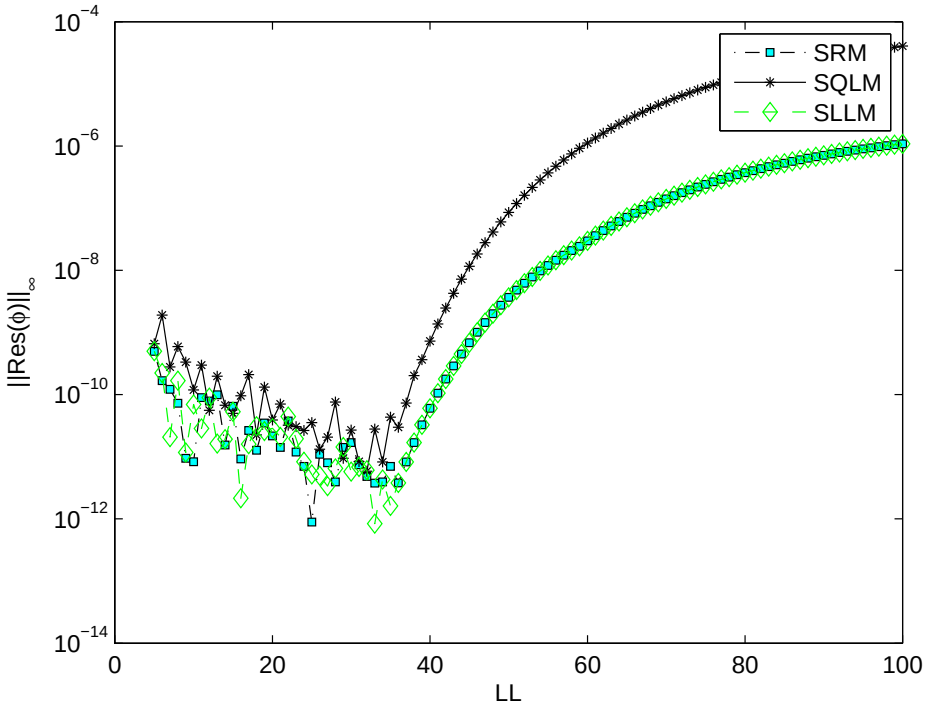

Figure 2.6: Effect of domain truncation on $||Res(\phi)||_\infty$

Figures 2.4-2.6 show the behavior of the residual error against the domain truncation. In Figure 2.4, as the domain truncation increases, the residual error decreases. The maximum residual error is attained when the domain truncation is between 20 and 30. When the length of scale increases past 30, the residual error keeps increasing hereby decreasing accuracy of the solution. This implies that for maximum residual to be maintained, the domain has to be truncated between 20 and 30. The maximum residual of the SQLM is at 10^{-09} while the maximum residual of the SRM and the SLLM are at 10^{-12} hence we can see that the SRM and the SQLM are comparable while the SQLM is not comparable to the rest. Figure 2.5 shows the maximum residual of the SQLM improving to 10^{-11} while the maximum residual of the SLLM and the SRM remains at 10^{-12}. When the domain is truncated after $L \geq 30$, the residual error increases for the three methods and at the same rate. At the maximum residual error (which is when $20<\mathbf{L}\leq 30$), the accuracy of the three methods can be said to be comparable. In Figure 2.6, the residual error of the three methods are seen to be slowly reducing until they attain their maximum residual. The SQLM attains a maximum residual error at 10^{-11} while the SRM and SLLM both attain maximum at 10^{-12}. Accuracy of the methods are best when the domain is truncated between $30 - 35$ and the three methods can be seen to be comparable. For $L \geq 35$, the residual errors of the methods are seen to increase therefore reducing the accuracy of the methods. The SQLM increases residual faster at this stage than the SRM and the SLLM.

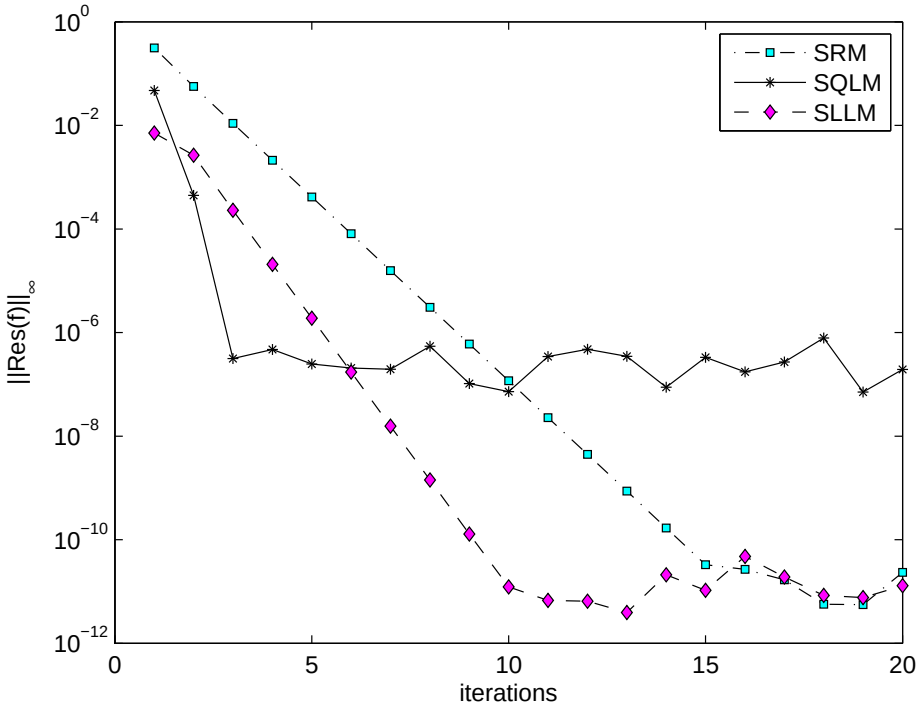

Figure 2.7: Effect of iterations on $||Res(f)||_\infty$

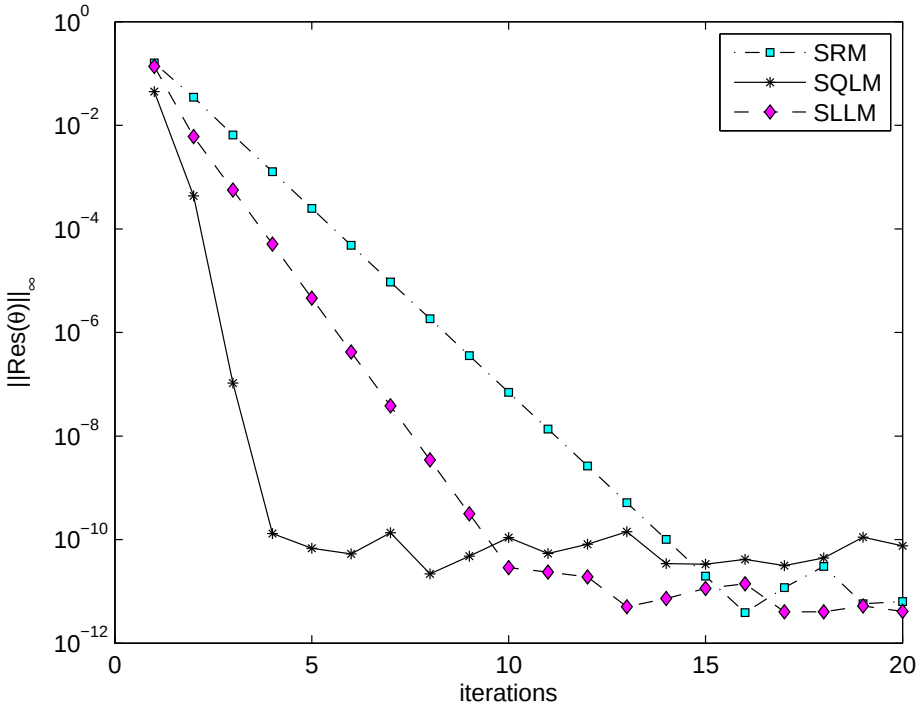

Figure 2.8: Effect of iterations on $||Res(\theta)||_\infty$

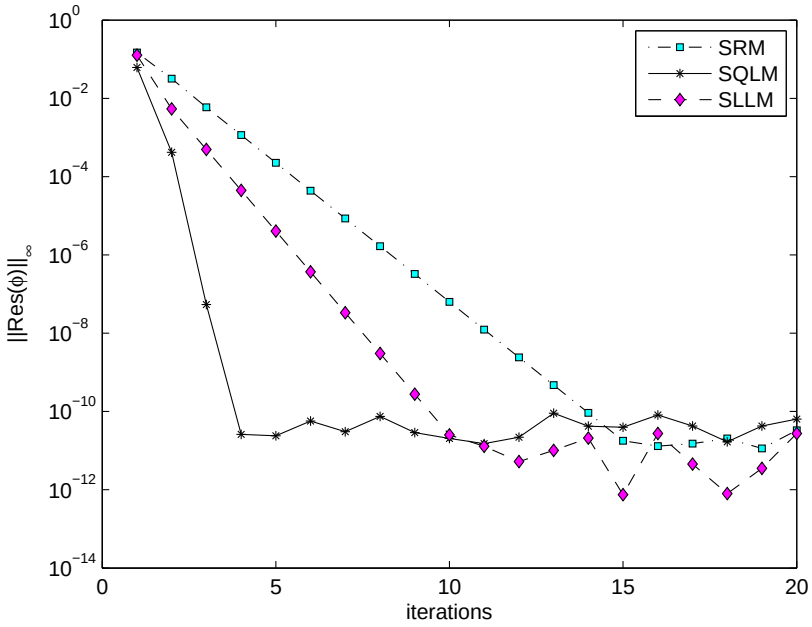

Figure 2.9: Effect of iterations on $||Res(\phi)||_{\infty}$

From Tables 2.1, 2.2 and 2.3, it was observed that the SQLM converged faster than the SRM and the SLLM which is a trend that is observed in the Figures 2.7, 2.8 and 2.9. As the number of iterations are increased, it is observed that the residual error improves thereby implying that accuracy of the methods improves accordingly. As shown in Figure 2.7, it can be seen that the residual error of the three methods decreases as the number of iterations increases which implies that accuracy improves after each iteration which is expected. Saturation point is reached when the optimal residual is obtained and convergence is observed from this point onwards irrespective of the amount of iterations added. It is observed that the residual error of the SQLM converges after 5 iterations between 10^{-6} and 10^{-8} which explains the result displayed in Table 2.1. The residual error of the SLLM can be seen to converge on 10^{-11} at the 10^{th} iteration while that of the SRM converges on 10^{-12} at the 16^{th} iteration which implies that the SQLM converges fastest and the SRM is the slowest to converge with an increase in number of iterations performed. It can also be seen that in terms of accuracy of the methods, the SQLM is not as accurate as the SRM and SLLM while the SRM and the SLLM are comparable. The convergence rate of the SQLM is 1.55 while the convergence rate of the SRM is 0.99 and the convergence rate of the SLLM is 0.99 which implies that the SQLM (that has a quadratic convergence) converges faster than the other methods that

converge linearly.

Figure 2.8 displays the influence of iterations on the residual $||Res(\theta)||_\infty$. It is seen that the three methods give similar residual error norms which implies that the methods are closely comparable in terms of their accuracies. The SQLM converges fastest after 4 iterations to a residual error norm of 10^{-11} which the SLLM converges to after 10 iterations and the SRM converges to the same norm after 15 iterations. The convergence rate of the SQLM is also observed to be faster than the other methods with a rate of 1.79 while the convergence rate of the SLLM is 1.003 and 0.99 for the SRM. The slope of the SQLM is seen to be steeper than the other two slopes which implies faster convergence than the SLLM and the SRM.

Figure 2.9 gives the graphical observation of how the number of iterations improves $||Res(\phi)||_\infty$. It is seen that the residual error of the SQLM is smaller than the other methods at the 5^{th} iteration at 10^{-10}. The residual of the SLLM is optimum at the 10^{th} iteration. The residual at this point is $10^{-11.5}$ which indicates the level of accuracy of the method. The residual of the SRM obtains optimum at the 15^{th} iteration. The optimal residual error of the SRM is at $10^{-11.5}$. The convergence rate of the SQLM is 1.8 while that of the SLLM is 1.01 and the SRM is 1.09 which implies that the SQLM has a faster convergence rate than the other methods while the SRM has the slowest convergence rate. The slope of the SQLM is observed to be steepest which further indicates that the SQLM converges faster than the SLLM and the SRM.

The fluctuations which are observed after the optimal residual errors of the three methods are obtained in Figures 2.7 - 2.9 occur as a result of round-off error which comes with the MATLAB package in some numerical computations. The behaviour of the methods after the saturation points is unpredictable.

2.5 Summary

This chapter successfully compared the spectral relaxation method (SRM), the spectral local linearization method (SLLM) and the spectral quasi-linearization method (SQLM) by

applying the methods on an unsteady free convective heat and mass transfer on a stretching surface in a porous medium with suction. The algorithms for the three methods were derived easily. Approximate solutions were obtained for the local skin friction coefficient, local Nusselt number and the local Sherwood number and comparison of the convergence of the three methods were carried out using these values. Computational efficiency of the methods were also investigated using the time taken to obtain solutions. Comparison was carried out with results obtained from published literature and it was observed that both set of results were in excellent agreement. Norm of the residual error was obtained for the three methods and was plotted against collocation points, the length of scale and the number of iterations.

One of the most significant findings to emerge from this study was that the number of grid (collocation) points to achieve very accurate results has to be controlled as a large amount of grid points led to loss of accuracy in solutions obtained by the SRM, SLLM and SQLM. It was also shown that the domain had to be truncated within a certain range to achieve very accurate solutions as an increase beyond a certain point was observed to produce less accurate solutions. The third major finding was that increasing the number of iterations improved the accuracy of the solutions. Unlike the other two observations, the number of iterations can be increased infinitely without any loss of accuracy. It was also observed that the three methods were computationally efficient as it took very short time for solutions to be generated.

These findings suggest that in general, the SRM, SLLM and the SQLM are very accurate methods for solving systems of ordinary differential equations but the SRM and the SLLM are more accurate methods than the SQLM. It is recommended that further comparative research be conducted on systems of partial differential equations to observe if the methods will behave differently on other types of differential equations.

Chapter 3

Unsteady boundary layer flow due to a stretching surface in a rotating fluid

3.1 Introduction

The study of the effect of stretching surfaces/sheets on boundary layer flow problems has been conducted extensively in the last few decades because of its applicability in various areas. Flow and heat transfer characteristics due to a stretching sheet in a static fluid is applied in the industrial manufacture of polymer and metal sheets as reported by Pop and Na (1996). It is also used in aerodynamic extrusion of plastic sheets (Takhar and Nath, 1998; Liao, 2006a).

In this chapter, the problem of unsteady boundary layer flow due to a stretching surface in a rotating fluid is investigated using the SRM, SLLM and SQLM to obtain numerical solutions. Nazar et al. (2004a) studied the unsteady boundary layer flow due to a stretching surface in a rotating fluid and obtained numerical solutions using the Keller-Box method to obtain numerical solutions at steady state. The equations that model the unsteady boundary layer flow due to a stretching surface in a rotating fluid are nonlinear partial differential equations (PDEs) that are in time and space. A transformation, introduced by Williams and Rhyne (1980) in transforming an infinite time scale $\tau = [0, \infty)$ of an unsteady flow problem to a finite domain $\xi = [0, 1]$ of integration, is applied to perform proper analysis on the system of PDEs.

The aim of this study is to extend the comparative study performed on the system of ordinary differential equations in the previous chapter to a system of partial differential equations using the SRM, SLLM and SQLM. A study carried out by Motsa et al. (2014) successfully introduced the SRM and SQLM for solving systems of partial differential equations that modeled boundary layer flow caused by an impulsively stretching plate and an unsteady MHD flow and mass transfer in a porous space. The application of the methods on the system of PDEs is as described in Chapter 1 but with an added usage of Crank-Nicolson finite difference method to solve in the direction of time. To effectively carry out the study in this chapter, some investigations will be carried out. The steps applied in developing the algorithms of the SRM, SLLM and SQLM for the system of partial differential equations will be fully shown. The number of iterations used to obtain converged solutions is also investigated as well to compare the speed of the methods. Finally, the effect of the dimensionless time ξ on the accuracy of the solutions obtained is also investigated.

As reported by Nazar et al. (2004a), the problem formulation is obtained by reducing the governing equations to similar equations produced by Rayleigh and Wang (1988) in the presence of initial unsteady flow ($t = 0$) and final steady state flow ($t \to \infty$). It is necessary to pick a time scale ξ such that the region of time integration becomes finite. These types of transformations were produced by Williams and Rhyne (1980).

3.2 Method formulation

In this section, the formulation of the mathematical equations that model an unsteady boundary layer flow due to a stretching surface in a rotating fluid are presented.

As described by Nazar et al. (2004a), consider the two-dimensional stretching of a surface in a rotating fluid as seen in Fig3.1. At an initial unsteady state $t = 0$, the surface at $z = 0$ is stretched impulsively in the x direction in the rotating fluid. Because of the Coriolis force (that is, force that deflects movement to different hemispheres due to the rotation of the earth) in place, the motion of the fluid is three-dimensional. Let (u, v, w) be the velocity components in the direction of the Cartesian axes (x, y, z), respectively, with the axes rotating at an angular

velocity Ω in the z direction.

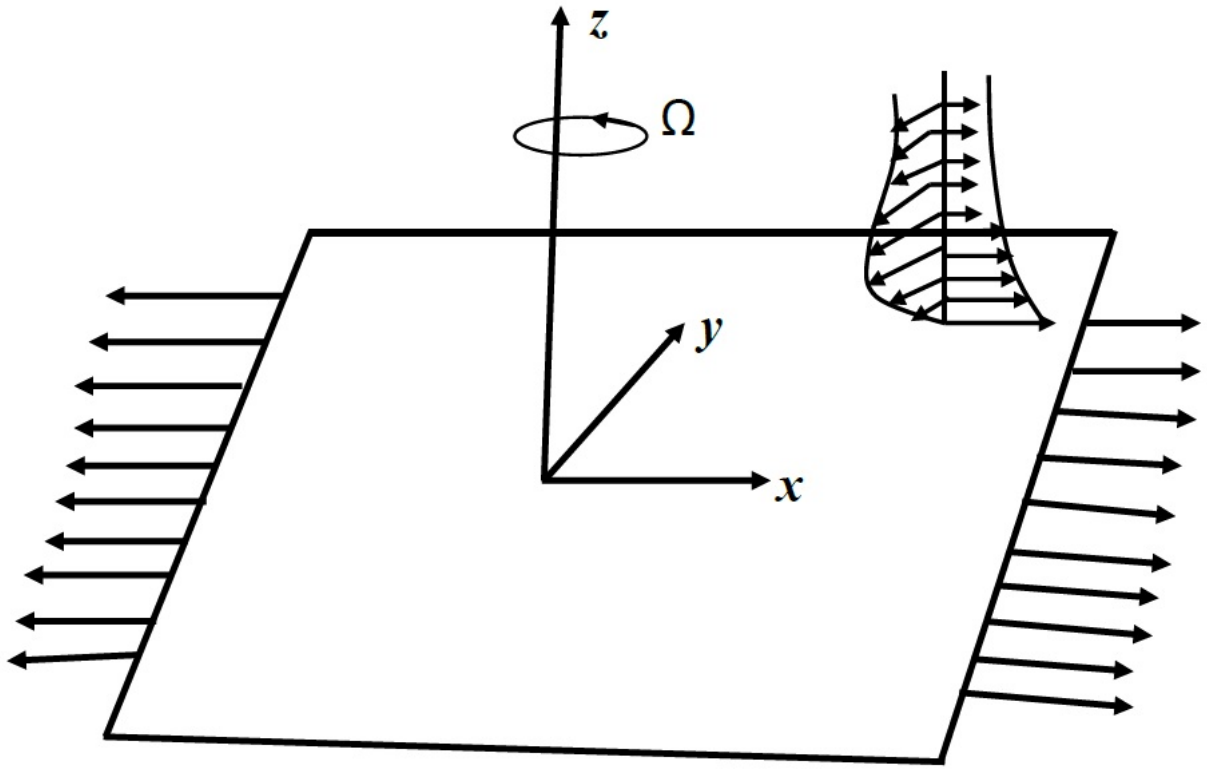

Figure 3.1: Physical model and coordinate system.

The unsteady Navier-Stokes equations that govern the fluid flow are

$$\begin{aligned}
\frac{\partial u}{\partial x}+\frac{\partial v}{\partial y}+\frac{\partial w}{\partial z} &= 0,\\
\frac{\partial u}{\partial t}+u\frac{\partial u}{\partial x}+v\frac{\partial u}{\partial y}+w\frac{\partial u}{\partial z}-2\Omega v &= -\frac{1}{\rho}\frac{\partial p}{\partial x}+\nu\nabla^2 u,\\
\frac{\partial v}{\partial t}+u\frac{\partial v}{\partial x}+v\frac{\partial v}{\partial y}+w\frac{\partial v}{\partial z}-2\Omega u &= -\frac{1}{\rho}\frac{\partial p}{\partial y}+\nu\nabla^2 v,\\
\frac{\partial w}{\partial t}+u\frac{\partial w}{\partial x}+v\frac{\partial w}{\partial y}+w\frac{\partial w}{\partial z} &= -\frac{1}{\rho}\frac{\partial p}{\partial z}+v\nabla^2 w,
\end{aligned} \tag{3.1}$$

where x, y and z are the longitudinal, the transverse and the normal directions respectively, u, v and w are the velocity components in the $x-$, $y-$ and $z-$directions respectively, p is the pressure, ρ is the density, v the kinematic viscosity and ∇ the three-dimensional Laplacean operator.

Chapter 3 – Unsteady boundary layer flow due to a stretching surface in a rotating fluid

Let the surface be impulsively stretched in the x direction such that the initial and boundary conditions are

$$\begin{aligned} t<0:\ u=v=w=0\ for\ any\ x,y,z,\\ t\geq 0:\ u=ax,\ \ v=w=0\ at\ z=0,\\ u\to 0,\ v\to 0\ as\ z\to\infty, \end{aligned} \tag{3.2}$$

where $a(>0)$ has a dimension of $[t^{-1}]$ and represents the stretching rate.

As reported by Nazar et al. (2004a), we introduce the following similarity variables:

$$\begin{aligned} \eta=(a/\nu)^{1/2}\xi^{-1/2}z,\ \ u=axf^{'}(\xi,\eta),\ \ v=axh(\xi,\eta),\\ w=-(a\nu)^{1/2}\xi^{1/2}f(\xi,\eta),\ \ \xi=1-\exp^{-\tau},\ \tau=at. \end{aligned} \tag{3.3}$$

After transformation, the system (3.1) becomes:

$$\begin{aligned} f^{'''}+\frac{1}{2}(1-\xi)\eta f^{''}+\xi(ff^{''}-f^{'2}+2\lambda h) &= \xi(1-\xi)\frac{\partial f^{'}}{\partial\xi},\\ h^{''}+\frac{1}{2}(1-\xi)\eta h^{'}+\xi(fh^{'}-f^{'}h-2\lambda f^{'}) &= \xi(1-\xi)\frac{\partial h}{\partial\xi}, \end{aligned} \tag{3.4}$$

with corresponding boundary conditions

$$f(0,\xi)=0,\quad f^{'}(0,\xi)=1,\quad h(0,\xi)=0,\quad h(\infty,\xi)=0,\quad f^{'}(\infty,\xi)=0, \tag{3.5}$$

where $\lambda=\Omega/a$ and the prime denotes differentiation with respect to η. The wall shear stresses (as a result of the pressure contained in the fluid) τ_w^x and τ_w^y in the x and y directions are related to the non-dimensional skin friction coefficient in x and y directions, C_f^x and C_f^y, respectively, according to:

$$\begin{aligned} C_f^x=\frac{\tau_w^x}{\rho(ax)^2} &= \frac{v}{(ax)^2}\left(\frac{\partial u}{\partial z}\right)_{z=0},\\ C_f^y=\frac{\tau_w^y}{\rho(ax)^2} &= \frac{v}{(ax)^2}\left(\frac{\partial \nu}{\partial z}\right)_{z=0}. \end{aligned} \tag{3.6}$$

Applying the variables (3.3), we obtain

$$C_f^x Re_x^{1/2}=\xi^{-1/2}f^{''}(\xi,0),\ \ C_f^y Re_x^{1/2}=\xi^{-1/2}h^{'}(\xi,0), \tag{3.7}$$

where $Re_x=(ax)x/v$ is the local Reynolds number.

Initial unsteady solution is obtained by setting $\xi = 0$ ($\tau = 0$) for the system of equations (3.4) and the new system is of the form

$$\begin{aligned} f''' + \frac{1}{2}\eta f'' &= 0, \\ h'' + \frac{1}{2}\eta h' &= 0, \end{aligned} \tag{3.8}$$

with corresponding boundary conditions

$$f(0,0) = 0, \quad f'(0,0) = 1, \quad f'(\infty,0) = 0, \quad h(0,0) = 0, \quad h(\infty,0) = 0. \tag{3.9}$$

The solutions to these equations are

$$\begin{aligned} f(\eta,0) &= \eta erfc(\eta/2) + \frac{2}{\sqrt{\pi}}\left(1 - \exp^{-\eta^2/4}\right), \\ h(\eta,0) &= 0, \end{aligned} \tag{3.10}$$

where $erfc(\eta)$ is the complementary error function defined as

$$erfc(\eta) = \frac{2}{\sqrt{\pi}} \int_{\eta}^{\infty} \exp^{-s^2} ds. \tag{3.11}$$

The steady state solution at $\xi = 1$, corresponding to $\tau \to +\infty$, is obtained from

$$\begin{aligned} f''' + ff'' - f'^2 + 2\lambda h &= 0, \\ h'' + fh' - f'h - 2\lambda f' &= 0, \end{aligned} \tag{3.12}$$

with boundary conditions

$$f(0,0) = 0, \quad f'(0,0) = 1, \quad f'(\infty,0) = 0, \quad h(0,0) = 0, \quad h(\infty,0) = 0. \tag{3.13}$$

3.3 Solution Techniques

In this section, the spectral relaxation method (SRM), the spectral local linearization method (SLLM) and the spectral quasi-linearization method (SQLM) are all applied to obtain solutions to the system of equations (3.4). The steps taken to come up with the iteration scheme are shown in details.

3.3.1 Spectral Relaxation Method (SRM)

In this subsection, the SRM is applied on the system of equations (3.4) and the corresponding boundary conditions (3.5) by applying the idea of the Gauss-Seidel relaxation method to decouple the system and applying spectral collocation technique on the decoupled system.

The order of the first equation in the system (3.4) is reduced by setting $f^{'} = u$ and the reduced system of equations take on the form:

$$\begin{aligned} f^{'} &= u, \\ u^{''} + \frac{1}{2}(1-\xi)\eta u^{'} + \xi\left(fu^{'} - u^2 + 2\lambda h\right) &= \xi(1-\xi)\frac{\partial u}{\partial \xi}, \\ h^{''} + \frac{1}{2}(1-\xi)\eta h^{'} + \xi\left(fh^{'} - uh - 2\lambda u\right) &= \xi(1-\xi)\frac{\partial h}{\partial \xi}, \end{aligned} \tag{3.14}$$

with corresponding boundary conditions:

$$f(0,\xi) = 0, \quad u(0,\xi) = 1, \quad h(0,\xi) = 0, \quad h(\infty,\xi) = 0, \quad u(\infty,\xi) = 0. \tag{3.15}$$

After applying the concept of the Gauss-Seidel relaxation technique in order to decouple the system (3.14), the decoupled system becomes

$$\begin{aligned} u^{''}_{r+1} + \left(\frac{\eta}{2} - \frac{\eta}{2}\xi + \xi f_r\right)u^{'}_{r+1} - \xi u_r^2 + 2\xi\lambda h_r &= \xi(1-\xi)\frac{\partial u_{r+1}}{\partial \xi}, \\ h^{''}_{r+1} + \left(\frac{\eta}{2} - \frac{\eta}{2}\xi + \xi f_{r+1}\right)h^{'}_{r+1} - u_{r+1}h_{r+1} - 2\lambda u_{r+1} &= \xi(1-\xi)\frac{\partial h_{r+1}}{\partial \xi}, \\ f^{'}_{r+1} &= u_{r+1}, \end{aligned} \tag{3.16}$$

where linear terms are evaluated at the current iteration level $(r+1)$ and nonlinear terms at the previous iteration level (r). A compact form is given by

$$\begin{aligned} u^{''}_{r+1} + a_{1,r}u^{'}_{r+1} + a_{2,r} &= \xi(1-\xi)\frac{\partial u_{r+1}}{\partial \xi}, \\ h^{''}_{r+1} + b_{1,r}h^{'}_{r+1} - b_{2,r}h_{r+1} + b_{3,r} &= \xi(1-\xi)\frac{\partial h_{r+1}}{\partial \xi}, \\ f^{'}_{r+1} &= u_{r+1}, \end{aligned} \tag{3.17}$$

where

$$\begin{aligned} a_{1,r} &= \frac{\eta}{2} - \frac{\eta}{2}\xi + \xi f_r, \\ a_{2,r} &= -\xi u_r^2 + 2\xi\lambda h_r, \\ b_{1,r} &= \frac{\eta}{2} - \frac{\eta}{2}\xi + \xi f_{r+1}, \\ b_{2,r} &= u_{r+1}, \\ b_{3,r} &= -2\lambda u_{r+1}. \end{aligned}$$

The compact form (3.17) does not hold any significant meaning other than to make coding much easier or organized on the $MATLAB$ package.

Following (Trefethen (2000)), to solve partial differential equations that are dependent on time using spectral methods, finite differences is used to discretize the equation in time ξ while spectral collocation is used to discretize the equation in space η (as was described in the previous chapter). The Crank-Nicolson finite difference scheme (which is implicit in time) is applied with centering about a mid-point halfway between ξ^{n+1} and ξ^n to approximate the derivative with respect to ξ. The point is defined as $\xi^{n+\frac{1}{2}} = \left(\xi^{n+1} + \xi^n\right)/2$. Derivatives with respect to η are defined in terms of the Chebyshev differentiation matrices. Applying centering about $\xi^{n+\frac{1}{2}}$ to any function in space and time $u(\eta, \xi)$ and its corresponding derivative gives:

$$u\left(\eta_j, \xi^{n+\frac{1}{2}}\right) = u_j^{n+\frac{1}{2}} = \frac{u_j^{n+1} + u_j^n}{2}, \quad \left(\frac{\partial u}{\partial \xi}\right)^{n+\frac{1}{2}} = \frac{u_j^{n+1} - u_j^n}{\Delta\xi}. \tag{3.18}$$

Thus, when the Crank-Nicolson finite difference approach is applied on the compact system (3.17) and the system (3.19) is obtained:

$$\begin{aligned} \left(u_{r+1}^{''}\right)^{n+\frac{1}{2}} + \left(a_{1,r}\right)^{n+\frac{1}{2}} \left(u_{r+1}^{'}\right)^{n+\frac{1}{2}} + \left(a_{2,r}\right)^{n+\frac{1}{2}} &= \xi^{n+\frac{1}{2}} \left(1 - \xi^{n+\frac{1}{2}}\right) \left(\frac{u_{r+1}^{n+1} - u_{r+1}^n}{\Delta\xi}\right), \\ \left(h_{r+1}^{''}\right)^{n+\frac{1}{2}} + \left(b_{1,r}\right)^{n+\frac{1}{2}} \left(h_{r+1}^{'}\right)^{n+\frac{1}{2}} - \left(b_{2,r}\right)^{n+\frac{1}{2}} \left(h_{r+1}\right)^{n+\frac{1}{2}} + \left(b_{3,r}\right)^{n+\frac{1}{2}} &= \\ \xi^{n+\frac{1}{2}} \left(1 - \xi^{n+\frac{1}{2}}\right) \left(\frac{h_{r+1}^{n+1} - h_{r+1}^n}{\Delta\xi}\right), & \\ \left(f_{r+1}^{'}\right)^{n+\frac{1}{2}} = \left(u_{r+1}\right)^{n+\frac{1}{2}}. & \end{aligned} \tag{3.19}$$

The Chebyshev pseudo-spectral collocation technique is then applied to integrate system (3.19). The pseudo-spectral collocation technique (contained in Hussaini and Zang (1987), Trefethen (2000) and described in the previous chapter) uses a differentiation matrix that is applied in approximating derivatives of unknown functions and is denoted $\mathbf{D}$ which does the approximation at the collocation points (grid points) as the matrix vector product

$$\frac{dF}{d\eta}(\eta_j) = \sum_{k=0}^{N_x} \mathbf{D}_{jk} f(Y_k) = \mathbf{DF}, \quad j = 0, 1, ..., N_x, \tag{3.20}$$

where $\eta = \frac{(Y+1)\eta_\infty}{2}$, $N_x + 1$ is the number of collocation points, $\mathbf{D} = 2D/\eta_\infty$, and

$$\mathbf{F} = \left[f(Y_0), f(Y_1), \cdots, f(Y_{N_x})\right]^T, \tag{3.21}$$

is the vector function at the collocation points. Higher order derivatives are obtained as powers of $\mathbf{D}$, that is

$$\mathbf{F}^{(p)} = \mathbf{D}^p \mathbf{F}, \tag{3.22}$$

where p is the order of the derivative. The matrix D is of the size $(N_x + 1) \times (N_x + 1)$. The grid points on (η, ξ) are defined as

$$Y_j = \cos\frac{\pi j}{N_x}, \quad \xi^n = n\Delta\xi, \quad j = 0, 1, ..., N_x, \quad n = 0, 1, ..., N_t, \tag{3.23}$$

where $N_x + 1$, and $N_t + 1$ are the total number of collocation points in the space (η) and time (ξ) directions respectively and $\Delta\xi$ is the spacing in the time ξ-direction.

Now, rewriting (3.19) in the spectral collocation form, the system becomes:

$$\begin{aligned}
\left(\mathbf{D}^2\mathbf{u}_{r+1}\right)^{n+\frac{1}{2}} + \left(\mathbf{a}_{1,r}\right)^{n+\frac{1}{2}} \left(\mathbf{D}\mathbf{u}_{r+1}\right)^{n+\frac{1}{2}} + \left(\mathbf{a}_{2,r}\right)^{n+\frac{1}{2}} \\
= \frac{\xi^{n+\frac{1}{2}}\left(1 - \xi^{n+\frac{1}{2}}\right)}{\Delta\xi}\left(\mathbf{u}_{r+1}^{n+1} - \mathbf{u}_{r+1}^{n}\right), \\
\left(\mathbf{D}^2\mathbf{h}_{r+1}\right)^{n+\frac{1}{2}} + \left(\mathbf{b}_{1,r}\right)^{n+\frac{1}{2}} \left(\mathbf{D}\mathbf{h}_{r+1}\right)^{n+\frac{1}{2}} - \left(\mathbf{b}_{2,r}\right)^{n+\frac{1}{2}} \left(\mathbf{h}_{r+1}\right)^{n+\frac{1}{2}} + \left(\mathbf{b}_{3,r}\right)^{n+\frac{1}{2}} \\
= \frac{\xi^{n+\frac{1}{2}}\left(1 - \xi^{n+\frac{1}{2}}\right)}{\Delta\xi}\left(\mathbf{h}_{r+1}^{n+1} - \mathbf{h}_{r+1}^{n}\right), \\
\left(\mathbf{D}\mathbf{f}_{r+1}\right)^{n+\frac{1}{2}} = \left(\mathbf{u}_{r+1}\right)^{n+\frac{1}{2}}.
\end{aligned} \tag{3.24}$$

From (3.24), taking terms at the next time level $(n + 1)$ to the left and terms at the current

time level(n) and nonlinear terms to the right, the new system is obtained:

$$\begin{aligned}
&\left[\frac{1}{2}\left(\mathbf{D}^2+\mathbf{diag}\left[\mathbf{a}_{1,r}^{n+\frac{1}{2}}\right]\mathbf{D}\right)-\frac{\xi^{n+\frac{1}{2}}\left(1-\xi^{n+\frac{1}{2}}\right)}{\Delta\xi}\right]\mathbf{U}_{r+1}^{n+1}\\
&=\left[-\frac{1}{2}\left(\mathbf{D}^2+\mathbf{diag}\left[\mathbf{a}_{1,r}^{n+\frac{1}{2}}\right]\mathbf{D}\right)-\frac{\xi^{n+\frac{1}{2}}\left(1-\xi^{n+\frac{1}{2}}\right)}{\Delta\xi}\right]\mathbf{U}_{r+1}^{n}-\mathbf{a}_{2,r}^{n+\frac{1}{2}},\\
&\left[\frac{1}{2}\left(\mathbf{D}^2+\mathbf{diag}\left[\mathbf{b}_{1,r}^{n+\frac{1}{2}}\right]\mathbf{D}-\mathbf{b}_{2,r}^{n+\frac{1}{2}}\right)-\frac{\xi^{n+\frac{1}{2}}\left(1-\xi^{n+\frac{1}{2}}\right)}{\Delta\xi}\right]\mathbf{H}_{r+1}^{n+1}\\
&=\left[-\frac{1}{2}\left(\mathbf{D}^2+\mathbf{diag}\left[\mathbf{b}_{1,r}^{n+\frac{1}{2}}\right]\mathbf{D}-\mathbf{b}_{2,r}^{n+\frac{1}{2}}\right)-\frac{\xi^{n+\frac{1}{2}}\left(1-\xi^{n+\frac{1}{2}}\right)}{\Delta\xi}\right]\mathbf{H}_{r+1}^{n}-\mathbf{b}_{3,r}^{n+\frac{1}{2}},
\end{aligned}\tag{3.25}$$

where

$$\mathbf{diag}[\mathbf{a}_{1,r}]=\begin{bmatrix}a_{1,r}(x_0) & & & & \\ & a_{1,r}(x_1) & & & \\ & & \ddots & & \\ & & & \ddots & \\ & & & & a_{1,r}(x_{N_x})\end{bmatrix},\quad \mathbf{diag}[\mathbf{b}_{1,r}]=\begin{bmatrix}b_{1,r}(x_0) & & & & \\ & b_{1,r}(x_1) & & & \\ & & \ddots & & \\ & & & \ddots & \\ & & & & b_{1,r}(x_{N_x})\end{bmatrix},$$

$$\mathbf{diag}[\mathbf{b}_{1,r}]=\begin{bmatrix}b_{1,r}(x_0) & & & & \\ & b_{1,r}(x_1) & & & \\ & & \ddots & & \\ & & & \ddots & \\ & & & & b_{1,r}(x_{N_x})\end{bmatrix}.$$

Equation (3.25) can be written in a compact form as:

$$\begin{aligned}
\mathbf{A}_1\mathbf{U}_{r+1}^{n+1} &= \mathbf{B}_1\mathbf{U}_{r+1}^{n}+\mathbf{K}_1,\\
\mathbf{A}_2\mathbf{H}_{r+1}^{n+1} &= \mathbf{B}_2\mathbf{H}_{r+1}^{n}+\mathbf{K}_2,\\
\mathbf{A}_3\mathbf{F}_{r+1} &= \mathbf{K}_3,
\end{aligned}\tag{3.26}$$

where

$$\begin{aligned}
\mathbf{A}_1 &= \frac{1}{2}\left(\mathbf{D}^2 + \mathbf{a}_{1,r}^{n+\frac{1}{2}}\mathbf{D}\right) - \frac{\xi^{n+\frac{1}{2}}\left(1-\xi^{n+\frac{1}{2}}\right)}{\Delta\xi}\mathbf{I},\\
\mathbf{B}_1 &= -\frac{1}{2}\left(\mathbf{D}^2 + \mathbf{a}_{1,r}^{n+\frac{1}{2}}\mathbf{D}\right) - \frac{\xi^{n+\frac{1}{2}}\left(1-\xi^{n+\frac{1}{2}}\right)}{\Delta\xi}\mathbf{I},\\
\mathbf{K}_1 &= -\mathbf{a}_{2,r}^{n+\frac{1}{2}},\\
\mathbf{A}_2 &= \frac{1}{2}\left(\mathbf{D}^2 + \mathbf{b}_{1,r}^{n+\frac{1}{2}}\mathbf{D} - \mathbf{b}_{2,r}^{n+\frac{1}{2}}\right) - \frac{\xi^{n+\frac{1}{2}}\left(1-\xi^{n+\frac{1}{2}}\right)}{\Delta\xi}\mathbf{I},\\
\mathbf{B}_2 &= -\frac{1}{2}\left(\mathbf{D}^2 + \mathbf{b}_{1,r}^{n+\frac{1}{2}}\mathbf{D} - \mathbf{b}_{2,r}^{n+\frac{1}{2}}\right) - \frac{\xi^{n+\frac{1}{2}}\left(1-\xi^{n+\frac{1}{2}}\right)}{\Delta\xi}\mathbf{I},\\
\mathbf{K}_2 &= -\mathbf{b}_{3,r}^{n+\frac{1}{2}},\\
\mathbf{A}_3 &= \mathbf{D},\\
\mathbf{K}_3 &= \mathbf{U}_{r+1}.
\end{aligned}$$

The boundary conditions are implemented on the system in the form below:

$$\begin{aligned}
\mathbf{M}_1\mathbf{P}_1 &= \mathbf{Q}_1,\\
\mathbf{M}_2\mathbf{P}_2^{n+1} &= \mathbf{Q}_2\mathbf{P}_2^{n} + \mathbf{R}_1,\\
\mathbf{M}_3\mathbf{P}_3^{n+1} &= \mathbf{Q}_3\mathbf{P}_3^{n} + \mathbf{R}_2,
\end{aligned} \tag{3.27}$$

where $\mathbf{M}_1 = \begin{bmatrix} \mathbf{A}_3 \\ \hline 0 \;\; 0 \;\; \cdots \;\; 0 \;\; 1 \end{bmatrix}$, $\mathbf{P}_1 = \begin{bmatrix} f_{r+1,0} \\ f_{r+1,1} \\ \vdots \\ \vdots \\ \hline f_{r+1,N} \end{bmatrix}$, $\mathbf{Q}_1 = \begin{bmatrix} \mathbf{K}_3 \\ \hline 0 \end{bmatrix}$, $\mathbf{R}_1 = \begin{bmatrix} 0 \\ \hline \mathbf{K}_2 \\ \hline 1 \end{bmatrix}$, $\mathbf{R}_2 = \begin{bmatrix} 0 \\ \hline \mathbf{K}_1 \\ \hline 1 \end{bmatrix}$,

$$\mathbf{M}_2=\begin{bmatrix} 1 & 0 & \cdots & 0 & 0 \\ \hline & & & & \\ & & \mathbf{A}_2 & & \\ & & & & \\ \hline 0 & 0 & \cdots & 0 & 1 \end{bmatrix}, \quad \mathbf{P}_2^{n+1}=\begin{bmatrix} h_{r+1,0}^{n+1} \\ \hline h_{r+1,1}^{n+1} \\ \vdots \\ \vdots \\ \hline h_{r+1,N}^{n+1} \end{bmatrix}, \quad \mathbf{Q}_2=\begin{bmatrix} 0 & 0 & \cdots & 0 & 0 \\ \hline & & & & \\ & & \mathbf{B}_2 & & \\ & & & & \\ \hline 0 & 0 & \cdots & 0 & 0 \end{bmatrix}, \quad \mathbf{P}_2^{n}=\begin{bmatrix} h_{r+1,0}^{n} \\ \hline h_{r+1,1}^{n} \\ \vdots \\ \vdots \\ \hline h_{r+1,N}^{n} \end{bmatrix},$$

$$\mathbf{M}_3=\begin{bmatrix} 1 & 0 & \cdots & 0 & 0 \\ \hline & & & & \\ & & \mathbf{A}_1 & & \\ & & & & \\ \hline 0 & 0 & \cdots & 0 & 1 \end{bmatrix}, \quad \mathbf{P}_3^{n+1}=\begin{bmatrix} u_{r+1,0}^{n+1} \\ \hline u_{r+1,1}^{n+1} \\ \vdots \\ \vdots \\ \hline u_{r+1,N}^{n+1} \end{bmatrix}, \quad \mathbf{Q}_3=\begin{bmatrix} 0 & 0 & \cdots & 0 & 0 \\ \hline & & & & \\ & & \mathbf{B}_1 & & \\ & & & & \\ \hline 0 & 0 & \cdots & 0 & 0 \end{bmatrix}, \quad \mathbf{P}_3^{n}=\begin{bmatrix} u_{r+1,0}^{n} \\ \hline u_{r+1,1}^{n} \\ \vdots \\ \vdots \\ \hline u_{r+1,N}^{n} \end{bmatrix}.$$

3.3.2 Spectral Local Linearization Method(SLLM)

In this subsection, the SLLM is applied on the system (3.4) and the corresponding boundary conditions (3.5). This application is done by identifying nonlinear terms of the same function and its derivative in each of the equations of the system (3.4), applying Taylor series expansion on the nonlinear terms so as to linearize the system of equations which will be decoupled before applying spectral collocation technique on the system.

In order to apply the SLLM, let $f^{'} = u$ to reduce the order of (3.4) and the resulting equations become:

$$\begin{aligned} f^{'} &= u, \\ u^{''} + \frac{1}{2}(1-\xi)\eta u^{'} + \xi\left(fu^{'} - u^2 + 2\lambda h\right) &= \xi(1-\xi)\frac{\partial u}{\partial \xi}, \\ h^{''} + \frac{1}{2}(1-\xi)\eta h^{'} + \xi\left(fh^{'} - uh - 2\lambda u\right) &= \xi(1-\xi)\frac{\partial h}{\partial \xi}, \end{aligned} \tag{3.28}$$

with corresponding boundary conditions:

$$f(0,\xi)=0, \quad u(0,\xi)=1, \quad h(0,\xi)=0, \quad h(\infty,\xi)=0, \quad u(\infty,\xi)=0. \tag{3.29}$$

The nonlinear term in the system (3.28) is u^2 which is linearized as shown below:

$$\begin{aligned} u_{r+1}^2 &= u_r^2 + 2u_r\left(u_{r+1} - u_r\right) \\ &= 2u_r u_{r+1} - u_r^2. \end{aligned} \tag{3.30}$$

The solution obtained in equation (3.30) is substituted into (3.28) and the nonlinear system is decoupled using the concept of the Gauss-Seidel relaxation method to obtain:

$$\begin{aligned} u_{r+1}^{''} + \left(\frac{\eta}{2} - \frac{\eta}{2}\xi + \xi f_r\right) u_{r+1}^{'} - 2\xi u_r u_{r+1} + \xi u_r^2 + 2\xi\lambda h_r &= \xi(1-\xi)\frac{\partial u_{r+1}}{\partial \xi}, \\ h_{r+1}^{''} + \left(\frac{\eta}{2} - \frac{\eta}{2}\xi + \xi f_{r+1}\right) h_{r+1}^{'} - u_{r+1}h_{r+1} - 2\lambda u_{r+1} &= \xi(1-\xi)\frac{\partial h_{r+1}}{\partial \xi}, \\ f_{r+1}^{'} &= u_{r+1}, \end{aligned} \tag{3.31}$$

where linear terms are evaluated at the current iteration level $(r+1)$ and nonlinear terms at the previous iteration level (r). Equation (3.32) is written in a compact form as:

$$\begin{aligned} u_{r+1}^{''} + a_{1,r}u_{r+1}^{'} + a_{2,r}u_{r+1} + a_{3,r} &= \xi(1-\xi)\frac{\partial u_{r+1}}{\partial \xi}, \\ h_{r+1}^{''} + b_{1,r}h_{r+1}^{'} - b_{2,r}h_{r+1} + b_{3,r} &= \xi(1-\xi)\frac{\partial h_{r+1}}{\partial \xi}, \\ f_{r+1}^{'} &= u_{r+1}, \end{aligned} \tag{3.32}$$

where

$$\begin{aligned} a_{1,r} &= \frac{\eta}{2} - \frac{\eta}{2}\xi + \xi f_r, \\ a_{2,r} &= -2\xi u_r, \\ a_{3,r} &= \xi u_r^2 + 2\xi\lambda h_r, \\ b_{1,r} &= \frac{\eta}{2} - \frac{\eta}{2}\xi + \xi f_{r+1}, \\ b_{2,r} &= u_{r+1}, \\ b_{3,r} &= -2\lambda u_{r+1}. \end{aligned}$$

The Crank-Nicolson finite difference approach is applied on the system (3.33) and the new system obtained is:

$$
\begin{aligned}
(u_{r+1}^{''})^{n+\frac{1}{2}} + (a_{1,r})^{n+\frac{1}{2}}(u_{r+1}^{'})^{n+\frac{1}{2}} + (a_{2,r})^{n+\frac{1}{2}}(u_{r+1})^{n+\frac{1}{2}} + (a_{3,r})^{n+\frac{1}{2}} &= \xi^{n+\frac{1}{2}}(1-\xi^{n+\frac{1}{2}})(\frac{u_{r+1}^{n+1}-u_{r+1}^{n}}{\Delta\xi}),\\
(h_{r+1}^{''})^{n+\frac{1}{2}} + (b_{1,r})^{n+\frac{1}{2}}(h_{r+1}^{'})^{n+\frac{1}{2}} - (b_{2,r})^{n+\frac{1}{2}}(h_{r+1})^{n+\frac{1}{2}} + (b_{3,r})^{n+\frac{1}{2}} &= \xi^{n+\frac{1}{2}}(1-\xi^{n+\frac{1}{2}})(\frac{h_{r+1}^{n+1}-h_{r+1}^{n}}{\Delta\xi}),\\
(f_{r+1}^{'})^{n+\frac{1}{2}} &= (u_{r+1})^{n+\frac{1}{2}}.
\end{aligned} \tag{3.33}
$$

At this point, the Chebyshev pseudo-spectral collocation technique is applied to integrate the system (3.33).

(3.33) is rewritten in the spectral collocation form to obtain:

$$
\begin{aligned}
(\mathbf{D}^2\mathbf{u}_{r+1})^{n+\frac{1}{2}} + (\mathbf{a}_{1,r})^{n+\frac{1}{2}}(\mathbf{D}\mathbf{u}_{r+1})^{n+\frac{1}{2}} + (\mathbf{a}_{2,r})^{n+\frac{1}{2}}(\mathbf{u}_{r+1})^{n+\frac{1}{2}} + (\mathbf{a}_{3,r})^{n+\frac{1}{2}}&\\
= \frac{\xi^{n+\frac{1}{2}}(1-\xi^{n+\frac{1}{2}})}{\Delta\xi}(\mathbf{u}_{r+1}^{n+1}-\mathbf{u}_{r+1}^{n}),&\\
(\mathbf{D}^2\mathbf{h}_{r+1})^{n+\frac{1}{2}} + (\mathbf{b}_{1,r})^{n+\frac{1}{2}}(\mathbf{D}\mathbf{h}_{r+1})^{n+\frac{1}{2}} - (\mathbf{b}_{2,r})^{n+\frac{1}{2}}(\mathbf{h}_{r+1})^{n+\frac{1}{2}} + (\mathbf{b}_{3,r})^{n+\frac{1}{2}}&\\
= \frac{\xi^{n+\frac{1}{2}}(1-\xi^{n+\frac{1}{2}})}{\Delta\xi}(\mathbf{h}_{r+1}^{n+1}-\mathbf{h}_{r+1}^{n}),&\\
(\mathbf{D}\mathbf{f}_{r+1})^{n+\frac{1}{2}} = (\mathbf{u}_{r+1})^{n+\frac{1}{2}}.&
\end{aligned} \tag{3.34}
$$

From (3.34), taking terms at the next time level $(n+1)$ to the left and terms at the current time level (n) and nonlinear terms to the right, the system takes on the form:

$$
\begin{aligned}
&\left[\frac{1}{2}\left(\mathbf{D}^2 + \mathbf{diag}\left[\mathbf{a}_{1,r}^{n+\frac{1}{2}}\right]\mathbf{D} + \mathbf{diag}\left[\mathbf{a}_{2,r}^{n+\frac{1}{2}}\right]\right) - \frac{\xi^{n+\frac{1}{2}}\left(1-\xi^{n+\frac{1}{2}}\right)}{\Delta\xi}\right]\mathbf{U}_{r+1}^{n+1}\\
&= \left[-\frac{1}{2}\left(\mathbf{D}^2 + \mathbf{diag}\left[\mathbf{a}_{1,r}^{n+\frac{1}{2}}\right]\mathbf{D} + \mathbf{diag}\left[\mathbf{a}_{2,r}^{n+\frac{1}{2}}\right]\right) - \frac{\xi^{n+\frac{1}{2}}\left(1-\xi^{n+\frac{1}{2}}\right)}{\Delta\xi}\right]\mathbf{U}_{r+1}^{n} - \mathbf{a}_{3,r}^{n+\frac{1}{2}},\\
&\left[\frac{1}{2}\left(\mathbf{D}^2 + \mathbf{diag}\left[\mathbf{b}_{1,r}^{n+\frac{1}{2}}\right]\mathbf{D} - \mathbf{diag}\left[\mathbf{b}_{2,r}^{n+\frac{1}{2}}\right]\right) - \frac{\xi^{n+\frac{1}{2}}\left(1-\xi^{n+\frac{1}{2}}\right)}{\Delta\xi}\right]\mathbf{H}_{r+1}^{n+1}\\
&= \left[-\frac{1}{2}\left(\mathbf{D}^2 + \mathbf{diag}\left[\mathbf{b}_{1,r}^{n+\frac{1}{2}}\right]\mathbf{D} - \mathbf{diag}\left[\mathbf{b}_{2,r}^{n+\frac{1}{2}}\right]\right) - \frac{\xi^{n+\frac{1}{2}}\left(1-\xi^{n+\frac{1}{2}}\right)}{\Delta\xi}\right]\mathbf{H}_{r+1}^{n} - \mathbf{b}_{3,r}^{n+\frac{1}{2}}.
\end{aligned} \tag{3.35}
$$

This is written in a compact form as:

$$
\begin{aligned}
\mathbf{A}_1\mathbf{U}_{r+1}^{n+1} &= \mathbf{B}_1 + \mathbf{K}_1,\\
\mathbf{A}_2\mathbf{H}_{r+1}^{n+1} &= \mathbf{B}_2 + \mathbf{K}_2,\\
\mathbf{A}_3\mathbf{F}_{r+1} &= \mathbf{K}_3.
\end{aligned} \tag{3.36}
$$

where

$$\begin{aligned}
\mathbf{A}_1 &= \frac{1}{2}\left(\mathbf{D}^2 + \mathbf{diag}\left[\mathbf{a}_{1,r}^{n+\frac{1}{2}}\right]\mathbf{D} + \mathbf{diag}\left[\mathbf{a}_{2,r}^{n+\frac{1}{2}}\right]\right) - \frac{\xi^{n+\frac{1}{2}}\left(1-\xi^{n+\frac{1}{2}}\right)}{\Delta\xi}\mathbf{I},\\
\mathbf{B}_1 &= -\frac{1}{2}\left(\mathbf{D}^2 + \mathbf{diag}\left[\mathbf{a}_{1,r}^{n+\frac{1}{2}}\right]\mathbf{D} + \mathbf{diag}\left[\mathbf{a}_{2,r}^{n+\frac{1}{2}}\right]\right) - \frac{\xi^{n+\frac{1}{2}}\left(1-\xi^{n+\frac{1}{2}}\right)}{\Delta\xi}\mathbf{I},\\
\mathbf{K}_1 &= -\mathbf{a}_{3,r}^{n+\frac{1}{2}},\\
\mathbf{A}_2 &= \frac{1}{2}\left(\mathbf{D}^2 + \mathbf{diag}\left[\mathbf{b}_{1,r}^{n+\frac{1}{2}}\right]\mathbf{D} - \mathbf{diag}\left[\mathbf{b}_{2,r}^{n+\frac{1}{2}}\right]\right) - \frac{\xi^{n+\frac{1}{2}}\left(1-\xi^{n+\frac{1}{2}}\right)}{\Delta\xi}\mathbf{I},\\
\mathbf{B}_2 &= -\frac{1}{2}\left(\mathbf{D}^2 + \mathbf{diag}\left[\mathbf{b}_{1,r}^{n+\frac{1}{2}}\right]\mathbf{D} - \mathbf{diag}\left[\mathbf{b}_{2,r}^{n+\frac{1}{2}}\right]\right) - \frac{\xi^{n+\frac{1}{2}}\left(1-\xi^{n+\frac{1}{2}}\right)}{\Delta\xi}\mathbf{I},\\
\mathbf{K}_2 &= -\mathbf{b}_{3,r}^{n+\frac{1}{2}},\\
\mathbf{A}_3 &= \mathbf{D},\\
\mathbf{K}_3 &= \mathbf{U}_{r+1}.
\end{aligned}$$

3.3.3 Spectral Quasi-Linearization Method(SQLM)

In this subsection, the SQLM is applied on the system (3.4) and the corresponding boundary conditions (3.5). This is done by identifying both univariate and multivariate nonlinear terms and applying Taylor series expansion on the nonlinear terms so as to obtain a linear coupled system of equations. In this case however, unlike with the other two methods (SRM and SLLM), the system of equations are solved in a coupled manner.

$$\begin{aligned}
f''' + \frac{1}{2}(1-\xi)\eta f'' + \xi(ff'' - f'^2 + 2\lambda h) &= \xi(1-\xi)\frac{\partial f'}{\partial \xi}, \\
h'' + \frac{1}{2}(1-\xi)\eta h' + \xi(fh' - f'h - 2\lambda f') &= \xi(1-\xi)\frac{\partial h}{\partial \xi},
\end{aligned} \tag{3.37}$$

with corresponding boundary conditions

$$f(0,\xi) = 0, \quad f'(0,\xi) = 1, \quad h(0,\xi) = 0, \quad h(\infty,\xi) = 0, \quad f'(\infty,\xi) = 0. \tag{3.38}$$

From (3.38), Taylor series expansion is applied on the nonlinear terms $f'^2,\ ff'',\ fh'\ \ f'h$ in the forms shown below:

$$\begin{aligned} f_{r+1}^{'2} &= f_r^{'2} + 2f_{'r}\left(f_{r+1}^{'} - f_r^{'}\right) \\ &= 2f_{'r}f_{r+1}^{'2} - f_r^{'2}, \end{aligned} \tag{3.39}$$

,

$$\begin{aligned} f_{r+1}f_{r+1}^{''} &= f_r f_r^{''} + f_r\left(f_{r+1}^{''} - f_r^{''}\right) + f_r^{''}\left(f_{r+1} - f_r\right) \\ &= f_r f_{r+1}^{''} + f_r^{''} f_{r+1} - f_r f_r^{''}, \end{aligned} \tag{3.40}$$

,

$$\begin{aligned} f_{r+1}h_{r+1}^{'} &= f_r h_r^{'} + h_r^{'}\left(f_{r+1} - f_r\right) + f_r\left(h_{r+1} - h_r\right) \\ &= f_r h_{r+1}^{'} + h_r^{'} f_{r+1} - f_r h_r^{'}, \end{aligned} \tag{3.41}$$

$$\begin{aligned} f_{r+1}^{'}h_{r+1} &= f_r^{'}h_r + h_r\left(f_{r+1}^{'} - f_r^{'}\right) + f_r^{'}\left(h_{r+1} - h_r\right) \\ &= f_r^{'}h_{r+1} + h_r f_{r+1}^{'} - f_r^{'}h_r. \end{aligned} \tag{3.42}$$

The solutions obtained in (3.39 - 3.42) are inserted into the system (3.38) and the linear coupled system is obtained:

$$\begin{aligned} f_{r+1}^{'''} + \left(\frac{\eta}{2} - \frac{\eta}{2}\xi + \xi f_r\right) f_{r+1}^{''} - 2\xi f_r^{'} f_{r+1}^{'} + \xi f_r^{''} f_{r+1} - \xi f_r f_r^{''} + \xi f_r^{'2} \\ +2\xi\lambda h_{r+1} = \xi(1-\xi)\frac{\partial f_{r+1}^{'}}{\partial\xi}, \\ h_{r+1}^{''} + \left(\frac{\eta}{2} - \frac{\eta}{2}\xi + \xi f_r\right) h_{r+1}^{'} - \xi f_r^{'} h_{r+1} + \xi h_r^{'} f_{r+1} - (\xi h_r - 2\lambda) f_{r+1}^{'} - \xi f_r h_r^{'} \\ +\xi f_r^{'} h_r = \xi(1-\xi)\frac{\partial h_{r+1}}{\partial\xi}, \end{aligned} \tag{3.43}$$

where linear terms are evaluated at the current iteration level $(r+1)$ and nonlinear terms at the previous iteration level (r). (3.43) is given in a compact form as;

$$\begin{aligned} f_{r+1}^{'''} + a_{1,r}f_{r+1}^{''} + a_{2,r}f_{r+1}^{'} + a_{3,r}f_{r+1} + a_{4,r}h_{r+1} + a_{5,r} &= \xi(1-\xi)\frac{\partial f_{r+1}^{'}}{\partial\xi}, \\ h_{r+1}^{''} + b_{1,r}h_{r+1}^{'} + b_{2,r}h_{r+1} + b_{3,r}f_{r+1}^{'} + b_{4,r}f_{r+1} + b_{5,r} &= \xi(1-\xi)\frac{\partial h_{r+1}}{\partial\xi}, \end{aligned} \tag{3.44}$$

where

$$\begin{aligned}
a_{1,r} &= \frac{\eta}{2} - \frac{\eta}{2}\xi + \xi f_r, \\
a_{2,r} &= -2\xi f_r^{'}, \\
a_{3,r} &= \xi f_r^{''}, \\
a_{4,r} &= 2\xi\lambda, \\
a_{5,r} &= -\xi f_r f_r^{''} + \xi f_r^{'2}, \\
b_{1,r} &= \frac{\eta}{2} - \frac{\eta}{2}\xi + \xi f_r, \\
b_{2,r} &= -\xi f_r^{'}, \\
b_{3,r} &= -2\xi\lambda - \xi h_r, \\
b_{4,r} &= \xi h_r^{'}, \\
b_{5,r} &= -\xi f_r h_r^{'} + \xi f_r^{'} h_r.
\end{aligned} \tag{3.45}$$

The Crank-Nicolson finite difference approach is applied on the system (3.44) and the system becomes:

$$\begin{aligned}
&(f_{r+1}^{'''})^{n+\frac{1}{2}} + (a_{1,r})^{n+\frac{1}{2}}(f_{r+1}^{''})^{n+\frac{1}{2}} + (a_{2,r})^{n+\frac{1}{2}}(f_{r+1}^{'})^{n+\frac{1}{2}} + (a_{3,r})^{n+\frac{1}{2}}(f_{r+1})^{n+\frac{1}{2}} + \\
&\qquad (a_{4,r})^{n+\frac{1}{2}}(h_{r+1})^{n+\frac{1}{2}} + (a_{5,r})^{n+\frac{1}{2}} = \xi^{n+\frac{1}{2}}(1-\xi^{n+\frac{1}{2}})\frac{f^{'n+1}_{r+1} - f^{'n}_{r+1}}{\Delta\xi}, \\
&(h_{r+1}^{''})^{n+\frac{1}{2}} + (b_{1,r})^{n+\frac{1}{2}}(h_{r+1}^{'})^{n+\frac{1}{2}} + (b_{2,r})^{n+\frac{1}{2}}(h_{r+1})^{n+\frac{1}{2}} + (b_{3,r})^{n+\frac{1}{2}}(f_{r+1}^{'})^{n+\frac{1}{2}} + \\
&\qquad (b_{4,r})^{n+\frac{1}{2}}(f_{r+1})^{n+\frac{1}{2}} + (b_{5,r})^{n+\frac{1}{2}} = \xi^{n+\frac{1}{2}}(1-\xi^{n+\frac{1}{2}})\frac{h^{n+1}_{r+1} - h^{n}_{r+1}}{\Delta\xi}.
\end{aligned} \tag{3.46}$$

The Chebyshev pseudo-spectral collocation technique is applied to integrate system (3.46). System (3.46) is rewritten in the spectral collocation form to obtain:

$$\begin{aligned}
&(D^2 f_{r+1}^{'})^{n+\frac{1}{2}} + (a_{1,r})^{n+\frac{1}{2}}(Df_{r+1}^{'})^{n+\frac{1}{2}} + (a_{2,r})^{n+\frac{1}{2}}(f_{r+1}^{'})^{n+\frac{1}{2}} + (a_{3,r})^{n+\frac{1}{2}}(f_{r+1})^{n+\frac{1}{2}} + \\
&\qquad (a_{4,r})^{n+\frac{1}{2}}(h_{r+1})^{n+\frac{1}{2}} + (a_{5,r})^{n+\frac{1}{2}} = \xi^{n+\frac{1}{2}}(1-\xi^{n+\frac{1}{2}})\frac{f^{'n+1}_{r+1} - f^{'n}_{r+1}}{\Delta\xi}, \\
&(D^2 h_{r+1})^{n+\frac{1}{2}} + (b_{1,r})^{n+\frac{1}{2}}(Dh_{r+1})^{n+\frac{1}{2}} + (b_{2,r})^{n+\frac{1}{2}}(h_{r+1})^{n+\frac{1}{2}} + (b_{3,r})^{n+\frac{1}{2}}(f_{r+1}^{'})^{n+\frac{1}{2}} + \\
&\qquad (b_{4,r})^{n+\frac{1}{2}}(f_{r+1})^{n+\frac{1}{2}} + (b_{5,r})^{n+\frac{1}{2}} = \xi^{n+\frac{1}{2}}(1-\xi^{n+\frac{1}{2}})\frac{h^{n+1}_{r+1} - h^{n}_{r+1}}{\Delta\xi}.
\end{aligned} \tag{3.47}$$

From (3.47), taking terms at the next time level $(n+1)$ to the left and terms at the current time level (n) and nonlinear terms to the right, the system becomes:

$$\left[\frac{1}{2}\left(\mathbf{D}^3+\mathbf{a}_{1,r}^{n+\frac{1}{2}}\mathbf{D}^2+\mathbf{a}_{3,r}^{n+\frac{1}{2}}\right)-\frac{\xi^{n+\frac{1}{2}}\left(1-\xi^{n+\frac{1}{2}}\right)}{\Delta\xi}\mathbf{D}\right]\mathbf{F}_{r+1}^{n+1}+\frac{1}{2}\mathbf{a}_{4,r}^{n+\frac{1}{2}}\mathbf{H}_{r+1}^{n+1}=$$
$$\left[-\frac{1}{2}\left(\mathbf{D}^3+\mathbf{a}_{1,r}^{n+\frac{1}{2}}\mathbf{D}^2+\mathbf{a}_{3,r}^{n+\frac{1}{2}}\right)-\frac{\xi^{n+\frac{1}{2}}\left(1-\xi^{n+\frac{1}{2}}\right)}{\Delta\xi}\mathbf{D}\right]\mathbf{F}_{r+1}^{n}-\frac{1}{2}\mathbf{a}_{4,r}^{n+\frac{1}{2}}\mathbf{H}_{r+1}^{n}-\mathbf{a}_{5,r}^{n+\frac{1}{2}},$$
$$\left[\frac{1}{2}\left(\mathbf{b}_{3,r}^{n+\frac{1}{2}}\mathbf{D}+\mathbf{b}_{4,r}^{n+\frac{1}{2}}\right)\right]\mathbf{F}_{r+1}^{n+1}+\left[\frac{1}{2}\left(\mathbf{D}^2+\mathbf{b}_{1,r}^{n+\frac{1}{2}}\mathbf{D}+\mathbf{b}_{2,r}^{n+\frac{1}{2}}\right)-\frac{\xi^{n+\frac{1}{2}}\left(1-\xi^{n+\frac{1}{2}}\right)}{\Delta\xi}\right]\mathbf{H}_{r+1}^{n+1}=$$
$$\left[-\frac{1}{2}\left(\mathbf{b}_{3,r}^{n+\frac{1}{2}}\mathbf{D}+\mathbf{b}_{4,r}^{n+\frac{1}{2}}\right)\right]\mathbf{F}_{r+1}^{n}+\left[-\frac{1}{2}\left(\mathbf{D}^2+\mathbf{b}_{1,r}^{n+\frac{1}{2}}\mathbf{D}+\mathbf{b}_{2,r}^{n+\frac{1}{2}}\right)-\frac{\xi^{n+\frac{1}{2}}\left(1-\xi^{n+\frac{1}{2}}\right)}{\Delta\xi}\right]\mathbf{H}_{r+1}^{n}-\mathbf{b}_{5,r}^{n+\frac{1}{2}}. \tag{3.48}$$

The system (3.48) is written in a compact form as:

$$\begin{aligned}\mathbf{A}_{11}\mathbf{F}_{r+1}^{n+1}+\mathbf{A}_{12}\mathbf{H}_{r+1}^{n+1} &= \mathbf{B}_{11}\mathbf{F}_{r+1}^{n}+\mathbf{B}_{12}\mathbf{H}_{r+1}^{n}+\mathbf{K}_1,\\ \mathbf{A}_{21}\mathbf{F}_{r+1}^{n+1}+\mathbf{A}_{22}\mathbf{H}_{r+1}^{n+1} &= \mathbf{B}_{21}\mathbf{F}_{r+1}^{n}+\mathbf{B}_{22}\mathbf{H}_{r+1}^{n}+\mathbf{K}_2,\end{aligned} \tag{3.49}$$

where

$$\begin{aligned}\mathbf{A}_{11} &= \frac{1}{2}\left(\mathbf{D}^3+\mathbf{a}_{1,r}^{n+\frac{1}{2}}\mathbf{D}^2+\mathbf{a}_{2,r}^{n+\frac{1}{2}}\mathbf{D}+\mathbf{a}_{3,r}^{n+\frac{1}{2}}\right)-\frac{\xi^{n+\frac{1}{2}}\left(1-\xi^{n+\frac{1}{2}}\right)}{\Delta\xi}\mathbf{D},\\ \mathbf{A}_{12} &= \frac{1}{2}\mathbf{a}_{4,r}^{n+\frac{1}{2}},\\ \mathbf{B}_{11} &= -\frac{1}{2}\left(\mathbf{D}^3+\mathbf{a}_{1,r}^{n+\frac{1}{2}}\mathbf{D}^2+\mathbf{a}_{2,r}^{n+\frac{1}{2}}\mathbf{D}+\mathbf{a}_{3,r}^{n+\frac{1}{2}}\right)-\frac{\xi^{n+\frac{1}{2}}\left(1-\xi^{n+\frac{1}{2}}\right)}{\Delta\xi}\mathbf{D},\\ \mathbf{B}_{12} &= -\frac{1}{2}\mathbf{a}_{4,r}^{n+\frac{1}{2}},\\ \mathbf{A}_{21} &= \frac{1}{2}\left(\mathbf{b}_{3,r}^{n+\frac{1}{2}}\mathbf{D}+\mathbf{b}_{4,r}^{n+\frac{1}{2}}\right),\\ \mathbf{A}_{22} &= \frac{1}{2}\left(\mathbf{D}^2+\mathbf{b}_{1,r}^{n+\frac{1}{2}}\mathbf{D}+\mathbf{b}_{2,r}^{n+\frac{1}{2}}\right)-\frac{\xi^{n+\frac{1}{2}}\left(1-\xi^{n+\frac{1}{2}}\right)}{\Delta\xi}\mathbf{I},\\ \mathbf{B}_{21} &= -\frac{1}{2}\left(\mathbf{b}_{3,r}^{n+\frac{1}{2}}\mathbf{D}+\mathbf{b}_{4,r}^{n+\frac{1}{2}}\right),\\ \mathbf{B}_{22} &= -\frac{1}{2}\left(\mathbf{D}^2+\mathbf{b}_{1,r}^{n+\frac{1}{2}}\mathbf{D}+\mathbf{b}_{2,r}^{n+\frac{1}{2}}\right)-\frac{\xi^{n+\frac{1}{2}}\left(1-\xi^{n+\frac{1}{2}}\right)}{\Delta\xi}\mathbf{I},\\ \mathbf{K}_1 &= -\mathbf{a}_{5,r}^{n+\frac{1}{2}},\\ \mathbf{K}_2 &= -b_{5,r}^{n+\frac{1}{2}}.\end{aligned}$$

The system (3.49) is solved in a matrix system as shown below.

$$\begin{bmatrix} \mathbf{A}_{11} & \mathbf{A}_{12} \\ \mathbf{A}_{21} & \mathbf{A}_{22} \end{bmatrix} \times \begin{bmatrix} \mathbf{F}_{r+1}^{n+1} \\ \mathbf{H}_{r+1}^{n+1} \end{bmatrix} = \begin{bmatrix} \mathbf{B}_{11} & \mathbf{B}_{12} \\ \mathbf{B}_{21} & \mathbf{B}_{22} \end{bmatrix} \times \begin{bmatrix} \mathbf{F}_{r+1}^{n} \\ \mathbf{H}_{r+1}^{n} \end{bmatrix} + \begin{bmatrix} \mathbf{K}_1 \\ \mathbf{K}_2 \end{bmatrix},$$

where all the entries of the coupled matrix system are all matrices and boundary conditions are imposed on all the matrices as follows:

$$\mathbf{A}_{11} = \begin{bmatrix} \mathbf{D}_{0,0} & \mathbf{D}_{0,1} & \cdots & \mathbf{D}_{0,N-1} & \mathbf{D}_{0,N} \\ \hline & & \mathbf{A}_{11} & & \\ \hline \mathbf{D}_{N,0} & \mathbf{D}_{N,1} & \cdots & \mathbf{D}_{N,N-1} & \mathbf{D}_{N,N} \\ \hline 0 & 0 & \cdots & 0 & 1 \end{bmatrix}, \quad \mathbf{A}_{12} = \begin{bmatrix} 0 & 0 & \cdots & 0 & 0 \\ \hline & & \mathbf{A}_{12} & & \\ \hline 0 & 0 & \cdots & 0 & 0 \\ \hline 0 & 0 & \cdots & 0 & 0 \end{bmatrix},$$

$$\mathbf{A}_{21} = \begin{bmatrix} 0 & 0 & \cdots & 0 & 0 \\ \hline & & \mathbf{A}_{21} & & \\ & & & & \\ \hline 0 & 0 & \cdots & 0 & 0 \end{bmatrix}, \quad \mathbf{A}_{22} = \begin{bmatrix} 1 & 0 & \cdots & 0 & 0 \\ \hline & & \mathbf{A}_{22} & & \\ & & & & \\ \hline 0 & 0 & \cdots & 0 & 1 \end{bmatrix}, \quad \mathbf{B}_{11} = \begin{bmatrix} 0 & 0 & \cdots & 0 & 0 \\ \hline & & \mathbf{B}_{11} & & \\ \hline 0 & 0 & 0 & 0 & \\ \hline 0 & 0 & \cdots & 0 & 0 \end{bmatrix},$$

$$\mathbf{B}_{12} = \begin{bmatrix} 0 & 0 & \cdots & 0 & 0 \\ \hline & & \mathbf{B}_{12} & & \\ \hline 0 & 0 & \cdots & 0 & 0 \\ \hline 0 & 0 & \cdots & 0 & 0 \end{bmatrix}, \quad \mathbf{B}_{21} = \begin{bmatrix} 0 & 0 & \cdots & 0 & 0 \\ \hline & & \mathbf{B}_{21} & & \\ & & & & \\ \hline 0 & 0 & \cdots & 0 & 0 \end{bmatrix}, \quad \mathbf{B}_{22} = \begin{bmatrix} 0 & 0 & \cdots & 0 & 0 \\ \hline & & \mathbf{B}_{22} & & \\ & & & & \\ \hline 0 & 0 & \cdots & 0 & 0 \end{bmatrix},$$

$$\mathbf{K}_1 = \begin{bmatrix} 0 \\ \hline \\ \mathbf{K}_1 \\ \\ \hline 1 \\ \hline 0 \end{bmatrix}, \quad \mathbf{K}_2 = \begin{bmatrix} 0 \\ \hline \\ \mathbf{K}_2 \\ \\ \hline 0 \end{bmatrix}, \quad \mathbf{F}_{r+1}^{n+1} = \begin{bmatrix} f_{r+1,0}^{n+1} \\ \hline \vdots \\ \\ \vdots \\ \hline f_{r+1,N-1}^{n+1} \\ \hline f_{r+1,N}^{n+1} \end{bmatrix}, \quad \mathbf{H}_{r+1}^{n+1} = \begin{bmatrix} h_{r+1,0}^{n+1} \\ \hline \vdots \\ \\ \\ \vdots \\ \hline h_{r+1,N}^{n+1} \end{bmatrix},$$

$$\mathbf{F}^{n}_{r+1}=\begin{bmatrix} f^{n}_{r+1,0} \\ \hline \vdots \\ \vdots \\ \hline f^{n}_{r+1,N-1} \\ \hline f^{n}_{r+1,N} \end{bmatrix}, \quad \mathbf{H}^{n}_{r+1}=\begin{bmatrix} h^{n}_{r+1,0} \\ \hline \vdots \\ \vdots \\ \\ \hline h^{n}_{r+1,N} \end{bmatrix}.$$

3.4 Results and Discussion

In this section, the numerical solutions for the system of partial differential equations (3.4) with their corresponding boundary conditions (3.5) by applying the SRM, SLLM and SQLM are presented. The results for the reduced skin frictions $f''(\xi,0)$ and $h'(\xi,0)$ at selected time (ξ) are displayed. Comparison is carried out on the solutions obtained by the three methods (SRM, SLLM and SQLM) to investigate how well they compare with each other. Comparison will be carried out by noting the effect of iterations and the effect of the time (ξ) on the accuracy of the solutions.

For the purpose of this study, the parameters used were assigned specific values except where mentioned otherwise. The value of the dimensionless angular velocity parameter was set at $\lambda = 1$. The number of grid points used in the space direction was $N_x = 100$ while the number of grid points in the time direction was $N_t = 1000$ and the truncated interval length $L = 20$.

Table 3.1: Comparison of skin friction $-f^{''}(0)$ obtained by the SRM, SLLM and the SQLM and number of iterations

ξ	SRM	It	SQLM	It	SLLM	It
0.1	0.61428287	4	0.61428287	2	0.61428287	4
0.3	0.73654114	4	0.73654114	2	0.73654114	4
0.5	0.89009105	4	0.89009105	2	0.89009105	4
0.7	1.07496070	4	1.07496070	2	1.07496070	4
0.8	1.17552926	4	1.17552926	2	1.17552926	4
0.9	1.268509	4	1.268509	3	1.268509	4
0.95	1.29784374	4	1.29784374	3	1.29784374	4
0.98	1.30642538	4	1.30642538	3	1.30642538	4

Table 3.2: Comparison of skin friction $-h^{'}(0)$ obtained by the SRM, SLLM and the SQLM and number of iterations

ξ	SRM	It	SQLM	It	SLLM	It
0.1	0.11240250	4	0.11240250	2	0.11240250	4
0.3	0.33186306	4	0.33186306	2	0.33186306	4
0.5	0.53589926	4	0.53589926	2	0.53589926	4
0.7	0.70709868	4	0.70709868	2	0.70709868	4
0.8	0.76911999	4	0.76911999	2	0.76911999	4
0.9	0.80301605	4	0.80301605	3	0.80301605	4
0.95	0.80987344	4	0.80987344	3	0.80987344	4
0.98	0.82513649	4	0.82513649	3	0.82513649	4

Tables 3.1 and 3.2 show numerical solutions obtained by the SRM, SLLM and SQLM. The numerical solutions for the skin frictions $f^{''}$ and $h^{'}$ obtained for the three methods are consistent with each other at different values of ξ. It is observed from both Tables that the SQLM converges fastest to 8 decimal places than the SRM and the SQLM. The SQLM converged after 2 iterations for values of ξ between $0.1 \leq \xi \leq 0.8$ and after 3 iterations for the remaining values of ξ. The SRM and SLLM converged after 4 iterations for all values of ξ.

Figures 3.2 - 3.5 gives the graphical representation of the number of iterations and time on the residual error norm of the solutions obtained. Convergence and accuracy is determined by the use of the infinity norm for the residual error which is obtained by inserting the approximate solutions obtained with the SRM, SLLM and SQLM into the original system of partial differential equations (3.4). The residual error of the methods are obtained from:

$$\begin{aligned} Res(\mathbf{f}) &= f^{'''} + \frac{1}{2}(1-\xi)\eta f^{''} + \xi(ff^{''} - f^{'2} + 2\lambda h) - \xi(1-\xi)\frac{\partial f^{'}}{\partial \xi}, \\ Res(\mathbf{h}) &= h^{''} + \frac{1}{2}(1-\xi)\eta h^{'} + \xi(fh^{'} - f^{'}h - 2\lambda f^{'}) - \xi(1-\xi)\frac{\partial h}{\partial \xi}, \end{aligned} \tag{3.50}$$

where the system of equations (3.50) are made up of approximate solutions that are obtained using the SRM, SLLM and SQLM. The infinity norms in (3.50) are defined as

$$\begin{aligned} IN_r(\mathbf{f}) &= ||Res(\mathbf{f})||_\infty, \\ IN_r(\mathbf{h}) &= ||Res(\mathbf{h})||_\infty. \end{aligned} \tag{3.51}$$

The residual error is obtained at each iteration level for a fixed time ξ. The point where the residual error is smallest is referred to as the *optimal residual error* and this point is used to estimate the number of iterations it takes each method to converge fully.

Table 3.3: Convergence of $||Res(\mathbf{f})||_\infty$ obtained using the SRM, SLLM and SQLM at $\xi = 0.2$

	SQLM	SRM	SLLM
iterations	$\|\|Res(\mathbf{f})\|\|_\infty$	$\|\|Res(\mathbf{f})\|\|_\infty$	$\|\|Res(\mathbf{f})\|\|_\infty$
1	8.2×10^{-5}	1.1×10^{-2}	1.5×10^{-2}
2	1.2×10^{-10}	9.0×10^{-6}	3.2×10^{-6}
3	2.3×10^{-10}	8.0×10^{-9}	1.3×10^{-9}
4	2.7×10^{-10}	7.6×10^{-12}	6.3×10^{-13}
5	2.4×10^{-10}	1.5×10^{-12}	6.3×10^{-13}
6	2.2×10^{-10}	1.5×10^{-12}	6.3×10^{-13}
7	3.2×10^{-10}	1.5×10^{-12}	6.3×10^{-13}
8	2.4×10^{-10}	1.5×10^{-12}	6.3×10^{-13}
9	2.4×10^{-10}	1.5×10^{-12}	6.3×10^{-13}
10	2.4×10^{-10}	1.5×10^{-12}	6.3×10^{-13}
11	2.8×10^{-10}	1.5×10^{-12}	6.3×10^{-13}
12	2.1×10^{-10}	1.5×10^{-12}	6.3×10^{-13}
13	2.6×10^{-10}	1.5×10^{-12}	6.3×10^{-13}
14	2.3×10^{-10}	1.5×10^{-12}	6.3×10^{-13}
15	2.4×10^{-10}	1.5×10^{-12}	6.3×10^{-13}

Table 3.4: Convergence of $||Res(\mathbf{h})||_\infty$ obtained using the SRM, SLLM and SQLM at $\xi = 0.2$

iterations	SQLM $\|\|Res(\mathbf{f})\|\|_\infty$	SRM $\|\|Res(\mathbf{f})\|\|_\infty$	SLLM $\|\|Res(\mathbf{f})\|\|_\infty$
1	1.7×10^{-4}	2.1×10^{-4}	2.1×10^{-4}
2	6.4×10^{-14}	4.5×10^{-8}	5.8×10^{-7}
3	8.0×10^{-14}	3.2×10^{-11}	1.1×10^{-10}
4	1.1×10^{-13}	2.8×10^{-14}	1.1×10^{-13}
5	1.6×10^{-13}	1.1×10^{-14}	1.1×10^{-13}
6	5.7×10^{-14}	1.1×10^{-14}	1.1×10^{-13}
7	1.2×10^{-13}	1.1×10^{-14}	1.1×10^{-13}
8	1.1×10^{-13}	1.1×10^{-14}	1.1×10^{-13}
9	1.5×10^{-13}	1.1×10^{-14}	1.1×10^{-13}
10	8.9×10^{-14}	1.1×10^{-14}	1.1×10^{-13}
11	9.4×10^{-14}	1.1×10^{-14}	1.1×10^{-13}
12	1.5×10^{-13}	1.1×10^{-14}	1.1×10^{-13}
13	1.7×10^{-13}	1.1×10^{-14}	1.1×10^{-13}
14	1.8×10^{-13}	1.1×10^{-14}	1.1×10^{-13}
15	1.3×10^{-13}	1.1×10^{-14}	1.1×10^{-13}

Tables 3.3 and 3.4 display the residual error norm of the solutions for the system of partial differential equations (3.4) obtained using the SRM, SLLM and the SQLM. It is seen from the tables that as the number of iterations increase, the norm of the residual decreases implying that accuracy of the approximate solutions obtained using the three methods improve as the number of iterations increase. The norm of the residual decreases continually until convergence is achieved. The point of convergence gives the level of accuracy of the methods. It can be seen from Tables 3.3 and 3.4 that the SQLM converges immediately at the 2^{nd} iteration making it faster than the SRM and the SLLM that both take 4 iterations to converge. It is also observed that the SQLM does not attain full convergence as the residual norms are slightly different while the SRM and the SLLM attain full convergence. Furthermore, it is observed in Table 3.3 that the SQLM converges to a larger residual error norm than the SRM and SLLM which indicates that the SQLM has lesser accuracy when compared to the SRM and the SLLM while

in Table 3.4, the residual error norms of the three methods are closely comparable.

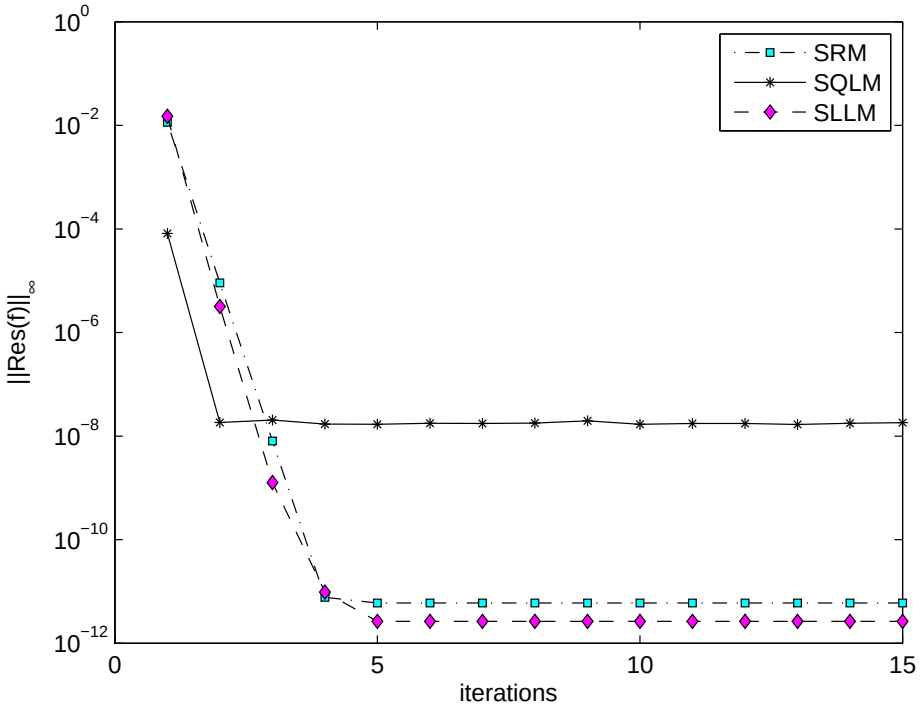

Figure 3.2: Effect of iterations on $||Res(f)||_{\infty}$ at $\xi = 0.2$

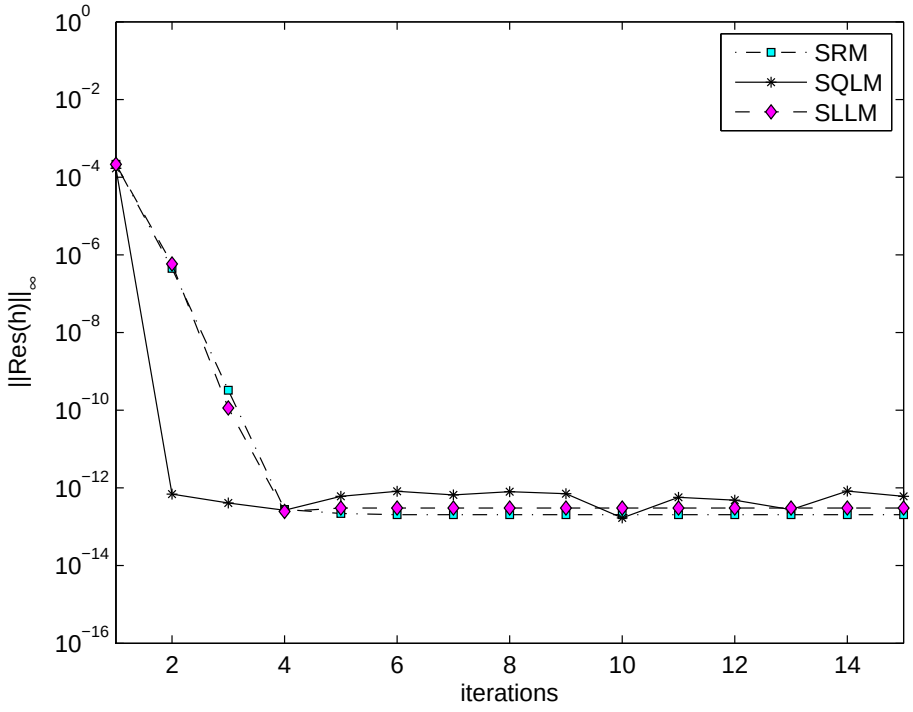

Figure 3.3: Effect of iterations on $||Res(h)||_{\infty}$ at $\xi = 0.2$

Figures 3.2 and 3.3 show the variation of the residual error against the number of iterations. As the number of iterations increase, the norm of the residual error of the three methods can be seen to decrease until a point where convergence of the norm is attained. At that point, *optimal residual error* is said to have been obtained.

Figure 3.2 shows that the residual error of the SQLM decreases sharply to an *optimum* value which is reached at the 2^{nd} iteration. The *optimal residual error norm* is attained at about 10^{-8}. The residual errors of the SRM and the SLLM are seen to decrease as the number of iterations increase and both residual errors are seen to decrease beyond the *optimal* residual error obtained by the SQLM which implies that the SQLM converges faster than the other methods but to a less accurate solution than the SRM and the SLLM. The *optimal* residual error of the SRM is obtained at the 4^{th} iteration and that of the SLLM at the 5^{th} iteration both to accuracies close to 10^{-12} hence implying that the SRM and the SLLM are comparable in terms of their accuracy. It can also be seen that due to the fact that the SQLM converges after the 2^{nd} iteration, convergence rate cannot be determined for the method but the SLLM

has a convergence rate of 0.92 while the SRM converges at the rate of 0.99 which implies that the SRM and SLLM converges linearly hence making the two methods also comparable in terms of their convergence rate.

From Figure 3.3, it can be observed that the residual error norm of the SQLM converges at 10^{-13} which is the same point where the SRM and the SLLM attains convergence as well. The SQLM converges after 2 iterations while the SLLM and the SRM take 4 iterations to attain the same accuracy. Hence the three methods can be seen to be comparable in terms of accuracy though it takes the SQLM fewer iterations to get to that point making it faster in convergence. The convergence rate of the SQLM cannot be determined here because it converges at the second iteration while the SRM has a convergence rate of 0.86 and the SLLM converges at a rate of 0.84. The SRM and the SLLM are comparable in terms of their convergence rate since they converge almost linearly. The slope of the SQLM can be seen to be steeper than the slopes for the SRM and the SLLM which indicates that the SQLM converges faster than the other methods.

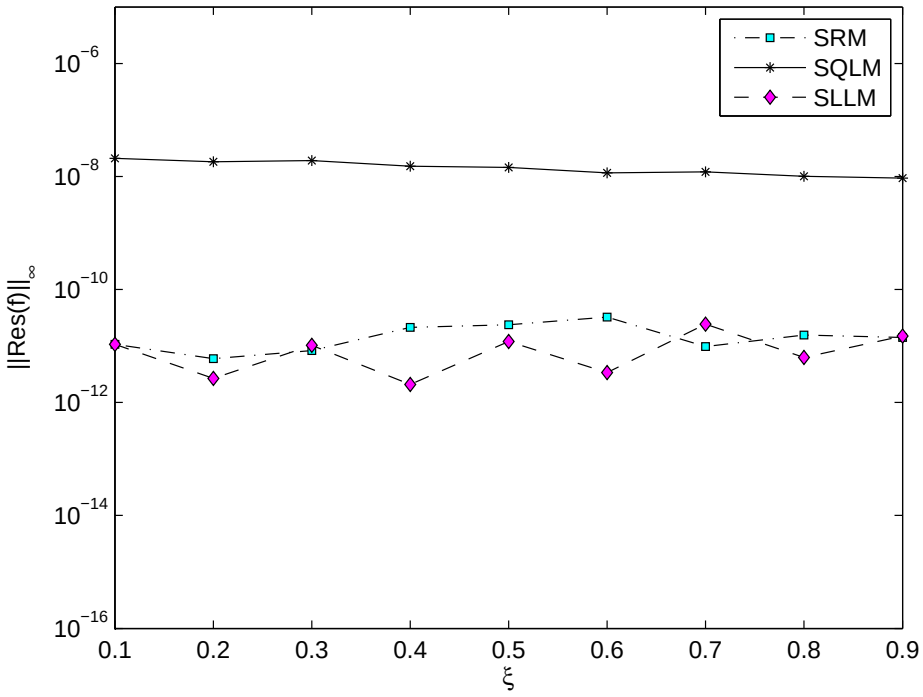

Figure 3.4: Effect of time (ξ) on $||Res(f)||_\infty$ at $\eta = 20$

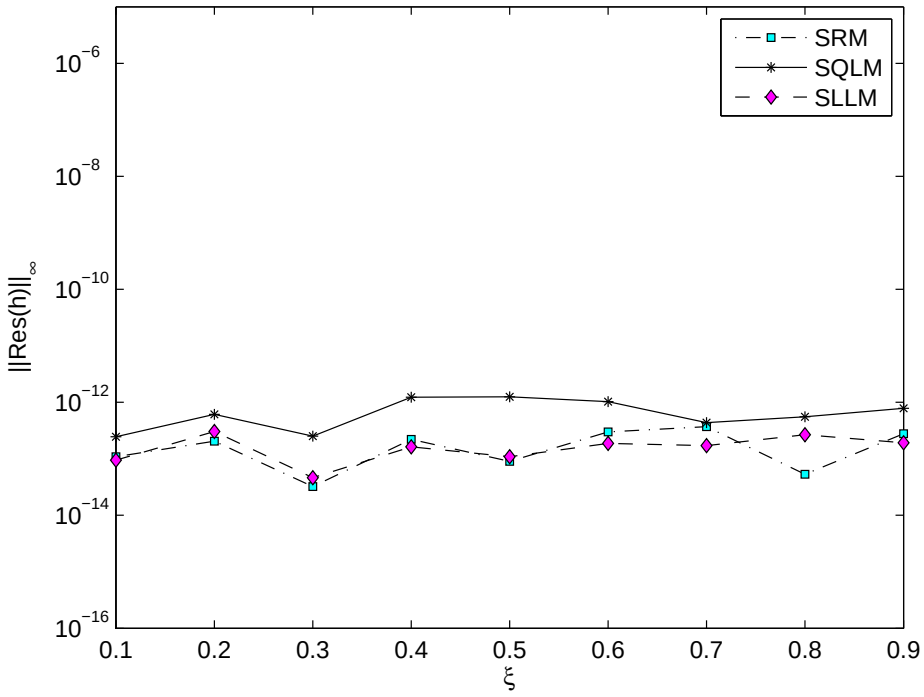

Figure 3.5: Effect of time (ξ) on $||Res(h)||_\infty$ at $\eta = 20$

Figures 3.4 - 3.5 show the variation of the residual errors with time ξ at the 15^{th} iteration at full convergence of each method. The figures are displayed at selected values of the grid points in the time direction Nt to observe the trend of the graphs properly.

As shown in Figure 3.4, it is seen that as the time ξ goes from unsteady state to steady state, the residual error norm of the three methods do not improve. The SQLM can be seen to maintain an accuracy close to 10^{-8} while the SRM and the SLLM both maintain accuracy of 10^{-11}. It is observed that the SRM and the SLLM compare well in terms of accuracy.

It can be seen in Figure 3.5 that the residual errors of the three methods are at about 10^{-13} for all values of ξ. The trend observed shows that when full convergence of solutions is attained, time ξ has no significant impact on the solutions obtained by the three numerical methods. This shows that the three methods are comparable in terms of their accuracies here.

3.5 Summary

This study successfully extended the SRM, SLLM and SQLM applied on the system of ordinary differential equations (2.8-2.10) in chapter 2 to a system of partial differential equations (3.4) which modeled an unsteady boundary layer flow due to a stretching surface in a rotating fluid. Approximate solutions were obtained for skin friction coefficients and comparison of the accuracy of the three methods was carried out using the values obtained. The solution obtained using the three methods were compared against one another for validation. The Norm of residual error was obtained for the three methods and was plotted against number of iterations taken to achieve convergence of solution and time (ξ).

The result obtained from this investigation follows the observation made on the system of ordinary differential equations in Chapter 2 regarding how iterations led to convergence of solutions. It was observed that an increase in the number of iterations improve the accuracy of solutions obtained till convergence was achieved. It was also shown that the time ξ did not really affect the accuracy of the solutions as accuracy was found to be uniform throughout ξ.

Taken together, these results suggest that the SRM, SLLM and SQLM are very efficient and produce accurate results but the SRM and the SLLM are more accurate than the SQLM. The SQLM was observed to take fewer iterations though to achieve best accuracy when compared to the other two methods. Also, it was noted that when the optimal accuracy was obtained for all three methods, an increase in the number of iterations neither increased nor decreased the accuracy of the solutions obtained.

In general, it was observed that the three methods are easy to implement, have straightforward algorithms, converge quite fast and have very good accuracies. The SRM, SLLM and SQLM have been applied on a system of ordinary differential equations and now a system of partial differential equations and similar conclusions have been drawn. In the next chapter, an unsteady three-dimensional MHD boundary layer flow and heat transfer over an impulsively stretching plate that is modeled by a system of three partial differential equations is investigated.

Chapter 4

Unsteady three-dimensional MHD boundary layer flow and heat transfer over an impulsively stretching plate

4.1 Introduction

In this chapter, the problem of an unsteady three-dimensional boundary layer flow and heat transfer induced by an impulsively stretched plane surface in two lateral directions in the presence of a magnetic field is studied using the SRM, SLLM and SQLM. The application of MHD flow problems extend to a variety of industrial fields. It is applied in metallurgical processes and in the molten metals purification (Takhar and Nath, 1998; Hang and Pop, 2007; Kumari and Nath, 2009). It is also applied in petroleum and agricultural processes (Pal and Mondal (2011)). The problem of unsteady MHD three-dimensional boundary layer flow and heat transfer over an impulsively stretching plate has been solved using other methods by some researchers. Kumari and Nath (2009) and Hang and Pop (2007) studied the unsteady MHD three-dimensional boundary layer flow and heat transfer over an impulsively stretching plate and obtained analytical and series solutions respectively. Dlamini et al. (2013a) also studied the unsteady three-dimensional MHD boundary layer flow and heat transfer over an impulsively stretching plate and obtained numerical solutions using the compact finite difference relaxation method (CFDRM).

The aim of this study is to extend the comparative studies performed on the system of ordinary differential equations and the system of partial differential equations in the previous chapters to another system of partial differential equations using the SRM, SLLM and SQLM. The ease of implementing the algorithms of the SRM, SLLM and SQLM to the system of partial differential equations is displayed. The previous chapter had 2 partial differential equations and the current study considers a system of three PDEs. The norm of the residual error of the approximate solutions obtained is used to carry out proper comparative study on the three methods. The number of iterations used in obtaining converged result is investigated to compare the speed at which the methods converge as well as the convergence rate of the methods. Finally, the effect of the dimensionless time ξ on the accuracy of the solutions obtained were also observed.

4.2 Problem formulation

In this section, the mathematical equations that model an unsteady three-dimensional MHD boundary layer flow and heat transfer are formulated, by applying similarity transformations.

Following Kumari and Nath (2009), consider prior to time $t = 0$, that a two-dimensional flat surface is put in an incompressible, laminar unbounded electrically quiescent fluid that is unbounded. Steady temperature T_∞ is kept for both surface and the fluid. The xy-plane is the same as the surface and the z-axis is perpendicular to the surface. At time $t = 0$, the surface is stretched impulsively in the two lateral directions x and y with respective velocities $u_w = ax$, $a > 0$ and $v_w = by$, $b > 0$, by introducing two equal and opposite forces in $x-$ and $y-$ directions so that the point (0,0,0) remains the same. At the same time, the surface temperature is increased suddenly from T_∞ to T_w. Unsteadiness in the flow and thermal fields are introduced by these impulsive changes. Magnetic field $\vec{B}(0, 0, B_0)$ is applied in $z-$direction. Given that the fluid is electrically conducting, the Lorentz force is given by $\vec{J} \times \vec{B}$ where $\vec{J} = \sigma\left(\vec{E} + \vec{V} \times \vec{B}\right)$ is the electrical current, $\vec{V}$ is the velocity vector and $\vec{E}$ is the electrical field, must be included in the equations of momentum (see Davidson (2001)). The terms due to the Lorentz force can be simplified when the following assumptions are made:

- That all the physical quantities are kept constant.
- The induced magnetic field is small in contrast to the applied magnetic field.
- The electric field $\vec{E} \ll \vec{V} \times \vec{B}$.

When the magnetic Reynolds number $Re_m = \mu_0 \sigma V_0 L \ll 1$ is small, where μ_0 is the magnetic permeability, σ is the electrical conductivity, V_0 and L are respectively the characteristic velocity and length, the assumptions made above are valid (Davidson (2001)). Under these assumptions, only the applied magnetic field contributes to the Lorentz force whose components in $x-$ and $y-$directions are $-\sigma B_0^2 u/\rho$ and $-\sigma B_0^2 v/\rho$, respectively. Effects of quantities like viscous dissipation, Hall current, Ohmic heating among others are neglected due to the fact they are basically small when the velocity of the stretching surface is small. As reported by Kumari and Nath (2009), the boundary layer equations based on the conservation of mass, momentum and energy that govern the unsteady three-dimensional flow and heat transfer on a stretching surface in the presence of a magnetic field can be expressed in dimensionless form as:

$$\begin{aligned} f''' + \frac{1}{2}(1-\xi)\eta f'' + \xi[(f+s)f'' - f'^2 - Mf'] &= \xi(1-\xi)\frac{\partial f'}{\partial \xi}, \\ s''' + \frac{1}{2}(1-\xi)\eta s'' + \xi[(f+s)s'' - s'^2 - Ms'] &= \xi(1-\xi)\frac{\partial s'}{\partial \xi}, \\ g'' + \frac{1}{2}Pr(1-\xi)\eta g' + Pr\xi(f+s)g' &= Pr\xi(1-\xi)\frac{\partial g}{\partial \xi}, \end{aligned} \tag{4.1}$$

with the boundary conditions given as

$$f(0,\xi) = s(0,\xi) = 0, \quad f'(0,\xi) = 1, \quad s'(0,\xi) = c, \quad g(0,\xi) = 1, \quad f'(\infty,\xi) = s'(\infty,\xi) = g(\infty,\xi) = 0, \tag{4.2}$$

where f' and s' are both dimensionless velocities, g is the dimensionless temperature, Pr the Prandtl number, c is the stretching ratio and M is the magnetic parameter.

$$\begin{aligned} \text{For } a > 0, \quad t^* = at, \quad \xi = 1 - \exp^{-t^*}, \quad \eta = (a/b)^{1/2} z, \\ u(x,y,z,t) = axf'(\eta,\xi), \quad v(x,y,z,t) = ays'(\eta,\xi), \\ w(x,y,z,t) = -(av\xi)^{1/2}[f(\eta,\xi) + s(\eta,\xi)] \end{aligned} \tag{4.3}$$

$$g(\eta,\xi) = [T(x,y,z,t) - T_\infty]/(T_W - T_\infty), T_W > T_\infty,$$

$$u_w = ax, \quad a > 0, \quad v_w = by, \quad b \geq 0, \quad c = b/a \geq 0, \quad M = \sigma B_0^2/(\rho a), \quad Pr = v/\alpha.$$

Transformations shown in equation (4.3) are obtained through Williams and Rhyne (1980).

The cartesian coordinate system are the $x-$(longitudinal), $y-$(transverse), $z-$(normal) directions respectively while $u,\ v,\ w$ are the velocity components along each directions respectively, T is the temperature, a and b velocity gradients, t is the time, c the stretching ratio, η the dimensionless transformed independent variable, t^* and ξ are the dimensionless time, ρ the density, v the kinematic viscosity and prime ($'$) denotes derivative with respect to η.

For the initial unsteady solution to be obtained, dimensionless time is set at $\xi = 0$ (at $t^* = 0$) in (4.1) and the following resulting equations are solved:

$$\begin{aligned} f''' + \frac{1}{2}\eta f'' &= 0, \\ s''' + \frac{1}{2}\eta s'' &= 0, \\ g'' + Pr\eta g' &= 0, \end{aligned} \tag{4.4}$$

with corresponding boundary conditions

$$\begin{aligned} f(0,0) = 0, \quad f'(0,0) = 1, \quad f'(\infty,0) = 0, \quad s(0,0) = 0, \quad s'(\infty,0) = 0 \\ s'(0,0) = c, \quad g(0,0) = 1, \quad g(\infty,0) = 0. \end{aligned} \tag{4.5}$$

Equations (4.4) have solutions in the form

$$\begin{aligned} f(\eta,0) &= \eta erfc\,(\eta/2) + \frac{2}{\sqrt{\pi}}\left(1 - \exp^{-\eta^2/4}\right), \\ s(\eta,0) &= c\left(\eta erfc(\eta/2) + \frac{2}{\sqrt{\pi}}\left(1 - \exp^{-\eta^2/4}\right)\right), \\ g(\eta,0) &= erfc\left(\frac{1}{2}\sqrt{Pr}\eta\right), \end{aligned} \tag{4.6}$$

where $erfc(\eta)$ is the complementary error function defined as

$$erfc(\eta) = \frac{2}{\sqrt{\pi}}\int_{\eta}^{\infty} \exp^{-s^2}\, ds. \tag{4.7}$$

At $\xi = 1$, system (4.1) reduces to

$$f''' + (f+s)f'' - f'^2 - Mf' = 0, \tag{4.8}$$

$$s''' + (f+s)s'' - s'^2 - Ms' = 0, \tag{4.9}$$

$$g'' + Pr(f+s)g' = 0, \tag{4.10}$$

with corresponding boundary conditions:

$$f(0,0)=0, \quad f^{'}(0,0)=1, \quad f^{'}(\infty,0)=0, \quad h(0,0)=0, \quad h(\infty,0)=0. \tag{4.11}$$

Steady state solution at $\xi=1$, where $c=0$ corresponding to $t\to+\infty$, renders $s=0$ and solution to equation (4.8) becomes

$$f(\eta,1) \;=\; \beta^{-1}\left[1-\exp^{-\beta\eta}\right], \quad \beta=(1+M)^{1/2}. \tag{4.12}$$

The solution gotten from (4.12) is substituted into equation (4.10) to obtain:

$$g^{''}+Pr\beta^{-1}\left[1-\exp^{-\beta\eta}\right]g^{'}=0. \tag{4.13}$$

Solution of (4.13) is expressed in terms of Kummer's function H (Kumari and Nath (2009)) as:

$$g(\eta,1)=\exp^{-\gamma\beta\eta}\left[H\left(\gamma,1+\gamma,\gamma\exp^{-\beta\eta}\right)/H\left(\gamma,1+\gamma,-\gamma\right)\right], \quad \gamma=Pr/\beta^2. \tag{4.14}$$

The local skin friction coefficients in the $x-$ and $y-$directions and the local Nusselt number are given as:

$$\begin{aligned} C_{fx} &= -\mu(\partial u/\partial z)_{z=0}/\rho(ax)^2=-Re_x^{-1/2}\xi^{-1/2}f^{''}(0,\eta), \\ C_{fy} &= -\mu(\partial v/\partial z)_{z=0}/\rho(ay)^2=-Re_y^{-1/2}\xi^{-1/2}s^{''}(0,\eta), \\ Nu_x &= -x(\partial T/\partial z)_{z=0}/\left(T_w-T_\infty\right)=-Re_x^{-1/2}\xi^{-1/2}g^{'}(0,\eta). \end{aligned} \tag{4.15}$$

4.3 Problem Solution Techniques

In this section, the spectral relaxation method (SRM), the spectral local linearization method (SLLM) and the spectral quasi-linearization method (SQLM) are all applied to obtain solutions to the system of equations (4.1). The steps taken to come up with the iteration schemes are shown in detail.

4.3.1 Spectral Relaxation Method (SRM)

In this subsection, the SRM is applied on the system of equations (4.1) and the corresponding boundary conditions (4.2) by applying the idea of the Gauss-Seidel relaxation technique to decouple the system and applying spectral collocation technique on the decoupled system.

In order to reduce the order of the system (4.1), set $f^{'} = u$ and $s^{'} = w$ and the resulting reduced system of equations is obtained:

$$\begin{aligned} f^{'} &= u, \\ s^{'} &= w, \\ u^{''} + \frac{1}{2}(1-\xi)\eta u^{'} + \xi\left[(f+s)\,u^{'} - u^2 - Mu\right] &= \xi(1-\xi)\frac{\partial u}{\partial \xi}, \\ w^{''} + \frac{1}{2}(1-\xi)\eta w^{'} + \xi\left[(f+s)w^{'} - w^2 - Mw\right] &= \xi(1-\xi)\frac{\partial w}{\partial \xi}, \\ g^{''} + \frac{1}{2}Pr\,(1-\xi)\,\eta g^{'} + Pr\xi(f+s)g^{'} &= Pr\xi(1-\xi)\frac{\partial g}{\partial \xi}, \end{aligned} \tag{4.16}$$

with corresponding boundary conditions

$$f(0,\xi) = s(0,\xi) = 0, \quad f^{'}(0,\xi) = 1, \quad s^{'}(0,\xi) = c, \;\; g(0,\xi) = 1, \quad f^{'}(\infty,\xi) = s^{'}(\infty,\xi) = g(\infty,\xi) = 0. \tag{4.17}$$

The system (4.17) is a coupled nonlinear system of equations that has to be decoupled for the system to be solved.

After applying the concept of the Gauss-Seidel relaxation technique in order to decouple the system (4.17), the decoupled system becomes

$$\begin{aligned} f^{'}_{r+1} &= u_{r+1}, \\ s^{'}_{r+1} &= w_{r+1}, \\ u^{''}_{r+1} + \frac{1}{2}\left[\frac{\eta}{2} - \frac{\xi\eta}{2} + \xi f_r + \xi s_r\right] u^{'}_{r+1} - \xi M u_{r+1} - u_r^2 &= \xi(1-\xi)\frac{\partial u_{r+1}}{\partial \xi}, \\ w^{''}_{r+1} + \frac{1}{2}\left[\frac{\eta}{2} - \frac{\xi\eta}{2} + \xi f_r + \xi s_r\right] w^{'}_{r+1} - \xi M w_{r+1} - w_r^2 &= \xi(1-\xi)\frac{\partial w_{r+1}}{\partial \xi}, \\ (1/Pr)g^{''}_{r+1} + \left(\frac{\eta}{2}(1-\xi) + \xi(f_r + s_r)\right) g^{'}_{r+1} &= \xi(1-\xi)\frac{\partial g_{r+1}}{\partial \xi}. \end{aligned} \tag{4.18}$$

Equation (4.19) is expressed in a compact form as

$$\begin{aligned} f_{r+1}^{'} &= u_{r+1}, \\ s_{r+1}^{'} &= w_{r+1}, \\ u_{r+1}^{''} + a_{1,r}u_{r+1}^{'} + a_{2,r}u_{r+1} + a_{3,r} &= \xi(1-\xi)\frac{\partial u_{r+1}}{\partial \xi}, \\ w_{r+1}^{''} + b_{1,r}w_{r+1}^{'} + b_{2,r}w_{r+1} + b_{3,r} &= \xi(1-\xi)\frac{\partial w_{r+1}}{\partial \xi}, \\ (1/Pr)g_{r+1}^{''} + c_{1,r}g_{r+1}^{'} &= \xi(1-\xi)\frac{\partial g_{r+1}}{\partial \xi}, \end{aligned} \tag{4.19}$$

(4.20)

where

$$\begin{aligned} a_{1,r} &= \frac{\eta}{2}(1-\xi) + \xi\left(f_r + s_r\right), \\ a_{2,r} &= -\xi M, \\ a_{3,r} &= -\xi u_r^2, \\ b_{1,r} &= \frac{\eta}{2}(1-\xi) + \xi\left(f_r + s_r\right), \\ b_{2,r} &= -\xi M, \\ b_{3,r} &= -\xi w_r^2, \\ c_{1,r} &= \frac{\eta}{2}(1-\xi) + \xi\left(f_r + s_r\right). \end{aligned}$$

The Crank-Nicolson finite difference method is applied on (4.20) and the system obtained is:

$$\begin{aligned} (u_{r+1}^{''})^{n+\frac{1}{2}} + (a_{1,r})^{n+\frac{1}{2}}(u_{r+1}^{'})^{n+\frac{1}{2}} + (a_{2,r})^{n+\frac{1}{2}}(u_{r+1})^{n+\frac{1}{2}} + (a_{3,r}) &= \xi^{n+\frac{1}{2}}(1-\xi^{n+\frac{1}{2}})\frac{\partial u_{r+1}}{\partial \xi}, \\ (w_{r+1}^{''})^{n+\frac{1}{2}} + (b_{1,r})^{n+\frac{1}{2}}(w_{r+1}^{'})^{n+\frac{1}{2}} + (b_{2,r})^{n+\frac{1}{2}}(w_{r+1})^{n+\frac{1}{2}} + (b_{3,r}) &= \xi^{n+\frac{1}{2}}(1-\xi^{n+\frac{1}{2}})\frac{\partial w_{r+1}}{\partial \xi}, \\ (1/Pr)^{n+\frac{1}{2}}(g_{r+1}^{''})^{n+\frac{1}{2}} + (c_{1,r})^{n+\frac{1}{2}}(g_{r+1}^{'})^{n+\frac{1}{2}} &= \xi^{n+\frac{1}{2}}(1-\xi^{n+\frac{1}{2}})\frac{\partial g_{r+1}}{\partial \xi}, \\ (f_{r+1}^{'})^{n+\frac{1}{2}} &= (u_{r+1})^{n+\frac{1}{2}}, \\ (s_{r+1}^{'})^{n+\frac{1}{2}} &= (w_{r+1})^{n+\frac{1}{2}}. \end{aligned} \tag{4.21}$$

Equation (4.21) is rewritten in the spectral collocation form to obtain:

$$\begin{aligned}
(D^2U_{r+1})^{n+\frac{1}{2}} + (a_{1,r})^{n+\frac{1}{2}}(DU_{r+1})^{n+\frac{1}{2}} + (a_{2,r})^{n+\frac{1}{2}}(U_{r+1})^{n+\frac{1}{2}} + (a_{3,r}) &= \xi^{n+\frac{1}{2}}(1-\xi^{n+\frac{1}{2}})\frac{U_{r+1}^{n+1}-U_{r+1}^{n}}{\Delta\xi},\\
(D^2W_{r+1})^{n+\frac{1}{2}} + (b_{1,r})^{n+\frac{1}{2}}(DW_{r+1})^{n+\frac{1}{2}} + (b_{2,r})^{n+\frac{1}{2}}(W_{r+1})^{n+\frac{1}{2}} + (b_{3,r}) &= \xi^{n+\frac{1}{2}}(1-\xi^{n+\frac{1}{2}})\frac{W_{r+1}^{n+1}-W_{r+1}^{n}}{\Delta\xi},\\
(1/Pr)^{n+\frac{1}{2}}(D^2G_{r+1})^{n+\frac{1}{2}} + (c_{1,r})^{n+\frac{1}{2}}(DG_{r+1})^{n+\frac{1}{2}} &= \xi^{n+\frac{1}{2}}(1-\xi^{n+\frac{1}{2}})\frac{G_{r+1}^{n+1}-G_{r+1}^{n}}{\Delta\xi},\\
(DF_{r+1})^{n+\frac{1}{2}} &= (U_{r+1})^{n+\frac{1}{2}}, \qquad (4.22)\\
(DS_{r+1})^{n+\frac{1}{2}} &= (W_{r+1})^{n+\frac{1}{2}}.
\end{aligned}$$

From (4.23), taking terms at the next time level $(n+1)$ to the left and terms at the current time level(n) and nonlinear terms to the right, the new system becomes:

$$\begin{aligned}
&\left[\frac{1}{2}\left(\mathbf{D}^2 + \mathbf{a}_{1,r}^{n+\frac{1}{2}}\mathbf{D} + \mathbf{a}_{2,r}^{n+\frac{1}{2}}\right) - \frac{\xi^{n+\frac{1}{2}}\left(1-\xi^{n+\frac{1}{2}}\right)}{\Delta\xi}\right]\mathbf{U}_{r+1}^{n+1}\\
&= \left[-\frac{1}{2}\left(\mathbf{D}^2 + \mathbf{a}_{1,r}^{n+\frac{1}{2}}\mathbf{D} + \mathbf{a}_{2,r}^{n+\frac{1}{2}}\right) - \frac{\xi^{n+\frac{1}{2}}\left(1-\xi^{n+\frac{1}{2}}\right)}{\Delta\xi}\right]\mathbf{U}_{r+1}^{n} - \mathbf{a}_{3,r},\\
&\frac{1}{2}\left(\mathbf{D}^2 + \mathbf{b}_{1,r}^{n+\frac{1}{2}}\mathbf{D} + \mathbf{b}_{2,r}^{n+\frac{1}{2}}\right) - \frac{\xi^{n+\frac{1}{2}}\left(1-\xi^{n+\frac{1}{2}}\right)}{\Delta\xi}\mathbf{W}_{r+1}^{n+1}\\
&= \left[-\frac{1}{2}\left(\mathbf{D}^2 + \mathbf{b}_{1,r}^{n+\frac{1}{2}}\mathbf{D} + \mathbf{b}_{2,r}^{n+\frac{1}{2}}\right) - \frac{\xi^{n+\frac{1}{2}}\left(1-\xi^{n+\frac{1}{2}}\right)}{\Delta\xi}\right]\mathbf{W}_{r+1}^{n} - \mathbf{b}_{3,r},\\
&\left[\frac{1}{2}\left((1/Pr)\,\mathbf{D}^2 + \mathbf{c}_{1,r}^{n+\frac{1}{2}}\mathbf{D}\right) - \frac{\xi^{n+\frac{1}{2}}\left(1-\xi^{n+\frac{1}{2}}\right)}{\Delta\xi}\right]\mathbf{G}_{r+1}^{n+1}\\
&= \left[-\frac{1}{2}\left((1/Pr)\,\mathbf{D}^2 + \mathbf{c}_{1,r}^{n+\frac{1}{2}}\mathbf{D}\right) - \frac{\xi^{n+\frac{1}{2}}\left(1-\xi^{n+\frac{1}{2}}\right)}{\Delta\xi}\right]\mathbf{G}_{r+1}^{n},\\
&\left(\mathbf{DF}_{r+1}\right)^{n+\frac{1}{2}} = \left(\mathbf{U}_{r+1}\right)^{n+\frac{1}{2}},\\
&\left(\mathbf{DS}_{r+1}\right)^{n+\frac{1}{2}} = \left(\mathbf{W}_{r+1}\right)^{n+\frac{1}{2}}.
\end{aligned}$$

Equation (4.23) is represented in a compact form as:

$$\begin{aligned}
\mathbf{A}_1\mathbf{U}_{r+1}^{n+1} &= \mathbf{B}_1\mathbf{U}_{r+1}^{n} + \mathbf{K}_1, \\
\mathbf{A}_2\mathbf{W}_{r+1}^{n+1} &= \mathbf{B}_2\mathbf{W}_{r+1}^{n} + \mathbf{K}_2, \\
\mathbf{A}_3\mathbf{G}_{r+1}^{n+1} &= \mathbf{B}_3\mathbf{G}_{r+1}^{n} + \mathbf{K}_3, \\
\mathbf{A}_4\mathbf{F}_{r+1} &= \mathbf{K}_4, \\
\mathbf{A}_5\mathbf{S}_{r+1} &= \mathbf{K}_5,
\end{aligned} \tag{4.23}$$

where

$$\begin{aligned}
\mathbf{A}_1 &= \frac{1}{2}\left(\mathbf{D}^2 + \mathbf{a}_{1,r}^{n+\frac{1}{2}}\mathbf{D} + \mathbf{a}_{2,r}^{n+\frac{1}{2}}\right) - \frac{\xi^{n+\frac{1}{2}}\left(1-\xi^{n+\frac{1}{2}}\right)}{\Delta\xi}\mathbf{I}, \\
\mathbf{B}_1 &= -\frac{1}{2}\left(\mathbf{D}^2 + \mathbf{a}_{1,r}^{n+\frac{1}{2}}\mathbf{D} + \mathbf{a}_{2,r}^{n+\frac{1}{2}}\right) - \frac{\xi^{n+\frac{1}{2}}\left(1-\xi^{n+\frac{1}{2}}\right)}{\Delta\xi}\mathbf{I}, \\
\mathbf{K}_1 &= -\mathbf{a}_{3,r}^{n+\frac{1}{2}}, \\
\mathbf{A}_2 &= \frac{1}{2}\left(\mathbf{D}^2 + \mathbf{b}_{1,r}^{n+\frac{1}{2}}\mathbf{D} + \mathbf{b}_{2,r}^{n+\frac{1}{2}}\right) - \frac{\xi^{n+\frac{1}{2}}\left(1-\xi^{n+\frac{1}{2}}\right)}{\Delta\xi}\mathbf{I}, \\
\mathbf{B}_2 &= -\frac{1}{2}\left(\mathbf{D}^2 + \mathbf{b}_{1,r}^{n+\frac{1}{2}}\mathbf{D} + \mathbf{b}_{2,r}^{n+\frac{1}{2}}\right) - \frac{\xi^{n+\frac{1}{2}}\left(1-\xi^{n+\frac{1}{2}}\right)}{\Delta\xi}\mathbf{I}, \\
\mathbf{K}_2 &= -\mathbf{b}_{3,r}^{n+\frac{1}{2}}, \\
\mathbf{A}_3 &= \frac{1}{2}\left((1/Pr)\,\mathbf{D}^2 + \mathbf{c}_{1,r}^{n+\frac{1}{2}}\mathbf{D}\right) - \frac{\xi^{n+\frac{1}{2}}\left(1-\xi^{n+\frac{1}{2}}\right)}{\Delta\xi}\mathbf{I}, \\
\mathbf{B}_3 &= -\frac{1}{2}\left((1/Pr)\,\mathbf{D}^2 + \mathbf{c}_{1,r}^{n+\frac{1}{2}}\mathbf{D}\right) - \frac{\xi^{n+\frac{1}{2}}\left(1-\xi^{n+\frac{1}{2}}\right)}{\Delta\xi}\mathbf{I}, \\
\mathbf{K}_3 &= \mathbf{0}, \\
\mathbf{A}_4 &= \mathbf{D}, \\
\mathbf{K}_4 &= \mathbf{U}_{r+1}^{n}, \\
\mathbf{A}_5 &= \mathbf{D}, \\
\mathbf{K}_5 &= \mathbf{W}_{r+1}^{n}.
\end{aligned}$$

Boundary conditions (4.2) are implemented on the system (4.23) in matrix form as shown below:

$$\begin{aligned}
\mathbf{M}_1\mathbf{P}_1 &= \mathbf{R}_1, \\
\mathbf{M}_2\mathbf{P}_2 &= \mathbf{R}_2, \\
\mathbf{M}_3\mathbf{P}_3^{n+1} &= \mathbf{Q}_3\mathbf{P}_3^{n} + \mathbf{R}_3, \\
\mathbf{M}_4\mathbf{P}_4^{n+1} &= \mathbf{Q}_4\mathbf{P}_4^{n} + \mathbf{R}_4, \\
\mathbf{M}_5\mathbf{P}_5^{n+1} &= \mathbf{Q}_5\mathbf{P}_5^{n} + \mathbf{R}_5,
\end{aligned} \tag{4.24}$$

where

$$\mathbf{M}_1=\begin{bmatrix} & & & & \\ & & \mathbf{A}_4 & & \\ & & & & \\ \hline 0 & 0 & \cdots & 0 & 1 \end{bmatrix}, \quad \mathbf{P}_1=\begin{bmatrix} f_{r+1,0}^{n+1} \\ f_{r+1,1}^{n+1} \\ \vdots \\ \vdots \\ \hline f_{r+1,N}^{n+1} \end{bmatrix}, \quad \mathbf{R}_1=\begin{bmatrix} & & \\ & \mathbf{K}_4 & \\ & & \\ \hline 0 \end{bmatrix},$$

$$\mathbf{M}_2=\begin{bmatrix} & & & & \\ & & \mathbf{A}_5 & & \\ & & & & \\ \hline 0 & 0 & \cdots & 0 & 1 \end{bmatrix}, \quad \mathbf{P}_2=\begin{bmatrix} s_{r+1,0}^{n+1} \\ s_{r+1,1}^{n+1} \\ \vdots \\ \vdots \\ \hline s_{r+1,N}^{n+1} \end{bmatrix}, \quad \mathbf{R}_2=\begin{bmatrix} & & \\ & \mathbf{K}_5 & \\ & & \\ \hline 0 \end{bmatrix},$$

$$\mathbf{M}_3=\begin{bmatrix} 1 & 0 & \cdots & 0 & 0 \\ \hline & & & & \\ & & \mathbf{A}_1 & & \\ & & & & \\ \hline 0 & 0 & \cdots & 0 & 1 \end{bmatrix}, \quad \mathbf{P}_3^{n+1}=\begin{bmatrix} u_{r+1,0}^{n+1} \\ \hline u_{r+1,1}^{n+1} \\ \vdots \\ \vdots \\ \hline u_{r+1,N}^{n+1} \end{bmatrix}, \quad \mathbf{Q}_3=\begin{bmatrix} 0 & 0 & \cdots & 0 & 0 \\ \hline & & & & \\ & & \mathbf{B}_1 & & \\ & & & & \\ \hline 0 & 0 & \cdots & 0 & 0 \end{bmatrix},$$

$$\mathbf{P}_3^{n}=\begin{bmatrix} u_{r+1,0}^{n} \\ \hline u_{r+1,1}^{n} \\ \vdots \\ \vdots \\ \hline u_{r+1,N}^{n} \end{bmatrix}, \quad \mathbf{R}_3=\begin{bmatrix} 0 \\ \hline & & \\ & \mathbf{K}_1 & \\ & & \\ \hline 1 \end{bmatrix}, \quad \mathbf{P}_5^{n}=\begin{bmatrix} g_{r+1,0}^{n} \\ \hline g_{r+1,1}^{n} \\ \vdots \\ \vdots \\ \hline g_{r+1,N}^{n} \end{bmatrix}, \quad \mathbf{R}_5=\begin{bmatrix} 0 \\ \hline & & \\ & \mathbf{K}_1 & \\ & & \\ \hline 1 \end{bmatrix},$$

$$\mathbf{M}_4=\begin{bmatrix} 1 & 0 & \cdots & 0 & 0 \\ \hline & & & & \\ & & \mathbf{A}_2 & & \\ & & & & \\ \hline 0 & 0 & \cdots & 0 & 1 \end{bmatrix}, \quad \mathbf{P}_4^{n+1}=\begin{bmatrix} w_{r+1,0}^{n+1} \\ \hline w_{r+1,1}^{n+1} \\ \vdots \\ \vdots \\ \hline w_{r+1,N}^{n+1} \end{bmatrix}, \quad \mathbf{Q}_4=\begin{bmatrix} 0 & 0 & \cdots & 0 & 0 \\ \hline & & & & \\ & & \mathbf{B}_2 & & \\ & & & & \\ \hline 0 & 0 & \cdots & 0 & 0 \end{bmatrix},$$

$$\mathbf{P}_4^{n}=\begin{bmatrix} w_{r+1,0}^{n} \\ \hline w_{r+1,1}^{n} \\ \vdots \\ \vdots \\ \hline w_{r+1,N}^{n} \end{bmatrix}, \quad \mathbf{R}_4=\begin{bmatrix} 0 \\ \hline \\ \mathbf{K}_2 \\ \\ \hline c \end{bmatrix},$$

$$\mathbf{M}_5=\begin{bmatrix} 1 & 0 & \cdots & 0 & 0 \\ \hline & & & & \\ & & \mathbf{A}_3 & & \\ & & & & \\ \hline 0 & 0 & \cdots & 0 & 1 \end{bmatrix}, \mathbf{P}_5^{n+1}=\begin{bmatrix} g_{r+1,0}^{n+1} \\ \hline g_{r+1,1}^{n+1} \\ \vdots \\ \vdots \\ \hline g_{r+1,N}^{n+1} \end{bmatrix}, \quad \mathbf{Q}_5=\begin{bmatrix} 0 & 0 & \cdots & 0 & 0 \\ \hline & & & & \\ & & \mathbf{B}_3 & & \\ & & & & \\ \hline 0 & 0 & \cdots & 0 & 0 \end{bmatrix}.$$

4.3.2 Spectral Local Linearization Method (SLLM)

In this subsection, the SLLM is applied on the system (4.1) and the corresponding boundary conditions (4.2). This is done by identifying the nonlinear terms of the same function and its derivative in each of the equations of the system (4.1), applying single term Taylor series expansion on the nonlinear terms so as to linearize the system of equations which is decoupled and spectral collocation technique is applied to integrate the system.

Let $f^{'}=u$ and $s^{'}=w$ and the resulting system of equations reduce to:

$$\begin{aligned} f^{'} &= u, \\ s^{'} &= w, \\ u^{''}+\frac{1}{2}(1-\xi)\eta u^{'}+\xi\left[(f+s)\,u^{'}-u^2-Mu\right] &= \xi(1-\xi)\frac{\partial u}{\partial \xi}, \\ w^{''}+\frac{1}{2}(1-\xi)\eta w^{'}+\xi\left[(f+s)\,w^{'}-w^2-Mw\right] &= \xi(1-\xi)\frac{\partial w}{\partial \xi}, \\ g^{''}+\frac{1}{2}Pr(1-\xi)\eta g^{'}+Pr\xi(f+s)g^{'} &= Pr\xi(1-\xi)\frac{\partial g}{\partial \xi}, \end{aligned} \tag{4.25}$$

with corresponding boundary conditions:

$$f(0,\xi) = s(0,\xi) = 0, \quad f^{'}(0,\xi) = 1, \quad s^{'}(0,\xi) = c, \;\; g(0,\xi) = 1, \quad f^{'}(\infty,\xi) = s^{'}(\infty,\xi) = g(\infty,\xi) = 0. \tag{4.26}$$

The system (4.26) is a coupled nonlinear system of equations which has to be decoupled for the system to be solved.

The nonlinear terms are u^2 and w^2 and Taylor series expansion is applied on the nonlinear terms in the form below:

$$\begin{aligned} u_{r+1}^2 &= u_r^2 + 2u_r\left(u_{r+1} - u_r\right) \\ &= 2u_r u_{r+1} - u_r^2. \end{aligned} \tag{4.27}$$

$$\begin{aligned} w_{r+1}^2 &= w_r^2 + 2w_r\left(w_{r+1} - w_r\right) \\ &= 2w_r w_{r+1} - w_r^2. \end{aligned} \tag{4.28}$$

The solutions gotten from (4.27) and (4.28) are substituted into (4.26) and the nonlinear system is decoupled using the concept of the Gauss-Seidel relaxation method to obtain:

$$\begin{aligned} f_{r+1}^{'} &= u_{r+1}, \\ s_{r+1}^{'} &= w_{r+1}, \\ u_{r+1}^{''} + \frac{1}{2}\left[\frac{\eta}{2} - \frac{\xi\eta}{2} + \xi f_r + \xi s_r\right] u_{r+1}^{'} - 2\xi u_r u_{r+1} - \xi M u_{r+1} + \xi u_r^2 &= \xi(1-\xi)\frac{\partial u_{r+1}}{\partial \xi}, \\ w_{r+1}^{''} + \frac{1}{2}\left[\frac{\eta}{2} - \frac{\xi\eta}{2} + \xi f_r + \xi s_r\right] w_{r+1}^{'} - 2\xi w_r w_{r+1} - \xi M w_{r+1} + {}_r^2 &= \xi(1-\xi)\frac{\partial w_{r+1}}{\partial \xi}, \\ (1/Pr) g_{r+1}^{''} + \left(\frac{\eta}{2}(1-\xi) + \xi\left(f_r + s_r\right)\right) g_{r+1}^{'} &= \xi(1-\xi)\frac{\partial g_{r+1}}{\partial \xi}, \end{aligned} \tag{4.29}$$

where linear terms are evaluated at the current iteration level $(r+1)$ and nonlinear terms at the previous iteration level (r). The system (4.30) is expressed in a compact form as:

$$\begin{aligned} f_{r+1}^{'} &= u_{r+1}, \\ s_{r+1}^{'} &= w_{r+1}, \\ u_{r+1}^{''} + a_{1,r} u_{r+1}^{'} + a_{2,r} u_{r+1} + a_{3,r} &= \xi(1-\xi)\frac{\partial u_{r+1}}{\partial \xi}, \\ w_{r+1}^{''} + b_{1,r} w_{r+1}^{'} + b_{2,r} w_{r+1} + b_{3,r} &= \xi(1-\xi)\frac{\partial w_{r+1}}{\partial \xi}, \\ (1/Pr) g_{r+1}^{''} + c_{1,r} g_{r+1}^{'} &= \xi(1-\xi)\frac{\partial g_{r+1}}{\partial \xi}, \end{aligned} \tag{4.30}$$

where

$$\begin{aligned}
a_{1,r} &= \frac{\eta}{2}(1-\xi)+\xi\left(f_r+s_r\right), \\
a_{2,r} &= -\xi M-2\xi u_r, \\
a_{3,r} &= \xi u_r^2, \\
b_{1,r} &= \frac{\eta}{2}(1-\xi)+\xi\left(f_r+s_r\right), \\
b_{2,r} &= -\xi M-2\xi w_r, \\
b_{3,r} &= \xi w_r^2, \\
c_{1,r} &= \frac{\eta}{2}(1-\xi)+\xi\left(f_r+s_r\right).
\end{aligned}$$

The Crank-Nicolson finite difference approach is applied to the system (4.31) and the new system obtained is:

$$\begin{aligned}
\left(u_{r+1}^{''}\right)^{n+\frac{1}{2}}+\left(a_{1,r}\right)^{n+\frac{1}{2}}\left(u_{r+1}^{'}\right)^{n+\frac{1}{2}}+\left(a_{2,r}\right)^{n+\frac{1}{2}}\left(u_{r+1}\right)^{n+\frac{1}{2}}+\left(a_{3,r}\right) &= \xi^{n+\frac{1}{2}}(1-\xi^{n+\frac{1}{2}})\frac{\partial u_{r+1}}{\partial \xi}, \\
\left(w_{r+1}^{''}\right)^{n+\frac{1}{2}}+\left(b_{1,r}\right)^{n+\frac{1}{2}}\left(w_{r+1}^{'}\right)^{n+\frac{1}{2}}+\left(b_{2,r}\right)^{n+\frac{1}{2}}\left(w_{r+1}\right)^{n+\frac{1}{2}}+\left(b_{3,r}\right) &= \xi^{n+\frac{1}{2}}\left(1-\xi^{n+\frac{1}{2}}\right)\frac{\partial w_{r+1}}{\partial \xi}, \\
(1/Pr)^{n+\frac{1}{2}}\left(g_{r+1}^{''}\right)^{n+\frac{1}{2}}+\left(c_{1,r}\right)^{n+\frac{1}{2}}\left(g_{r+1}^{'}\right)^{n+\frac{1}{2}} &= \xi^{n+\frac{1}{2}}\left(1-\xi^{n+\frac{1}{2}}\right)\frac{\partial g_{r+1}}{\partial \xi}, \\
\left(f_{r+1}^{'}\right)^{n+\frac{1}{2}} &= \left(u_{r+1}\right)^{n+\frac{1}{2}}, \qquad (4.31) \\
\left(s_{r+1}^{'}\right)^{n+\frac{1}{2}} &= \left(w_{r+1}\right)^{n+\frac{1}{2}}.
\end{aligned}$$

The Chebyshev pseudo-spectral collocation technique is applied to integrate the system (4.32). The system (4.32) is rewritten in the spectral collocation form to obtain:

$$\begin{aligned}
\left(D^2U_{r+1}\right)^{n+\frac{1}{2}} + (a_{1,r})^{n+\frac{1}{2}}\left(DU_{r+1}\right)^{n+\frac{1}{2}} + (a_{2,r})^{n+\frac{1}{2}}\left(U_{r+1}\right)^{n+\frac{1}{2}} + (a_{3,r}) \\
= \xi^{n+\frac{1}{2}}\left(1-\xi^{n+\frac{1}{2}}\right)\frac{U_{r+1}^{n+1}-U_{r+1}^{n}}{\Delta\xi}, \\
\left(D^2W_{r+1}\right)^{n+\frac{1}{2}} + (b_{1,r})^{n+\frac{1}{2}}\left(DW_{r+1}\right)^{n+\frac{1}{2}} + (b_{2,r})^{n+\frac{1}{2}}\left(W_{r+1}\right)^{n+\frac{1}{2}} + (b_{3,r}) \\
= \xi^{n+\frac{1}{2}}\left(1-\xi^{n+\frac{1}{2}}\right)\frac{W_{r+1}^{n+1}-W_{r+1}^{n}}{\Delta\xi}, \\
(1/Pr)^{n+\frac{1}{2}}\left(D^2G_{r+1}\right)^{n+\frac{1}{2}} + (c_{1,r})^{n+\frac{1}{2}}(DG_{r+1})^{n+\frac{1}{2}} \\
= \xi^{n+\frac{1}{2}}(1-\xi^{n+\frac{1}{2}})\frac{G_{r+1}^{n+1}-G_{r+1}^{n}}{\Delta\xi}, \\
(DF_{r+1})^{n+\frac{1}{2}} = (U_{r+1})^{n+\frac{1}{2}}, \\
(DS_{r+1})^{n+\frac{1}{2}} = (W_{r+1})^{n+\frac{1}{2}}.
\end{aligned} \tag{4.32}$$

From the system (4.32), taking terms at the next time level $(n+1)$ to the left and terms at the current time level (n) and nonlinear terms to the right, the system becomes:

$$\begin{aligned}
&\left[\frac{1}{2}\left(\mathbf{D}^2 + \mathbf{a}_{1,r}^{n+\frac{1}{2}}\mathbf{D} + \mathbf{a}_{2,r}^{n+\frac{1}{2}}\right) - \frac{\xi^{n+\frac{1}{2}}\left(1-\xi^{n+\frac{1}{2}}\right)}{\Delta\xi}\right]\mathbf{U}_{r+1}^{n+1} \\
&= \left[-\frac{1}{2}\left(\mathbf{D}^2 + \mathbf{a}_{1,r}^{n+\frac{1}{2}}\mathbf{D} + \mathbf{a}_{2,r}^{n+\frac{1}{2}}\right) - \frac{\xi^{n+\frac{1}{2}}\left(1-\xi^{n+\frac{1}{2}}\right)}{\Delta\xi}\right]\mathbf{U}_{r+1}^{n} - \mathbf{a}_{3,r}^{n+\frac{1}{2}}, \\
&\left[\frac{1}{2}\left(\mathbf{D}^2 + \mathbf{b}_{1,r}^{n+\frac{1}{2}}\mathbf{D} + \mathbf{b}_{2,r}^{n+\frac{1}{2}}\right) - \frac{\xi^{n+\frac{1}{2}}\left(1-\xi^{n+\frac{1}{2}}\right)}{\Delta\xi}\right]\mathbf{W}_{r+1}^{n+1} \\
&= \left[-\frac{1}{2}\left(\mathbf{D}^2 + \mathbf{b}_{1,r}^{n+\frac{1}{2}}\mathbf{D} + \mathbf{b}_{2,r}^{n+\frac{1}{2}}\right) - \frac{\xi^{n+\frac{1}{2}}\left(1-\xi^{n+\frac{1}{2}}\right)}{\Delta\xi}\right]\mathbf{W}_{r+1}^{n} - \mathbf{b}_{3,r}^{n+\frac{1}{2}}, \\
&\left[\frac{1}{2}\left((1/Pr)\,\mathbf{D}^2 + \mathbf{c}_{1,r}^{n+\frac{1}{2}}\mathbf{D}\right) - \frac{\xi^{n+\frac{1}{2}}\left(1-\xi^{n+\frac{1}{2}}\right)}{\Delta\xi}\right]\mathbf{G}_{r+1}^{n+1} \\
&= \left[-\frac{1}{2}\left((1/Pr)\,\mathbf{D}^2 + \mathbf{c}_{1,r}^{n+\frac{1}{2}}\mathbf{D}\right) - \frac{\xi^{n+\frac{1}{2}}\left(1-\xi^{n+\frac{1}{2}}\right)}{\Delta\xi}\right]\mathbf{G}_{r+1}^{n}, \\
&\left(\mathbf{DF}_{r+1}\right)^{n+\frac{1}{2}} = \left(\mathbf{U}_{r+1}\right)^{n+\frac{1}{2}}, \\
&\left(\mathbf{DS}_{r+1}\right)^{n+\frac{1}{2}} = \left(\mathbf{W}_{r+1}\right)^{n+\frac{1}{2}}.
\end{aligned} \tag{4.33}$$

The system (4.33) is represented in a compact form as:

$$\begin{aligned}
\mathbf{A}_1\mathbf{U}_{r+1}^{n+1} &= \mathbf{B}_1\mathbf{U}_{r+1}^{n} + \mathbf{K}_1,\\
\mathbf{A}_2\mathbf{W}_{r+1}^{n+1} &= \mathbf{B}_2\mathbf{W}_{r+1}^{n} + \mathbf{K}_2,\\
\mathbf{A}_3\mathbf{G}_{r+1}^{n+1} &= \mathbf{B}_3\mathbf{G}_{r+1}^{n} + \mathbf{K}_3,\\
\mathbf{A}_4\mathbf{F}_{r+1} &= \mathbf{K}_4,\\
\mathbf{A}_5\mathbf{S}_{r+1} &= \mathbf{K}_5,
\end{aligned} \tag{4.34}$$

where

$$\begin{aligned}
\mathbf{A}_1 &= \frac{1}{2}\left(\mathbf{D}^2 + \mathbf{a}_{1,r}^{n+\frac{1}{2}}\mathbf{D} + \mathbf{a}_{2,r}^{n+\frac{1}{2}}\right) - \frac{\xi^{n+\frac{1}{2}}\left(1-\xi^{n+\frac{1}{2}}\right)}{\Delta\xi}\mathbf{I},\\
\mathbf{B}_1 &= -\frac{1}{2}\left(\mathbf{D}^2 + \mathbf{a}_{1,r}^{n+\frac{1}{2}}\mathbf{D} + \mathbf{a}_{2,r}^{n+\frac{1}{2}}\right) - \frac{\xi^{n+\frac{1}{2}}\left(1-\xi^{n+\frac{1}{2}}\right)}{\Delta\xi}\mathbf{I},\\
\mathbf{K}_1 &= -\mathbf{a}_{3,r}^{n+\frac{1}{2}},\\
\mathbf{A}_2 &= \frac{1}{2}\left(\mathbf{D}^2 + \mathbf{b}_{1,r}^{n+\frac{1}{2}}\mathbf{D} + \mathbf{b}_{2,r}^{n+\frac{1}{2}}\right) - \frac{\xi^{n+\frac{1}{2}}\left(1-\xi^{n+\frac{1}{2}}\right)}{\Delta\xi}\mathbf{I},\\
\mathbf{B}_2 &= -\frac{1}{2}\left(\mathbf{D}^2 + \mathbf{b}_{1,r}^{n+\frac{1}{2}}\mathbf{D} + \mathbf{b}_{2,r}^{n+\frac{1}{2}}\right) - \frac{\xi^{n+\frac{1}{2}}\left(1-\xi^{n+\frac{1}{2}}\right)}{\Delta\xi}\mathbf{I},\\
\mathbf{K}_2 &= -\mathbf{b}_{3,r}^{n+\frac{1}{2}},\\
\mathbf{A}_3 &= \frac{1}{2}\left((1/Pr)\,\mathbf{D}^2 + \mathbf{c}_{1,r}^{n+\frac{1}{2}}\mathbf{D}\right) - \frac{\xi^{n+\frac{1}{2}}\left(1-\xi^{n+\frac{1}{2}}\right)}{\Delta\xi}\mathbf{I},\\
\mathbf{B}_3 &= -\frac{1}{2}\left((1/Pr)\,\mathbf{D}^2 + \mathbf{c}_{1,r}^{n+\frac{1}{2}}\mathbf{D}\right) - \frac{\xi^{n+\frac{1}{2}}\left(1-\xi^{n+\frac{1}{2}}\right)}{\Delta\xi}\mathbf{I},\\
\mathbf{A}_4 &= \mathbf{D},\\
\mathbf{K}_3 &= \mathbf{0},\\
\mathbf{K}_4 &= \mathbf{U}_{r+1},\\
\mathbf{A}_5 &= \mathbf{D},\\
\mathbf{K}_5 &= \mathbf{W}_{r+1}.
\end{aligned}$$

4.3.3 Spectral Quasi-Linearization Method (SQLM)

In this subsection, the SQLM is applied to the system (4.1) and the corresponding boundary conditions(4.2). This method is implemented by identifying all nonlinear terms and applying

Taylor series expansion on the nonlinear terms for the purpose of obtaining a linear coupled system of equations and spectral collocation method is applied on the linearized coupled system.

$$\begin{aligned} f''' + \frac{1}{2}(1-\xi)\eta f'' + \xi\left[(f+s)f'' - f'^2 - Mf'\right] &= \xi(1-\xi)\frac{\partial f'}{\partial \xi}, \\ s''' + \frac{1}{2}(1-\xi)\eta s'' + \xi\left[(f+s)s'' - s'^2 - Ms'\right] &= \xi(1-\xi)\frac{\partial s'}{\partial \xi}, \\ g'' + \frac{1}{2}Pr(1-\xi)\eta g' + Pr\xi(f+s)g' &= Pr\xi(1-\xi)\frac{\partial g}{\partial \xi}, \end{aligned} \tag{4.35}$$

with corresponding boundary conditions

$$\begin{aligned} f(0,\xi) = s(0,\xi) = 0, \quad f'(0,\xi) = 1, \quad s'(0,\xi) = c, \quad g(0,\xi) = 1, \\ f'(\infty,\xi) = s'(\infty,\xi) = g(\infty,\xi) = 0. \end{aligned} \tag{4.36}$$

The system (4.36) is a coupled nonlinear system of equations which has to be linearized for the system to be solved. The nonlinear terms $(f+s)f''$, $(f+s)s''$, $(f+s)g'$, f'^2 and s'^2 are linearized using Taylor series expansion as shown below.

$$\begin{aligned} f'^2_{r+1} &= f'^2_r + 2f'_r\left(f'_{r+1} - f'_r\right) \\ &= 2f'_r f'^2_{r+1} - f'^2_r. \end{aligned} \tag{4.37}$$

$$\begin{aligned} s'^2_{r+1} &= s'^2_r + 2s'_r\left(s'_{r+1} - s'_r\right) \\ &= 2s'_r s'^2_{r+1} - s'^2_r. \end{aligned} \tag{4.38}$$

$$\begin{aligned} (f_{r+1}+s_{r+1})f''_{r+1} &= (f_r+s_r)f''_r + f''_r(f_{r+1}-f_r) + f''_r(s_{r+1}-s_r) + f_r(f''_{r+1}-f''_r) + s_r(f''_{r+1}-f''_r) \\ &= (f_r+s_r)f''_{r+1} - (s_r+f_r)f''_r + f''_r s_{r+1} + f''_r f_{r+1}. \end{aligned} \tag{4.39}$$

$$\begin{aligned} (f_{r+1}+s_{r+1})s''_{r+1} &= (f_r+s_r)s''_r + s''_r(f_{r+1}-f_r) + s''_r(s_{r+1}-s_r) + f_r(s''_{r+1}-s''_r) + s_r(s''_{r+1}-s''_r) \\ &= (f_r+s_r)s''_{r+1} - (s_r+f_r)s''_r + s''_r s_{r+1} + s''_r f_{r+1}. \end{aligned} \tag{4.40}$$

$$\begin{aligned} (f_{r+1}+s_{r+1})g'_{r+1} &= (f_r+s_r)g'_r + g'_r(f_{r+1}-f_r) + g'_r(s_{r+1}-s_r) + f_r(g'_{r+1}-g'_r) + s_r(g'_{r+1}-g'_r) \\ &= (f_r+s_r)g'_{r+1} - (s_r+f_r)g'_r + g'_r s_{r+1} + g'_r f_{r+1}. \end{aligned} \tag{4.41}$$

The solutions obtained in (4.37 - 4.41) are inserted into the system (4.36) and the linear coupled system is obtained:

$$\begin{aligned}
f_{r+1}^{'''}+\frac{1}{2}\left[\frac{\eta}{2}-\frac{\xi\eta}{2}+\xi f_r+\xi s_r\right]f_{r+1}^{''}-\left[2\xi f'_r f_{r+1}^{'}+\xi M f_{r+1}^{'}\right]+\xi f_r^{''}f_{r+1}+\xi f_r^{''}s_{r+1}\\
-\xi\left(f_r f_r^{''}-s_r f_r^{''}\right)+\xi f_r^{'2}=\xi\left(1-\xi\right)\frac{\partial f_{r+1}^{'}}{\partial\xi},\\
s_{r+1}^{'''}+\frac{1}{2}\left[\frac{\eta}{2}-\frac{\xi\eta}{2}+\xi f_r+\xi s_r\right]s_{r+1}^{''}-\left[\xi s_r^{'}s_{r+1}^{'}+\xi M s_{r+1}^{'}\right]+\xi s_r^{''}f_{r+1}+\xi s_r^{''}s_{r+1}\\
-\xi\left(f_r s_r^{''}-s_r s_r^{''}\right)+\xi s_r^{'2}=\xi\left(1-\xi\right)\frac{\partial s_{r+1}^{'}}{\partial\xi},\\
\left(1/Pr\right)g_{r+1}^{''}+\left(\frac{\eta}{2}\left(1-\xi\right)+\xi\left(f_r+s_r\right)\right)g_{r+1}^{'}-\xi\left(f_r+s_r\right)g_r^{'}\\
+\left(f_{r+1}+s_{r+1}\right)g_r^{'}=\xi\left(1-\xi\right)\frac{\partial g_{r+1}}{\partial\xi},
\end{aligned}\tag{4.42}$$

where linear terms are evaluated at the current iteration level $(r+1)$ and nonlinear terms at the previous iteration level (r). (4.42) is expressed in a compact form as:

$$\begin{aligned}
f_{r+1}^{'''}+a_{1,r}f_{r+1}^{''}+a_{2,r}f_{r+1}^{'}+a_{3,r}f_{r+1}+a_{4,r}s_{r+1}+a_{5,r} &= \xi(1-\xi)\frac{\partial f_{r+1}^{'}}{\partial\xi},\\
s_{r+1}^{'''}+b_{1,r}s_{r+1}^{''}+b_{2,r}s_{r+1}^{'}+b_{3,r}s_{r+1}+b_{4,r}f_{r+1}+b_{5,r} &= \xi(1-\xi)\frac{\partial s_{r+1}^{'}}{\partial\xi},\\
(1/Pr)g_{r+1}^{''}+c_{1,r}g_{r+1}^{'}+c_{2,r}f_{r+1}+c_{3,r}s_{r+1}+c_{4,r} &= \xi(1-\xi)\frac{\partial g_{r+1}}{\partial\xi},
\end{aligned}$$

where

$$\begin{aligned}
a_{1,r} &= \frac{\eta}{2}(1-\xi)+\xi(f_r+s_r),\\
a_{2,r} &= -\xi M-2\xi f_r^{'},\\
a_{3,r} &= \xi f_r^{''},\\
a_{4,r} &= \xi f_r^{''},\\
a_{5,r} &= -\xi f_r f_r^{''}-\xi s_r f_r^{''}+\xi f_r^{'2},\\
b_{1,r} &= \frac{\eta}{2}(1-\xi)+\xi(f_r+s_r),\\
b_{2,r} &= -\xi M-2\xi s_r^{'},\\
b_{3,r} &= \xi s_r^{''},\\
b_{4,r} &= \xi s_r^{''},\\
b_{5,r} &= -\xi f_r s_r^{''}-\xi s_r s_r^{''}+\xi s_r^{'2},\\
c_{1,r} &= \frac{\eta}{2}(1-\xi)+\xi(f_r+s_r),\\
c_{2,r} &= \xi g_r^{'},\\
c_{3,r} &= \xi g_r^{'},\\
c_{4,r} &= -\xi f_r g_r^{'}-\xi s_r g_r^{'}.
\end{aligned}$$

The Crank-Nicolson finite difference approach is applied to the system (4.43) and the system becomes:

$$\begin{aligned}
&\left(f_{r+1}^{'''}\right)^{n+\frac{1}{2}}+(a_{1,r})^{n+\frac{1}{2}}\left(f_{r+1}^{''}\right)^{n+\frac{1}{2}}+(a_{2,r})^{n+\frac{1}{2}}\left(f_{r+1}^{'}\right)^{n+\frac{1}{2}}+(a_{3,r})^{\frac{1}{2}}(f_{r+1})^{n+\frac{1}{2}}\\
&\qquad+(a_{4,r})^{\frac{1}{2}}(s_{r+1})^{n+\frac{1}{2}}+(a_{5,r})=\xi^{n+\frac{1}{2}}\left(1-\xi^{n+\frac{1}{2}}\right)\frac{\partial f_{r+1}^{'}}{\partial\xi},\\
&\left(s_{r+1}^{'''}\right)^{n+\frac{1}{2}}+(b_{1,r})^{n+\frac{1}{2}}\left(s_{r+1}^{''}\right)^{n+\frac{1}{2}}+(b_{2,r})^{n+\frac{1}{2}}\left(s_{r+1}^{'}\right)^{n+\frac{1}{2}}+(b_{3,r})^{\frac{1}{2}}(s_{r+1})^{n+\frac{1}{2}}\\
&\qquad+(b_{4,r})^{\frac{1}{2}}(f_{r+1})^{n+\frac{1}{2}}+(b_{5,r})=\xi^{n+\frac{1}{2}}\left(1-\xi^{n+\frac{1}{2}}\right)\frac{\partial s_{r+1}^{'}}{\partial\xi},\\
&(1/Pr)\left(g_{r+1}^{''}\right)^{n+\frac{1}{2}}+(c_{1,r})^{n+\frac{1}{2}}\left(g_{r+1}^{'}\right)^{n+\frac{1}{2}}+(c_{2,r})^{n+\frac{1}{2}}(f_{r+1})^{n+\frac{1}{2}}\\
&\qquad+(c_{3,r})^{n+\frac{1}{2}}(s_{r+1})^{n+\frac{1}{2}}=\xi^{n+\frac{1}{2}}\left(1-\xi^{n+\frac{1}{2}}\right)\frac{\partial g_{r+1}}{\partial\xi}.
\end{aligned}\tag{4.43}$$

The Chebyshev pseudo-spectral collocation technique is applied to integrate system (4.43). System (4.43) is rewritten in the spectral collocation form to obtain:

$$\begin{aligned}
\left(D^3F_{r+1}\right)^{n+\frac{1}{2}} + (a_{1,r})^{n+\frac{1}{2}}\left(D^2F_{r+1}\right)^{n+\frac{1}{2}} + (a_{2,r})^{n+\frac{1}{2}}\left(DF_{r+1}\right)^{n+\frac{1}{2}} + (a_{3,r})^{\frac{1}{2}}\left(F_{r+1}\right)^{n+\frac{1}{2}} \\
+ (a_{4,r})^{\frac{1}{2}}\left(S_{r+1}\right)^{n+\frac{1}{2}} + (a_{5,r}) = D\xi^{n+\frac{1}{2}}\left(1-\xi^{n+\frac{1}{2}}\right)\frac{F_{r+1}^{n+1}-F_{r+1}^{n}}{\Delta\xi}, \\
\left(D^3S_{r+1}\right)^{n+\frac{1}{2}} + (b_{1,r})^{n+\frac{1}{2}}\left(D^2S_{r+1}\right)^{n+\frac{1}{2}} + (b_{2,r})^{n+\frac{1}{2}}\left(DS_{r+1}\right)^{n+\frac{1}{2}} + (b_{3,r})^{\frac{1}{2}}\left(S_{r+1}\right)^{n+\frac{1}{2}} \\
+ (b_{4,r})^{\frac{1}{2}}\left(F_{r+1}\right)^{n+\frac{1}{2}} + (b_{5,r}) = D\xi^{n+\frac{1}{2}}\left(1-\xi^{n+\frac{1}{2}}\right)\frac{S_{r+1}^{n+1}-S_{r+1}^{n}}{\Delta\xi}, \\
(1/Pr)^{n+\frac{1}{2}}\left(D^2G_{r+1}\right)^{n+\frac{1}{2}} + (c_{1,r})^{n+\frac{1}{2}}\left(DG_{r+1}\right)^{n+\frac{1}{2}} + (c_{2,r})^{n+\frac{1}{2}}\left(F_{r+1}\right)^{n+\frac{1}{2}} + (c_{3,r})^{n+\frac{1}{2}}\left(S_{r+1}\right)^{n+\frac{1}{2}} \\
+ (c_{4,r})^{n+\frac{1}{2}} = \xi^{n+\frac{1}{2}}\left(1-\xi^{n+\frac{1}{2}}\right)\frac{G_{r+1}^{n+1}-G_{r+1}^{n}}{\Delta\xi}.
\end{aligned} \tag{4.44}$$

From equation (4.44), taking terms at the next time level $(n+1)$ to the left and terms at the current time level (n) and nonlinear terms to the right, the system becomes:

$$\begin{aligned}
&\left[\frac{1}{2}\left(\mathbf{D}^3 + \mathbf{a}_{1,r}^{n+\frac{1}{2}}\mathbf{D}^2 + \mathbf{a}_{2,r}^{n+\frac{1}{2}}\mathbf{D} + \mathbf{a}_{3,r}^{n+\frac{1}{2}}\right) - \frac{\mathbf{D}\xi^{n+\frac{1}{2}}\left(1-\xi^{n+\frac{1}{2}}\right)}{\Delta\xi}\right]\mathbf{F}_{r+1}^{n+1} + \left[\frac{1}{2}\mathbf{a}_{4,r}^{n+\frac{1}{2}}\right]\mathbf{S}_{r+1}^{n+1} \\
&= \left[-\frac{1}{2}\left(\mathbf{D}^3 + \mathbf{a}_{1,r}^{n+\frac{1}{2}}\mathbf{D}^2 + \mathbf{a}_{2,r}^{n+\frac{1}{2}}\mathbf{D} + \mathbf{a}_{3,r}^{n+\frac{1}{2}}\right) - \frac{\mathbf{D}\xi^{n+\frac{1}{2}}\left(1-\xi^{n+\frac{1}{2}}\right)}{\Delta\xi}\right]\mathbf{F}_{r+1}^{n} - \left[\frac{1}{2}\mathbf{a}_{4,r}^{n+\frac{1}{2}}\right]\mathbf{S}_{r+1}^{n} - \mathbf{a}_{5,r}, \\
&\left[\frac{1}{2}\left(\mathbf{D}^3 + \mathbf{b}_{1,r}^{n+\frac{1}{2}}\mathbf{D}^2 + \mathbf{b}_{2,r}^{n+\frac{1}{2}}\mathbf{D} + \mathbf{b}_{3,r}^{n+\frac{1}{2}}\right) - \frac{\mathbf{D}\xi^{n+\frac{1}{2}}\left(1-\xi^{n+\frac{1}{2}}\right)}{\Delta\xi}\right]\mathbf{S}_{r+1}^{n+1} + \left[\frac{1}{2}\mathbf{b}_{4,r}^{n+\frac{1}{2}}\right]\mathbf{F}_{r+1}^{n+1} \\
&= \left[-\frac{1}{2}\left(\mathbf{D}^3 + \mathbf{b}_{1,r}^{n+\frac{1}{2}}\mathbf{D}^2 + \mathbf{b}_{2,r}^{n+\frac{1}{2}}\mathbf{D} + \mathbf{b}_{3,r}^{n+\frac{1}{2}}\right) - \frac{\mathbf{D}\xi^{n+\frac{1}{2}}\left(1-\xi^{n+\frac{1}{2}}\right)}{\Delta\xi}\right]\mathbf{S}_{r+1}^{n} - \left[\frac{1}{2}\mathbf{b}_{4,r}^{n+\frac{1}{2}}\right]\mathbf{F}_{r+1}^{n} - \mathbf{b}_{5,r}, \\
&\left[\frac{1}{2}\left((1/Pr)\,\mathbf{D}^2 + \mathbf{c}_{1,r}^{n+\frac{1}{2}}\mathbf{D}\right) - \frac{\xi^{n+\frac{1}{2}}\left(1-\xi^{n+\frac{1}{2}}\right)}{\Delta\xi}\right]\mathbf{G}_{r+1}^{n+1} + \left[\frac{1}{2}\mathbf{c}_{2,r}^{n+\frac{1}{2}}\right]\mathbf{F}_{r+1}^{n+1} + \left[\frac{1}{2}\mathbf{c}_{3,r}^{n+\frac{1}{2}}\right]\mathbf{S}_{r+1}^{n+1} \\
&= \left[-\frac{1}{2}\left((1/Pr)\,\mathbf{D}^2 + \mathbf{c}_{1,r}^{n+\frac{1}{2}}\mathbf{D}\right) - \frac{\xi^{n+\frac{1}{2}}\left(1-\xi^{n+\frac{1}{2}}\right)}{\Delta\xi}\right]\mathbf{G}_{r+1}^{n} - \left[\frac{1}{2}\mathbf{c}_{2,r}^{n+\frac{1}{2}}\right]\mathbf{F}_{r+1}^{n} - \left[\frac{1}{2}\mathbf{c}_{3,r}^{n+\frac{1}{2}}\right]\mathbf{S}_{r+1}^{n}.
\end{aligned} \tag{4.45}$$

The system (4.45) is written in a compact form as :

$$\begin{aligned}
\mathbf{A}_{11}\mathbf{F}_{r+1}^{n+1}+\mathbf{A}_{12}\mathbf{S}_{r+1}^{n+1}+\mathbf{A}_{13}\mathbf{G}_{r+1}^{n+1} &= \mathbf{B}_{11}\mathbf{F}_{r+1}^{n}+\mathbf{B}_{12}\mathbf{S}_{r+1}^{n}+\mathbf{B}_{13}\mathbf{G}_{r+1}^{n}+\mathbf{K}_1,\\
\mathbf{A}_{21}\mathbf{F}_{r+1}^{n+1}+\mathbf{A}_{32}\mathbf{S}_{r+1}^{n+1}+\mathbf{A}_{33}\mathbf{G}_{r+1}^{n+1} &= \mathbf{B}_{21}\mathbf{F}_{r+1}^{n}+\mathbf{B}_{22}\mathbf{S}_{r+1}^{n}+\mathbf{B}_{23}\mathbf{G}_{r+1}^{n}+\mathbf{K}_2,\\
\mathbf{A}_{31}\mathbf{F}_{r+1}^{n+1}+\mathbf{A}_{32}\mathbf{S}_{r+1}^{n+1}+\mathbf{A}_{33}\mathbf{G}_{r+1}^{n+1} &= \mathbf{B}_{31}\mathbf{F}_{r+1}^{n}+\mathbf{B}_{32}\mathbf{S}_{r+1}^{n}+\mathbf{B}_{33}\mathbf{G}_{r+1}^{n}+\mathbf{K}_3,
\end{aligned} \tag{4.46}$$

where

$$\begin{aligned}
\mathbf{A}_{11} &= \frac{1}{2}\left(\mathbf{D}^3+\mathbf{a}_{1,r}^{n+\frac{1}{2}}\mathbf{D}^2+\mathbf{a}_{2,r}^{n+\frac{1}{2}}\mathbf{D}+\mathbf{a}_{3,r}^{n+\frac{1}{2}}\right)-\frac{\mathbf{D}\xi^{n+\frac{1}{2}}\left(1-\xi^{n+\frac{1}{2}}\right)}{\Delta\xi},\\
\mathbf{B}_{11} &= -\frac{1}{2}\left(\mathbf{D}^3+\mathbf{a}_{1,r}^{n+\frac{1}{2}}\mathbf{D}^2+\mathbf{a}_{2,r}^{n+\frac{1}{2}}\mathbf{D}+\mathbf{a}_{3,r}^{n+\frac{1}{2}}\right)-\frac{\mathbf{D}\xi^{n+\frac{1}{2}}\left(1-\xi^{n+\frac{1}{2}}\right)}{\Delta\xi},\\
\mathbf{K}_1 &= -\mathbf{a}_{5,r}^{n+\frac{1}{2}},\quad \mathbf{A}_{12}=\frac{1}{2}\mathbf{a}_{4,r}^{n+\frac{1}{2}},\quad \mathbf{B}_{12}=-\frac{1}{2}\mathbf{a}_{4,r}^{n+\frac{1}{2}},\\
\mathbf{A}_{13} &= \mathbf{0},\quad \mathbf{B}_{13}=\mathbf{0},\quad \mathbf{A}_{21}=\frac{1}{2}\mathbf{b}_{4,r}^{n+\frac{1}{2}},\quad \mathbf{B}_{21}=-\frac{1}{2}\mathbf{b}_{4,r}^{n+\frac{1}{2}},\\
\mathbf{A}_{22} &= \frac{1}{2}\left(\mathbf{D}^3+\mathbf{b}_{1,r}^{n+\frac{1}{2}}\mathbf{D}^2+\mathbf{b}_{2,r}^{n+\frac{1}{2}}\mathbf{D}+\mathbf{b}_{3,r}^{n+\frac{1}{2}}\right)-\frac{\mathbf{D}\xi^{n+\frac{1}{2}}\left(1-\xi^{n+\frac{1}{2}}\right)}{\Delta\xi},\\
\mathbf{B}_{22} &= -\frac{1}{2}\left(\mathbf{D}^3+\mathbf{b}_{1,r}^{n+\frac{1}{2}}\mathbf{D}^2+\mathbf{b}_{2,r}^{n+\frac{1}{2}}\mathbf{D}+\mathbf{b}_{3,r}^{n+\frac{1}{2}}\right)-\frac{\mathbf{D}\xi^{n+\frac{1}{2}}\left(1-\xi^{n+\frac{1}{2}}\right)}{\Delta\xi},\\
\mathbf{A}_{23} &= \mathbf{0},\quad \mathbf{B}_{23}=\mathbf{0},\quad \mathbf{K}_2=-\mathbf{b}_{5,r},\quad \mathbf{A}_{31}=\frac{1}{2}\mathbf{c}_{2,r}^{n+\frac{1}{2}},\\
\mathbf{B}_{31} &= -\frac{1}{2}\mathbf{c}_{2,r}^{n+\frac{1}{2}},\quad \mathbf{A}_{32}=\frac{1}{2}\mathbf{c}_{3,r}^{n+\frac{1}{2}},\quad \mathbf{B}_{32}=-\frac{1}{2}\mathbf{c}_{3,r}^{n+\frac{1}{2}},\\
\mathbf{A}_{33} &= \frac{1}{2}\left((1/Pr)\,\mathbf{D}^2+\mathbf{c}_{1,r}^{n+\frac{1}{2}}\mathbf{D}\right)-\frac{\xi^{n+\frac{1}{2}}\left(1-\xi^{n+\frac{1}{2}}\right)}{\Delta\xi}\mathbf{I},\\
\mathbf{B}_{33} &= \frac{1}{2}\left((1/Pr)\,\mathbf{D}^2+\mathbf{c}_{1,r}^{n+\frac{1}{2}}\mathbf{D}\right)-\frac{\xi^{n+\frac{1}{2}}\left(1-\xi^{n+\frac{1}{2}}\right)}{\Delta\xi}\mathbf{I},\\
\mathbf{K}_3 &= -\mathbf{c}_{1,r}^{n+\frac{1}{2}}.
\end{aligned} \tag{4.47}$$

The system (4.46) is solved as a matrix form as shown below.

$$\begin{bmatrix}\mathbf{A}_{11} & \mathbf{A}_{12} & \mathbf{A}_{13}\\ \mathbf{A}_{21} & \mathbf{A}_{22} & \mathbf{A}_{23}\\ \mathbf{A}_{31} & \mathbf{A}_{32} & \mathbf{A}_{33}\end{bmatrix}\times\begin{bmatrix}\mathbf{F}_{r+1}^{n+1}\\ \mathbf{S}_{r+1}^{n+1}\\ \mathbf{G}_{r+1}^{n+1}\end{bmatrix}=\begin{bmatrix}\mathbf{B}_{11} & \mathbf{B}_{12} & \mathbf{B}_{13}\\ \mathbf{B}_{21} & \mathbf{B}_{22} & \mathbf{B}_{23}\\ \mathbf{B}_{31} & \mathbf{B}_{32} & \mathbf{B}_{33}\end{bmatrix}\times\begin{bmatrix}\mathbf{F}_{r+1}^{n}\\ \mathbf{S}_{r+1}^{n}\\ \mathbf{G}_{r+1}^{n}\end{bmatrix}+\begin{bmatrix}\mathbf{K}_1\\ \mathbf{K}_2\\ \mathbf{K}_3\end{bmatrix},$$

where all the entries of the matrix are matrices and boundary conditions are imposed on the matrices as shown below.

$$\mathbf{A}_{11}=\begin{bmatrix} \mathbf{D}_{0,0} & \mathbf{D}_{0,1} & \cdots & \mathbf{D}_{0,N-1} & \mathbf{D}_{0,N} \\ & & \mathbf{A}_{11} & & \\ \mathbf{D}_{N,0} & \mathbf{D}_{N,1} & \cdots & \mathbf{D}_{N,N-1} & \mathbf{D}_{N,N} \\ 0 & 0 & \cdots & 0 & 1 \end{bmatrix}, \quad \mathbf{A}_{12}=\begin{bmatrix} 0 & 0 & \cdots & 0 & 0 \\ & & \mathbf{A}_{12} & & \\ 0 & 0 & \cdots & 0 & 0 \\ 0 & 0 & \cdots & 0 & 0 \end{bmatrix},$$

$$\mathbf{A}_{21}=\begin{bmatrix} 0 & 0 & \cdots & 0 & 0 \\ & & \mathbf{A}_{21} & & \\ 0 & 0 & \cdots & 0 & 0 \end{bmatrix}, \quad \mathbf{A}_{22}=\begin{bmatrix} \mathbf{D}_{0,0} & \mathbf{D}_{0,1} & \cdots & \mathbf{D}_{0,N-1} & \mathbf{D}_{0,N} \\ & & \mathbf{A}_{22} & & \\ \mathbf{D}_{N,0} & \mathbf{D}_{N,1} & \cdots & \mathbf{D}_{N,N-1} & \mathbf{D}_{N,N} \\ 0 & 0 & \cdots & 0 & 1 \end{bmatrix},$$

$$\mathbf{A}_{13}=\begin{bmatrix} 0 & 0 & \cdots & 0 & 0 \\ & & \mathbf{A}_{13} & & \\ 0 & 0 & \cdots & 0 & 0 \\ 0 & 0 & \cdots & 0 & 0 \end{bmatrix}, \quad \mathbf{A}_{23}=\begin{bmatrix} 0 & 0 & \cdots & 0 & 0 \\ & & \mathbf{A}_{23} & & \\ 0 & 0 & \cdots & 0 & 0 \end{bmatrix},$$

$$\mathbf{A}_{31}=\begin{bmatrix} 0 & 0 & \cdots & 0 & 0 \\ & & \mathbf{A}_{31} & & \\ 0 & 0 & \cdots & 0 & 0 \end{bmatrix}, \quad \mathbf{A}_{32}=\begin{bmatrix} 0 & 0 & \cdots & 0 & 0 \\ & & \mathbf{A}_{32} & & \\ 0 & 0 & \cdots & 0 & 0 \end{bmatrix}, \quad \mathbf{A}_{33}=\begin{bmatrix} 1 & 0 & \cdots & 0 & 0 \\ & & \mathbf{A}_{33} & & \\ 0 & 0 & \cdots & 0 & 1 \end{bmatrix},$$

$$\mathbf{B}_{11}=\begin{bmatrix} 0 & 0 & \cdots & 0 & 0 \\ & & \mathbf{B}_{11} & & \\ 0 & 0 & \cdots & 0 & 0 \\ 0 & 0 & \cdots & 0 & 0 \end{bmatrix}, \quad \mathbf{B}_{12}=\begin{bmatrix} 0 & 0 & \cdots & 0 & 0 \\ & & \mathbf{B}_{12} & & \\ 0 & 0 & \cdots & 0 & 0 \\ 0 & 0 & \cdots & 0 & 0 \end{bmatrix}, \quad \mathbf{B}_{13}=\begin{bmatrix} 0 & 0 & \cdots & 0 & 0 \\ & & \mathbf{B}_{13} & & \\ 0 & 0 & \cdots & 0 & 0 \\ 0 & 0 & \cdots & 0 & 0 \end{bmatrix},$$

$$\mathbf{B}_{21}=\begin{bmatrix} 0 & 0 & \cdots & 0 & 0 \\ & & \mathbf{B}_{21} & & \\ 0 & 0 & \cdots & 0 & 0 \end{bmatrix}, \quad \mathbf{B}_{22}=\begin{bmatrix} 0 & 0 & \cdots & 0 & 0 \\ & & \mathbf{B}_{22} & & \\ 0 & 0 & \cdots & 0 & 0 \end{bmatrix}, \quad \mathbf{B}_{23}=\begin{bmatrix} 0 & 0 & \cdots & 0 & 0 \\ & & \mathbf{B}_{23} & & \\ 0 & 0 & \cdots & 0 & 0 \end{bmatrix},$$

$$\mathbf{B}_{31}=\begin{bmatrix} 0 & 0 & \cdots & 0 & 0 \\ \hline & & \mathbf{B}_{31} & & \\ \hline 0 & 0 & \cdots & 0 & 0 \end{bmatrix}, \quad \mathbf{B}_{32}=\begin{bmatrix} 0 & 0 & \cdots & 0 & 0 \\ \hline & & \mathbf{B}_{32} & & \\ \hline 0 & 0 & \cdots & 0 & 0 \end{bmatrix}, \quad \mathbf{B}_{33}=\begin{bmatrix} 0 & 0 & \cdots & 0 & 0 \\ \hline & & \mathbf{B}_{33} & & \\ \hline 0 & 0 & \cdots & 0 & 0 \end{bmatrix},$$

$$\mathbf{K}_1=\begin{bmatrix} 0 \\ \hline \\ \mathbf{K}_1 \\ \\ \hline 1 \\ \hline 0 \end{bmatrix}, \quad \mathbf{K}_2=\begin{bmatrix} 0 \\ \hline \\ \mathbf{K}_2 \\ \\ \hline c \\ \hline 0 \end{bmatrix}, \quad \mathbf{K}_3=\begin{bmatrix} 0 \\ \hline \\ \mathbf{K}_3 \\ \\ \hline 0 \end{bmatrix}, \quad \mathbf{F}^{n+1}_{r+1}=\begin{bmatrix} f^{n+1}_{r+1,0} \\ \hline \vdots \\ \vdots \\ \hline f^{n+1}_{r+1,N-1} \\ \hline f^{n+1}_{r+1,N} \end{bmatrix},$$

$$\mathbf{S}^{n+1}_{r+1}=\begin{bmatrix} s^{n+1}_{r+1,0} \\ \hline \vdots \\ \vdots \\ \hline s^{n+1}_{r+1,N-1} \\ \hline s^{n+1}_{r+1,N} \end{bmatrix}, \quad \mathbf{G}^{n+1}_{r+1}=\begin{bmatrix} g^{n+1}_{r+1,0} \\ \hline \vdots \\ \\ \vdots \\ \hline g^{n+1}_{r+1,N} \end{bmatrix}, \quad \mathbf{F}^{n}_{r+1}=\begin{bmatrix} f^{n}_{r+1,0} \\ \hline \vdots \\ \vdots \\ \hline f^{n}_{r+1,N-1} \\ \hline f^{n}_{r+1,N} \end{bmatrix}, \quad \mathbf{S}^{n}_{r+1}=\begin{bmatrix} s^{n}_{r+1,0} \\ \hline \vdots \\ \vdots \\ \hline s^{n}_{r+1,N-1} \\ \hline s^{n}_{r+1,N} \end{bmatrix},$$

$$\mathbf{G}^{n}_{r+1}=\begin{bmatrix} g^{n}_{r+1,0} \\ \hline \vdots \\ \\ \vdots \\ \hline g^{n}_{r+1,N} \end{bmatrix}.$$

4.4 Results and Discussion

In this section, the numerical solutions obtained for the system of partial differential equations (4.1) with their corresponding boundary conditions (4.2) are presented. The results obtained for the skin frictions $f''(\xi,0)$ and $s''(\xi,0)$ at selected time (ξ) values are displayed. Comparative study is carried out on the solutions obtained by the SRM, SLLM and SQLM to investigate how well they compare and to note if results obtained match one another and results from published literature. Comparison will be carried out by noting how number of iterations improve accuracy and the effect of the time (ξ) on the accuracy of the solutions.

For the purpose of this study, the parameters used were assigned specific values except where mentioned otherwise. The value of the stretching ratio was set to be $c = 0.5$. The Prandtl number chosen was $Pr = 0.7$. Magnetic parameter was set at $M = 1$. The number of grid points used in the space direction was $N_x = 100$ while the number of grid points in the time direction was $N_t = 500$ and the length of scale was $L = 20$.

Table 4.1: Comparison of Skin friction $-f''(0)$ obtained by the SRM, SLLM and the SQLM and the number of iterations used

ξ	SRM	It	SQLM	It	SLLM	It
0.1	0.67444361	5	0.67444361	2	0.67444361	4
0.3	0.88040763	5	0.88040763	2	0.88040763	4
0.5	0.06892987	5	0.06892987	2	0.06892987	4
0.7	1.24206762	5	1.24206762	2	1.24206762	4
0.9	1.40159803	5	1.40159803	3	1.40159803	4

Table 4.2: Comparison of Skin friction $-s''(0)$ obtained by the SRM, SLLM and the SQLM and the number of iterations used

ξ	SRM	It	SQLM	It	SLLM	It
0.1	0.32758579	5	0.32758579	2	0.32758579	4
0.3	0.41456520	5	0.41456520	2	0.41456520	4
0.5	0.49636949	5	0.49636949	2	0.49636949	4
0.7	0.57322434	5	0.57322434	2	0.57322434	4
0.9	0.64538300	5	0.64538300	2	0.64538300	4

Table 4.3: Comparison of Nusselt number $-g^{'}(0)$ obtained by the SRM, SLLM and the SQLM and the number of iterations used

ξ	SRM	It	SQLM	It	SLLM	It
0.1	0.48308513	5	0.48308513	2	0.48308513	4
0.3	0.50350549	5	0.50350549	2	0.50350549	4
0.5	0.52102092	5	0.52102092	2	0.52102092	4
0.7	0.53406454	5	0.53406454	2	0.53406454	4
0.9	0.53713012	5	0.53713012	2	0.53713012	4

Tables 4.1, 4.2 and 4.3 show the number of iterations used by the SRM, SLLM and SQLM in obtaining numerical solutions. It is observed that the solutions obtained for the Skin frictions $f^{''}$ and $s^{''}$ and the surface heat transfer rate $g^{'}$ obtained for the SRM, SLLM and SQLM are consistent with each other at different values of ξ after convergence is attained. As shown in Tables 4.1, 4.2 and 4.3, the SQLM converges fastest after 2 iterations to 8 decimal places except at $\xi = 0.9$ in Table 4.1 where it takes 3 iterations. The SLLM converges after 4 iterations while the SRM converges slowest after 5 iterations.

To further verify the solutions obtained using these methods, the solutions obtained using the SRM, SLLM and SQLM are validated against solutions obtained by other known numerical methods. Dlamini et al. (2013a) used the compact finite difference relaxation method (CFDRM) to solve an unsteady three-dimensional MHD boundary layer flow and heat transfer over an impulsively stretching plate and solutions obtained are presented in Table 4.4.

Table 4.4: Comparison of $-f^{''}(0)$ with those reported by Dlamini et al. (2013a)

ξ	Dlamini et al. (2013a)	Present work
0.1	0.674444	0.674444
0.3	0.880408	0.880408
0.5	0.068930	0.068930
0.7	1.242068	1.242068
0.9	1.401598	1.401598

Table 4.4 shows that both sets of solutions are in excellent agreement to six decimal places shown in their reported result. This validates the results obtained using the SRM, SLLM and SQLM.

Figures 4.1 - 4.6 show the effect of iterations and time ξ on the accuracy of the solutions obtained using the SRM, SLLM and the SQLM. From the figures, it is possible to investigate the importance of iterations and time (ξ) on the convergence and accuracy of numerical solutions obtained. In the previous chapter, observation was made on these effects on the system of two partial differential equations and it was observed that the number of iterations affected the accuracy of solutions and it was also noted that the time ξ had neither positive nor negative effect on the accuracies. However, the system (4.1) is a system of three partial differential equations and it will be observed if that brings about a change in what was observed in the previous chapter.

Accuracy is determined by the use of the infinity norm of the residual error which is obtained by inserting the approximate solutions gotten with the SRM, SLLM and SQLM into the original system of partial differential equations (4.1). The residual error of the SRM, SLLM and SQLM are obtained from:

$$\begin{aligned} Res(\mathbf{f}) &= \mathbf{f}^{'''} + \frac{1}{2}(1-\xi)\eta\mathbf{f}^{''} + \xi[(\mathbf{f}+\mathbf{s})\mathbf{f}^{''} - \mathbf{f}^{'2} - M\mathbf{f}^{'}] - \xi(1-\xi)\frac{\partial \mathbf{f}^{'}}{\partial \xi}, \\ Res(\mathbf{s}) &= \mathbf{s}^{'''} + \frac{1}{2}(1-\xi)\eta\mathbf{s}^{''} + \xi[(\mathbf{f}+\mathbf{s})\mathbf{s}^{''} - \mathbf{s}^{'2} - M\mathbf{s}^{'}] - \xi(1-\xi)\frac{\partial \mathbf{s}^{'}}{\partial \xi}, \\ Res(\mathbf{g}) &= \mathbf{g}^{''} + \frac{1}{2}Pr(1-\xi)\eta\mathbf{g}^{'} + Pr\xi(\mathbf{f}+\mathbf{s})\mathbf{g}^{'} - Pr\xi(1-\xi)\frac{\partial \mathbf{g}}{\partial \xi}, \end{aligned} \tag{4.48}$$

where the system of equations (4.48) are made up of approximate solutions that are gotten using the SRM, SLLM and SQLM. The infinity norms of (2.81) defined as

$$\begin{aligned} IN_r(f) &= ||Res(f)||_\infty, \\ IN_r(s) &= ||Res(s)||_\infty, \\ IN_r(g) &= ||Res(g)||_\infty, \end{aligned} \tag{4.49}$$

were used to identify the optimal solutions of (4.48). The residual error is obtained at each iteration level subject to the time ξ. The point where the residual error is smallest is referred

to as the *optimal residual error* and this point is used to determine the level of accuracy and the number of iterations required to achieve full convergence.

Table 4.5: Convergence of $||Res(\mathbf{f})||_\infty$ obtained using the SRM, SLLM and SQLM at $\xi = 0.8$

iterations	SQLM $\|\|Res(\mathbf{f})\|\|_\infty$	SRM $\|\|Res(\mathbf{f})\|\|_\infty$	SLLM $\|\|Res(\mathbf{f})\|\|_\infty$
1	1.7×10^{-2}	1.2×10^{-1}	2.8×10^{-2}
2	1.5×10^{-8}	8.0×10^{-4}	4.7×10^{-5}
3	3.8×10^{-10}	5.5×10^{-6}	6.3×10^{-8}
4	1.4×10^{-10}	3.7×10^{-8}	7.8×10^{-11}
5	2.8×10^{-10}	2.5×10^{-10}	2.7×10^{-12}
6	2.7×10^{-10}	1.8×10^{-12}	3.8×10^{-13}
7	2.3×10^{-10}	8.7×10^{-13}	3.8×10^{-13}
8	2.6×10^{-10}	8.7×10^{-13}	3.8×10^{-13}
9	1.6×10^{-10}	8.7×10^{-13}	3.8×10^{-13}
10	1.7×10^{-10}	8.7×10^{-13}	3.8×10^{-13}
11	2.7×10^{-10}	8.7×10^{-13}	3.8×10^{-13}
12	2.8×10^{-10}	8.7×10^{-13}	3.8×10^{-13}
13	2.5×10^{-10}	8.7×10^{-13}	3.8×10^{-13}
14	2.0×10^{-10}	8.7×10^{-13}	3.8×10^{-13}
15	2.6×10^{-10}	8.7×10^{-13}	3.8×10^{-13}

Table 4.6: Convergence of $||Res(\mathbf{s})||_\infty$ obtained using the SRM, SLLM and SQLM at $\xi = 0.8$

	SQLM	SRM	SLLM
iterations	$\|\|Res(\mathbf{s})\|\|_\infty$	$\|\|Res(\mathbf{s})\|\|_\infty$	$\|\|Res(\mathbf{s})\|\|_\infty$
1	6.9×10^{-3}	2.7×10^{-2}	1.7×10^{-2}
2	5.6×10^{-9}	8.6×10^{-5}	2.4×10^{-5}
3	9.5×10^{-11}	2.9×10^{-7}	3.3×10^{-8}
4	8.2×10^{-11}	1.0×10^{-9}	4.1×10^{-11}
5	9.0×10^{-11}	3.4×10^{-12}	2.4×10^{-13}
6	8.4×10^{-11}	6.7×10^{-13}	3.2×10^{-13}
7	3.9×10^{-11}	1.1×10^{-12}	3.2×10^{-13}
8	2.6×10^{-11}	1.1×10^{-12}	3.2×10^{-13}
9	3.2×10^{-11}	1.1×10^{-12}	3.2×10^{-13}
10	7.1×10^{-11}	1.1×10^{-12}	3.2×10^{-13}
11	7.6×10^{-11}	1.1×10^{-12}	3.2×10^{-13}
12	2.5×10^{-11}	1.1×10^{-12}	3.2×10^{-13}
13	8.1×10^{-11}	1.1×10^{-12}	3.2×10^{-13}
14	1.1×10^{-11}	1.1×10^{-12}	3.2×10^{-13}
15	6.2×10^{-11}	1.1×10^{-12}	3.2×10^{-13}

Table 4.7: Convergence of $||Res(\mathbf{g})||_\infty$ obtained using the SRM, SLLM and SQLM at $\xi = 0.8$

	SQLM	SRM	SLLM
iterations	$\|\|Res(\mathbf{g})\|\|_\infty$	$\|\|Res(\mathbf{g})\|\|_\infty$	$\|\|Res(\mathbf{g})\|\|_\infty$
1	3.2×10^{-3}	2.1×10^{-11}	4.8×10^{-2}
2	3.4×10^{-9}	2.6×10^{-12}	6.8×10^{-5}
3	1.6×10^{-12}	1.3×10^{-12}	9.9×10^{-8}
4	9.3×10^{-13}	1.6×10^{-12}	1.2×10^{-10}
5	2.6×10^{-12}	3.9×10^{-12}	1.3×10^{-12}
6	2.6×10^{-12}	6.5×10^{-12}	2.6×10^{-12}
7	2.6×10^{-12}	5.2×10^{-12}	2.6×10^{-12}
8	2.6×10^{-12}	5.2×10^{-12}	2.6×10^{-12}
9	1.3×10^{-12}	5.2×10^{-12}	2.6×10^{-12}
10	2.6×10^{-12}	5.2×10^{-12}	2.6×10^{-12}
11	2.6×10^{-12}	5.2×10^{-12}	2.6×10^{-12}
12	2.5×10^{-12}	5.2×10^{-12}	2.6×10^{-12}
13	1.3×10^{-12}	5.2×10^{-12}	2.6×10^{-12}
14	2.6×10^{-12}	5.2×10^{-12}	2.6×10^{-12}
15	9.6×10^{-13}	5.2×10^{-12}	2.6×10^{-12}

Tables 4.5, 4.6 and 4.7 display the residual error norm of the solutions for the system of partial differential equations (4.1) obtained using the SRM, SLLM and the SQLM. Observation is made from the tables that an increment in the number of iterations decreases the norm of the residual error resulting in an increase in the accuracy of the approximate solutions obtained using the three methods. A reduction in the norm of the residual occurs continually until convergence is achieved and the level of accuracy of the methods is deduced using the point of convergence. It can be seen from Tables 4.5, 4.6 and 4.7 that the SQLM converges fastest at the 3^{rd} iteration making it faster than the SRM that takes 7 iterations and the SLLM that takes 6 iterations to converge. It is seen that the SQLM does not attain full convergence as the residual norms are slightly different while the SRM and the SLLM attain full convergence. Furthermore, it is observed in Table 4.5 that the SQLM converges to a larger residual error norm than the SRM and SLLM which indicates that the SQLM has lesser accuracy when

compared to the SRM and the SLLM while in Table 4.6, the residual error norms of the three methods are closely comparable but the SLLM has a higher accuracy. It is also seen from Table 4.7 that the three methods converge to similar residual error norms which shows that the methods are comparable in terms of their accuracy.

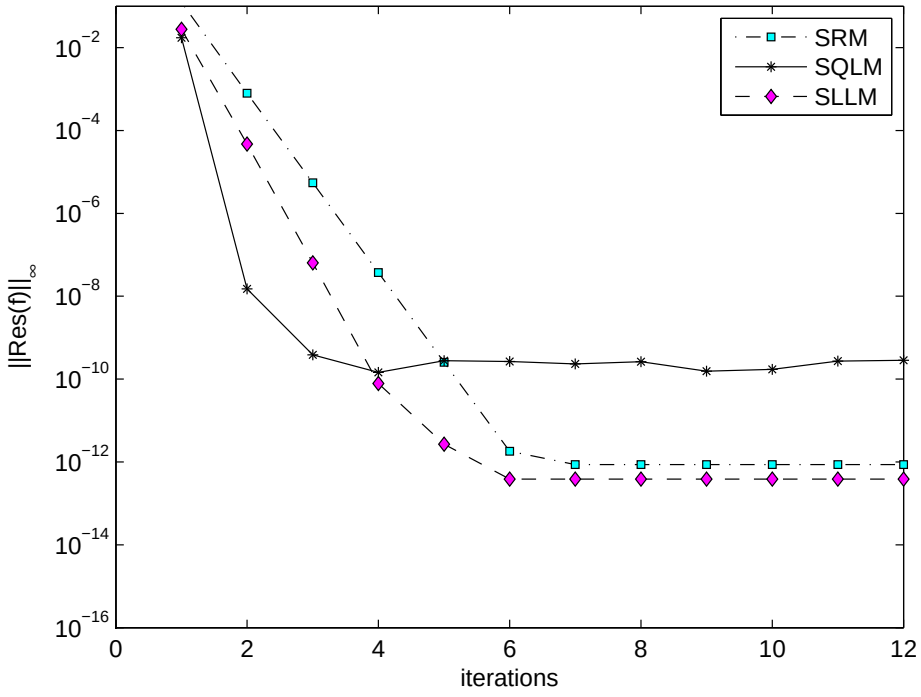

Figure 4.1: Effect of iterations on $||Res(f)||_\infty$ at $\xi = 0.4$

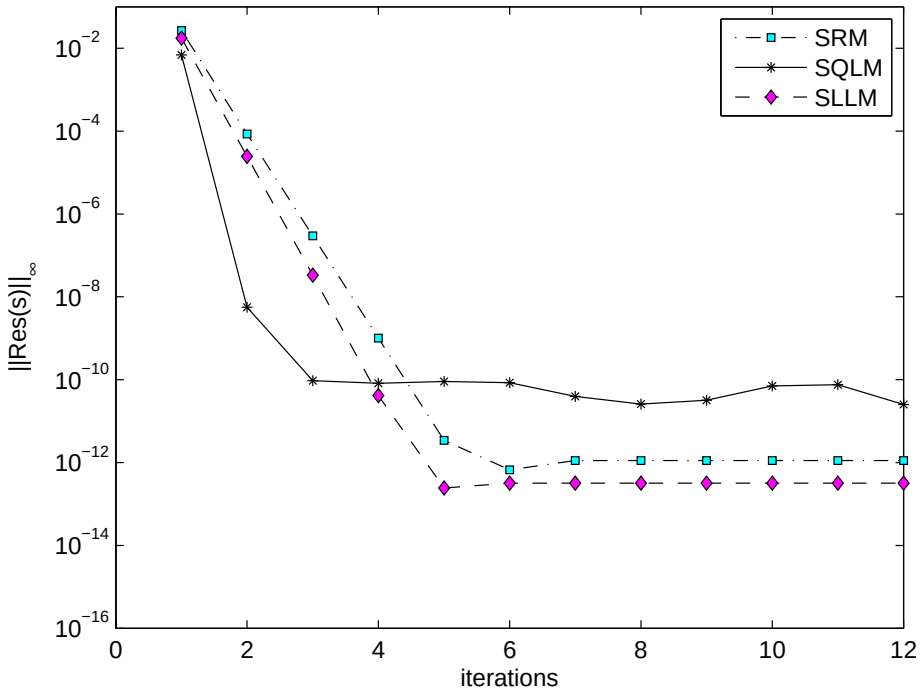

Figure 4.2: Effect of iterations on $||Res(s)||_\infty$ at $\xi = 0.4$

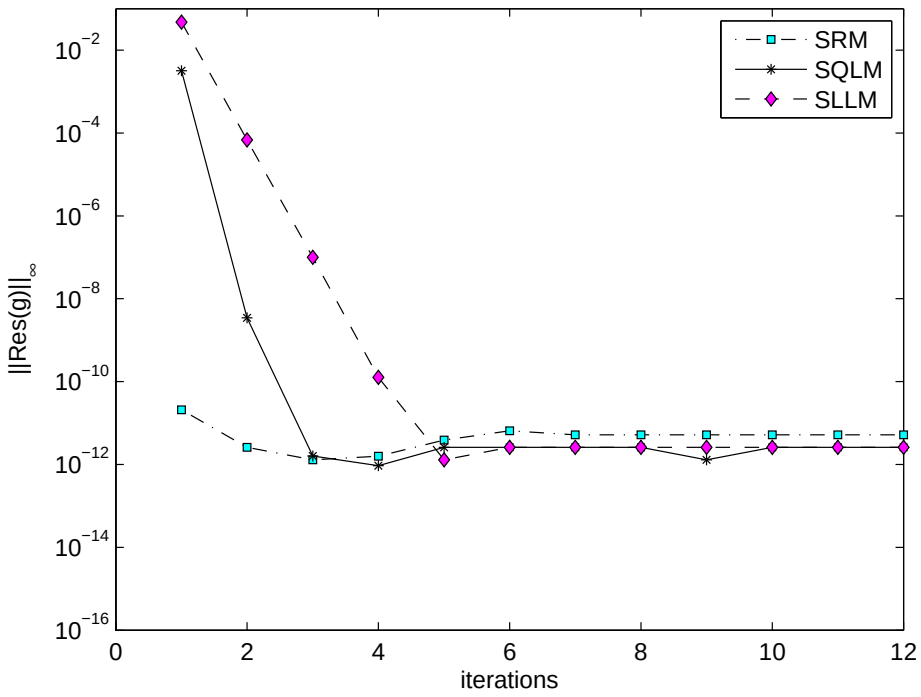

Figure 4.3: Effect of iterations on $||Res(g)||_\infty$ at $\xi = 0.4$

Figures 4.1 - 4.3 show the convergence of the norm of the residual error of each numerical method as the number of iterations increase and it is observed that as the number of iterations increases, the norm of the residual error of the three methods improves until a point where the residual error norm cannot improve further. At that point, *optimal residual error norm* is said to have been obtained and it is deduced that at that point, the solutions have converged fully.

It can be seen from Figure 4.1 that as the number of iterations increase, the norm of the residual error decreases rapidly to a point where they don't improve. At that saturation point, *convergence* has been attained and it is noted that increase in the number of iterations from that point onwards doesn't affect the *convergence* either positively or negatively. So this means just a few amount of iterations are needed to obtain converged numerical solutions. It is observed that the SQLM attains convergence after just two iterations at about 10^{-08} while at about 10^{-11}, it takes the SLLM 5 iterations and the SRM 6 iterations to attain *convergence*. This implies that fewer amount of iterations are required by the SQLM to attain convergence than the SRM and the SLLM but it converges to a lesser accuracy than the other two methods and the SRM and the SLLM are comparable in terms of accuracy. The SQLM and the SLLM can be observed to have the same starting points but the slope of the SQLM is steeper than the SLLM which further indicates that the SQLM converges faster than the SLLM. The convergence rate of the SQLM is calculated to be 0.26 while that of the SRM is 0.99 and the SLLM is 1.04 which implies that the SRM and the SLLM have a faster convergence rate than the SQLM.

From Figure 4.2, we observed that the SQLM attains convergence at a norm of 10^{-08} after 2 iterations while both the SRM and the SLLM attain convergence after 6 and 5 iterations respectively at a norm of about 10^{-12}. This means that the SQLM takes lesser amount of iterations to converge but converges to a lesser accuracy than the other methods while the SRM and the SLLM take more iterations but are comparable in terms of accuracy. The slope of the SQLM can also be observed to be steeper than the slopes of the SRM and the SLLM showing that the SQLM converges faster than the other methods. The convergence rate of the SQLM is 0.29 (superlinear convergence) which is lower than the SLLM and SRM that are

both at 1.004 (sublinear convergence) shows that the SQLM has a slower convergence rate than the other methods.

As shown in Figure 4.3, it is instantly observed that the SRM starts at a higher accuracy after a single iteration and obtains its convergence at the 2^{nd} iteration at an accuracy close to 10^{-12} but converges fully at the 5^{th} iteration to about 10^{-10} which is the point of convergence obtained by the SQLM after 3 iterations and the SLLM at the 5^{th} iteration. The SQLM takes fewer iterations to maintain a consistent accuracy and the three methods are comparable in terms of accuracy here. The convergence rate of the SQLM is 0.56 while the convergence rate of the SLLM is 1.00 which implies that the SLLM has a faster convergence rate than the SQLM.

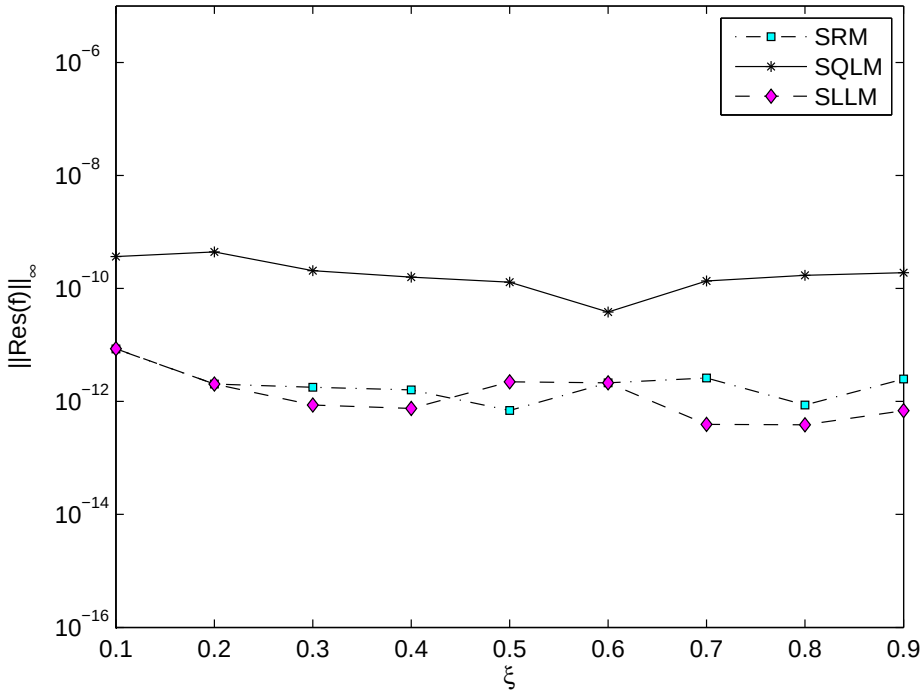

Figure 4.4: Effect of time (ξ) on $||Res(f)||_\infty$ when $\eta = 20$

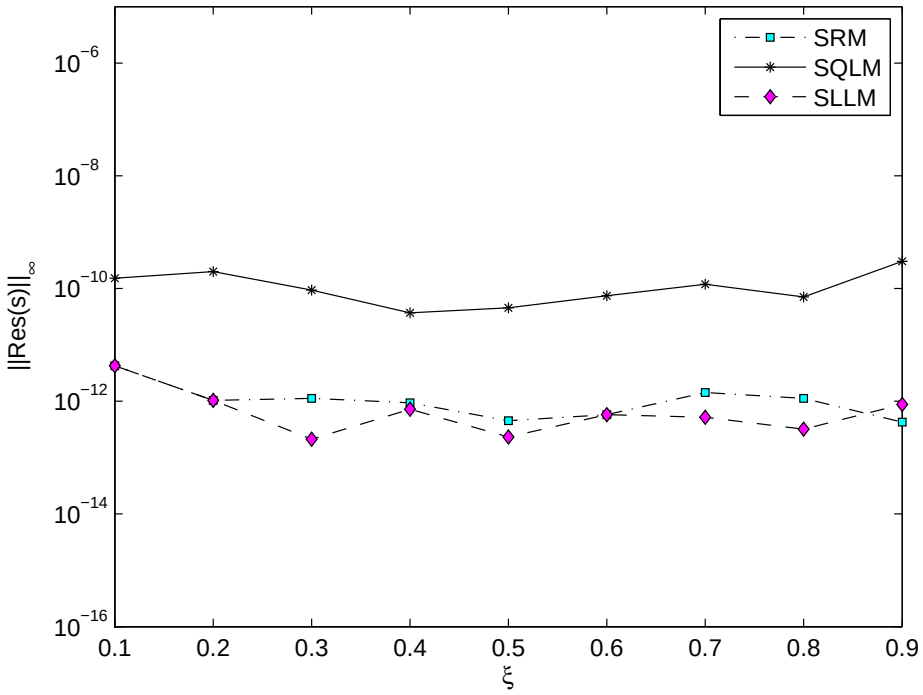

Figure 4.5: Effect of time (ξ) on $||Res(s)||_\infty$ when $\eta = 20$

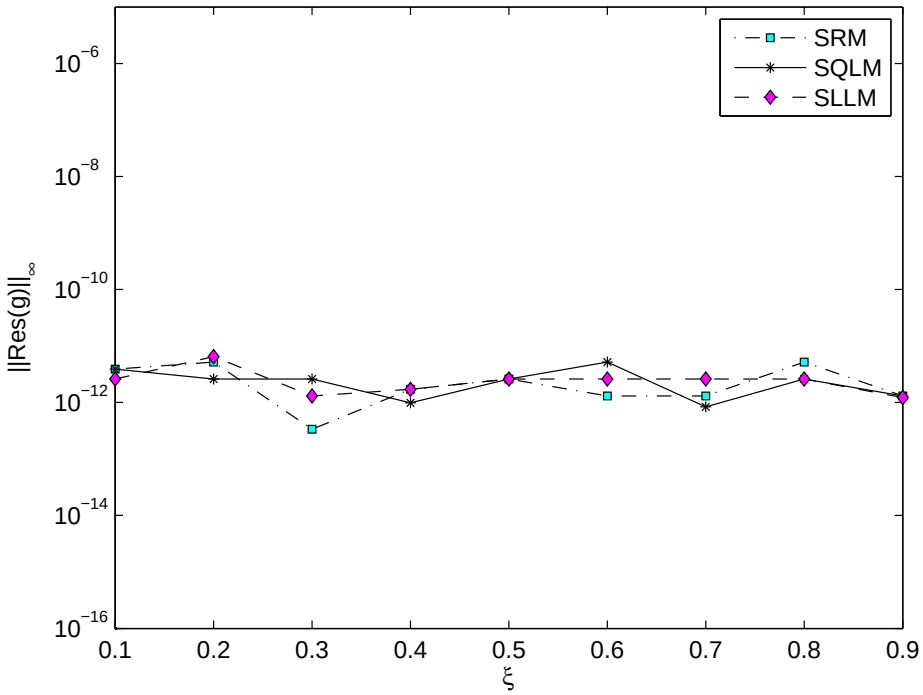

Figure 4.6: Effect of time (ξ) on $||Res(g)||_\infty$ when $\eta = 20$

Figures 4.4 - 4.6 show the effect of the time function ξ on the system of partial differential equations 4.48 using the SRM, SLLM and SQLM. In the three Figures, the effect of the time function moving from $\xi = 0$ to $\xi = 1$ on the accuracy of the methods is observed.

As shown in Figure 4.4, it is observed that as the time ξ changes, the norm of the residual error of the three methods remains the same. The SQLM can be seen to maintain a residual error norm close to 10^{-8} while the norm of the residual of the SRM and the SLLM oscillates between 10^{-10} and 10^{-12}. It is observed that the SRM and the SLLM compare well in terms of accuracy. Figure 4.5 shows that as the time ξ increases, the residual error of the three methods remain bounded within a certain range. The same accuracy is maintained in a distorted manner but the solutions are convergent at a point. The SQLM can be seen to maintain an accuracy of 10^{-8} while the SRM and the SLLM both maintain accuracy of 10^{-11}. Hence we see that the SRM and the SLLM compare well in terms of accuracy. It can be seen from Figure 4.6 that the norm of the residual errors of the three methods remain bounded between 10^{-10} and 10^{-12} . This shows that the three methods are comparable in terms of their accuracies.

4.5 Summary

In this chapter, the SRM, SLLM and SQLM that were applied on a system of ordinary differential equations (2.8) - (2.10) in chapter 2 and a system of partial differential equations (3.4) in chapter 3 have been extended to another system of partial differential equations (4.1). Approximate solutions were obtained for the system (4.1) and comparison of the convergence and accuracy of the three methods were carried out using the values obtained. Validation of the three methods was done by comparing against result from published literature. The norm of the residual error was obtained for the three methods and was varied against iterations used and time (ξ).

A recurring observation made was that an increase in the number of iterations improve the accuracy of solutions obtained till full convergence to consistent solution was achieved. The second major finding was that the time function ξ had very little effect on the accuracy of

the solutions though it was observed that there was a slightly better accuracy obtained at the unsteady state ($\xi = 0$).

In general, it is apparent from the results presented in this chapter and the previous ones that the SRM, SLLM and SQLM are very efficient and produce accurate results but the spectral relaxation method (SRM) and the spectral local linearization method (SLLM) were more accurate than the spectral quasilinearization method (SQLM). The SQLM was observed to take fewer amount of iterations to achieve its' best accuracy when compared to the SRM and SLLM. It was also noted that when the maximum accuracy was obtained for all three methods, an increase in the number of iterations did not improve the accuracy of the solutions obtained. Finally, conclusion is drawn that algorithms of the methods are very straightforward to come up with. The three methods use few grid points for analysis. The methods also take few iterations to give accurate results.

Chapter 5

Conclusion

In this dissertation, a comparative study was carried out on the SRM, SLLM and SQLM to observe how efficient, convergent and accurate the spectral based numerical methods are. The test problems in chapters 3 and 4 that were chosen were boundary layer problems that went through transformations produced by Williams and Rhyne (1980). A generalized observation made on each problem is provided below.

In Chapter 2, an unsteady free convective heat and mass transfer on a stretching surface in a porous medium with suction was observed by applying the SRM, SLLM and SQLM. The model equations were described by a nonlinear system of ordinary differential equations. Validation was made on the approximate solutions obtained using these numerical methods by comparing against solutions obtained from published literature and using residual error analysis. Comparison on the accuracies of the numerical methods showed that the three numerical methods were very efficient but the SRM and SLLM were more accurate than the SQLM but the SQLM converged fastest of the three methods.

In Chapter 3, an unsteady boundary layer flow due to a stretching surface in a rotating fluid was investigated. The model equations were described by a nonlinear system of partial differential equations. Validation was made on the approximate solutions by comparing the numerical solutions gotten by the SRM, SLLM and SQLM. Comparison made on the three methods also proved them to be very efficient but it was observed that the SRM and the

SLLM were more efficient in terms of accuracy than the SQLM. The SQLM was also seen to converge faster than the SRM and the SLLM.

In Chapter 4, an unsteady three-dimensional MHD boundary layer flow and heat transfer over an impulsively stretching plate was investigated using the SRM, SLLM and SQLM. The model equations were described by a nonlinear system of partial differential equations. The approximate solutions obtained were validated against solutions from published literature. Comparison on the accuracies of the SRM, SLLM and SQLM proved that they were very efficient methods. The investigation revealed that the SRM and SLLM were more accurate than the SQLM but the SQLM converged faster than the SRM and SLLM.

In conclusion, one common phenomena observed was that the SRM, SLLM and SQLM are very efficient and accurate numerical methods. The steps taken to develop their respective algorithms were found to be very straightforward and easy to come up with when applying the numerical methods on ODEs and PDEs. Further research can be carried out under other conditions to observe if the behavior of the methods remain the same as what was seen in this study.

Bibliography

Acton, F. S. (1990). *Numerical methods that usually work*. Mathematical Association of America Washington, DC.

Ahmad, B., J. J. Nieto, and N. Shahzad (2001). The Bellman–Kalaba–Lakshmikantham quasilinearization method for neumann problems. *Journal of mathematical analysis and applications 257*(2), 356–363.

Ahmad, B., J. J. Nieto, and N. Shahzad (2002). Generalized quasilinearization method for mixed boundary value problems. *Applied mathematics and computation 133*(2), 423–429.

Ali, F. M., R. Nazar, and N. M. Arafin (2010). Numerical solutions of unsteady boundary layer flow due to an impulsively stretching surface. *Journal of Applied Computer Science and Mathematics 8*(4), 25–30.

Anderson, J. D. et al. (1995). *Computational fluid dynamics*, Volume 206. Springer.

Ariel, P. (2003). Generalized three-dimensional flow due to a stretching sheet. *ZAMM - Journal of Applied Mathematics and Mechanics / Zeitschrift fr Angewandte Mathematik und Mechanik 83*(12), 844–852.

Awad, F. G., P. Sibanda, S. S. Motsa, and O. D. Makinde (2011). Convection from an inverted cone in a porous medium with cross-diffusion effects. *Computers & Mathematics with Applications 61*(5), 1431–1441.

Babolian, E., M. Bromilow, R. England, and M. Saravi (2007). A modification of pseudo-spectral method for solving a linear ODEs with singularity. *Applied mathematics and computation 188*(2), 1260–1266.

Baltensperger, R. and J.-P. Berrut (1999). The errors in calculating the pseudospectral differentiation matrices for chebyshev-gauss-lobatto points. *Computers & Mathematics with Applications 37*(1), 41–48.

Bellman, R., J. Jacquez, R. Kalaba, and S. Schwimmer (1967). Quasilinearization and the estimation of chemical rate constants from raw kinetic data. *Mathematical Biosciences 1*(1), 71–76.

Bellman, R. E. and R. E. Kalaba (1965). Quasilinearization and nonlinear boundary-value problems. *American Elsevier, New York, USA*.

Boyd, J. P. (2001). *Chebyshev and Fourier spectral methods*. Courier Dover Publications.

Canuto, C., M. Y. Husseini, A. Quarteroni, and T. A. Zang (1988). *Spectral Methods in Fluid Dynamics*. Springer-Verlag, Berlin.

Chamkha, A. J., A. M. Aly, and M. A. Mansour (2010). Similarity solution for unsteady heat and mass transfer from a stretching surface embedded in a porous medium with suction/injection and chemical reaction effects. *Chemical Engineering Communications 197*(6), 846–858.

Chang, Q., J. Erhui, and W. Sun (1999). Difference schemes for solving the generalized nonlinear schrödinger equation. *Journal of Computational Physics 148*(2), 397–415.

Cheng, A. H.-D., M. A. Golberg, E. J. Kansa, and G. Zammito (2003). Exponential convergence and h-c multiquadric collocation method for partial differential equations. *Numerical Methods for Partial Differential Equations 19*(5), 571–594.

Cueto-Felgueroso, L. and R. Juanes (2009). Adaptive rational spectral methods for the linear stability analysis of nonlinear fourth-order problems. *Journal of Computational Physics 228*(17), 6536–6552.

Davidson, P. A. (2001). *An introduction to magnetohydrodynamics*, Volume 25. Cambridge university press.

Dlamini, P. G., S. S. Motsa, and M. Khumalo (2013a). Higher order compact finite difference schemes for unsteady boundary layer flow problems. *Advances in Mathematical Physics*. vol. 2013, Article ID 941096, 10 pages, 2013. doi:10.1155/2013/941096.

Dlamini, P. G., S. S. Motsa, and M. Khumalo (2013b). On the comparison between compact finite difference and pseudospectral approaches for solving similarity boundary layer problems. *Mathematical Problems in Engineering*. vol. 2013, Article ID 746489, 15 pages, 2013. doi:10.1155/2013/746489.

Elbashbeshy, E. M. A. and M. A. A. Bazid (2003). Heat transfer over an unsteady stretching surface with internal heat generation. *Applied Mathematics and Computation 138*(23), 239 – 245.

Elbashbeshy, E. M. A. and M. A. A. Bazid (2004). Heat transfer over an unsteady stretching surface. *Heat and Mass Transfer 41*(1), 1–4.

Erickson, L. E., L. T. Fan, and V. G. Fox (1966). Heat and mass transfer on moving continuous flat plate with suction or injection. *Industrial Engineering Chemistry Fundamentals 5*(1), 19–25.

Gheorghiu, C. I. (2007). Spectral methods for differential problems. *Casa Cartii de Stiinta Publishing House, Cluj-Napoca*.

Gottlieb, S. and D. Gottlieb (2009). Spectral methods. *Scholarpedia 4*(9), 7504. revision 91796.

Gupta, P. S. and A. S. Gupta (1977). Heat and mass transfer on a stretching sheet with suction or blowing. *The Canadian Journal of Chemical Engineering 55*(6), 744–746.

Hang, X., S. L. and I. Pop (2007). Series solutions of unsteady three-dimensional MHD flow and heat transfer in the boundary layer over an impulsively stretching plate. *European Journal of Mechanics - B/Fluids 26*(1), 15 – 27.

Hu, B., Y. Xu, and J. Hu (2008). Crank-nicolson finite difference scheme for the rosenau-burgers equation. *Applied Mathematics and Computation 204*(1), 311–316.

Hussaini, M. Y. and T. A. Zang (1987). Spectral methods in fluid dynamics. *Annual Review of Fluid Mechanics 19*(1), 339–367.

Ishak, A., R. Nazar, and I. Pop (2006). Unsteady mixed convection boundary layer flow due to a stretching vertical surface. *Arabian Journal for Science Engineering (Springer Science Business Media B.V.) 31*(2B), 165 – 182.

Ishak, A., R. Nazar, and I. Pop (2008). Hydromagnetic flow and heat transfer adjacent to a stretching vertical sheet. *Heat and Mass Transfer 44*(8), 921 – 927.

Ishak, A., R. Nazar, and I. Pop (2009). Heat transfer over an unsteady stretching permeable surface with prescribed wall temperature. *Nonlinear Analysis: Real World Applications 10*, 2909 – 2913.

Ishak, A., I. Pop, and R. Nazar (2006). Mixed convection on the stagnation point flow toward a vertical, continuously stretching sheet. *Journal of Heat Transfer 129*, 1087 – 1090.

Jaddu, H. (2002). Direct solution of nonlinear optimal control problems using quasilinearization and chebyshev polynomials. *Journal of the Franklin Institute 339*(4), 479–498.

Juang, H.-M. H. and M. Kanamitsu (1994). The nmc nested regional spectral model. *Monthly Weather Review 122*(1), 3–26.

Kameswaran, P., P. Sibanda, and S. Motsa (2013). A spectral relaxation method for thermal dispersion and radiation effects in a nanofluid flow. *Boundary Value Problems*. Vol. 2013, page 242, 2013. doi:10.1186/1687-2770-2013-242.

Kameswaran, P. K., Z. G. Makukula, P. Sibanda, S. S. Motsa, and P. V. S. N. Murthy (2014). A new algorithm for internal heat generation in nanofluid flow due to a stretching sheet in a porous medium. *International Journal of Numerical Methods for Heat & Fluid Flow 24*(5), 1020–1043.

Keller, J. B. and H. Cebeci (1971). Accurate numerical methods for boundary layer flows in two dimensional laminar flows. *In Proceedings of the second international conference on numerical methods in fluid dynamics*. pp. 92-100, Springer.

Krivec, R. and V. B. Mandelzweig (2001). Numerical investigation of quasilinearization method in quantum mechanics. *Computer Physics Communications 138*(1), 69–79.

Kumari, M. and G. Nath (2009). Analytical solution of unsteady three-dimensional MHD boundary layer flow and heat transfer due to impulsively stretched plane surface. *Communications in Nonlinear Science and Numerical Simulation 14*(8), 3339 – 3350.

Kumari, M., A. Slaouti, H. S. Takhar, S. Nakamura, and G. Nath (1996). Unsteady free convection flow over a continuous moving vertical surface. *Acta Mechanica 116*(1-4), 75–82.

Lakshmikantham, V. (1994). An extension of the method of quasilinearization. *Journal of Optimization Theory and Applications 82*(2), 315–321.

Lakshmikantham, V., N. Shahzad, and J. J. Nieto (1996). Methods of generalized quasilinearization for periodic boundary value problems. *Nonlinear Analysis: Theory, Methods & Applications 27*(2), 143–151.

Liao, S. (2003). *Beyond perturbation: introduction to the homotopy analysis method*. CRC press.

Liao, S. (2006a). An analytic solution of unsteady boundary-layer flows caused by an impulsively stretching plate. *Communications in Nonlinear Science and Numerical Simulation 11*(3), 326 – 339.

Liao, S. (2006b). Series solutions of unsteady boundary-layer flows over a stretching flat plate. *Studies in Applied Mathematics 117*(3), 239–263.

Makukula, Z. G., S. S. Motsa, and S. Shateyi (2014). Numerical analysis for the synthesis of biodiesel using spectral relaxation method. *Mathematical Problems in Engineering*. vol. 2014, Article ID 601374, 6 pages, 2014. doi:10.1155/2014/601374.

Makukula, Z. G., P. Sibanda, and S. S. Motsa (2010a). A note on the solution of the von kármán equations using series and chebyshev spectral methods. *Boundary Value Problems*. Vol. 2010, page 471793, 2010. doi:10.1155/2010/471793.

Makukula, Z. G., P. Sibanda, and S. S. Motsa (2010b). A novel numerical technique for two-dimensional laminar flow between two moving porous walls. *Mathematical Problems in Engineering*. vol. 2010, Article ID 528956, 15 pages, 2010. doi:10.1155/2010/528956.

Makukula, Z. G., P. Sibanda, and S. S. Motsa (2010c). On new solutions for heat transfer in a visco-elastic fluid between parallel plates. *International journal of mathematical models and methods in applied sciences 4*(4), 221–230.

Makukula, Z. G., P. Sibanda, and S. S. Motsa (2012a). On a linearisation method for reiner-rivlin swirling flow. *Computational & Applied Mathematics 31*(1), 95–125.

Makukula, Z. G., P. Sibanda, and S. S. Motsa (2012b). On a quasilinearisation method for the von kármán flow problem with heat transfer. *Latin American Applied Research 42*(1). http://www.laar.uns.edu.ar/.

Makukula, Z. G., P. Sibanda, S. S. Motsa, and S. Shateyi (2011). On new numerical techniques for the MHD flow past a shrinking sheet with heat and mass transfer in the presence of a chemical reaction. *Mathematical Problems in Engineering*. Volume 2011 (Article ID 489217, doi:10.1155/2011/489217), 19 pages.

Mandelzweig, V. B. and F. Tabakin (2001). Quasilinearization approach to nonlinear problems in physics with application to nonlinear ODEs. *Computer Physics Communications 141*(2), 268–281.

Mantzaris, N. V., P. Daoutidis, and F. Srienc (2001). Numerical solution of multi-variable cell population balance models. ii. spectral methods. *Computers & Chemical Engineering 25*(11), 1441–1462.

Mehmood, A. and A. Ali (2006). Analytic solution of generalized three-dimensional flow and heat transfer over a stretching plane wall. *International Communications in Heat and Mass Transfer 33*(10), 1243 – 1252.

Motsa, S. S. (2011). A new algorithm for solving nonlinear boundary value problems arising in heat transfer. *International Journal of Modeling, Simulation, and Scientific Computing 2*(03), 355–373.

Motsa, S. S. (2013a). A new spectral local linearization method for nonlinear boundary layer flow problems. *Journal of Applied Mathematics*. vol. 2013, Article ID 423628, 15 pages, 2013. doi:10.1155/2013/423628.

Motsa, S. S. (2013b). A new spectral relaxation method for similarity variable nonlinear boundary layer flow systems. *Chemical Engineering Communications 201*(2), 241–256.

Motsa, S. S., P. G. Dlamini, and M. Khumalo (2013). Solving hyperchaotic systems using the spectral relaxation method. *Abstract and Applied Analysis*. vol. 2012, Article ID 203461, 18 pages, 2012. doi:10.1155/2012/203461.

Motsa, S. S., P. G. Dlamini, and M. Khumalo (2014). Spectral relaxation method and spectral quasilinearization method for solving unsteady boundary layer flow problems. *Advances in Mathematical Physics*. vol. 2014, Article ID 341964, 12 pages, 2014. doi:1155/2014/341964.

Motsa, S. S., Y. Khan, and S. Shateyi (2012). A new numerical solution of maxwell fluid over a shrinking sheet in the region of a stagnation point. *Mathematical Problems in Engineering*. vol. 2012, Article ID 290615, 11 pages, 2012. doi:10.1155/2012/290615.

Motsa, S. S., Z. G. Makukula, and S. Shateyi (2013). Spectral local linearisation approach for natural convection boundary layer flow. *Mathematical Problems in Engineering*. vol. 2013, Article ID 765013, 7 pages, 2013. doi:10.1155/2013/765013.

Motsa, S. S. and S. Shateyi (2011). Successive linearisation solution of free convection non-darcy flow with heat and mass transfer. *Advanced Topics in Mass Transfer*. Vol. 2011, page 14519, 2011. doi:10.5772/14519.

Motsa, S. S. and S. Shateyi (2012a). The effects of chemical reaction, hall, and ion-slip currents on MHD micropolar fluid flow with thermal diffusivity using a novel numerical technique. *Journal of Applied Mathematics*. vol. 2012, Article ID 689015, 30 pages, 2012. doi:10.1155/2012/689015.

Motsa, S. S. and S. Shateyi (2012b). New analytic solution to the lane-emden equation of index 2. *Mathematical Problems in Engineering*. vol. 2012, Article ID 614796, 19 pages, 2012. doi:10.1155/2012/614796.

Motsa, S. S. and S. Shateyi (2012c). Successive linearisation analysis of unsteady heat and mass transfer from a stretching surface embedded in a porous medium with suction/injection and thermal radiation effects. *The Canadian Journal of Chemical Engineering 90*(5), 1323–1335.

Motsa, S. S. and S. Shateyi (2012d). Successive linearization analysis of the effects of partial slip, thermal diffusion, and diffusion-thermo on steady MHD convective flow due to a ro-

tating disk. *Mathematical Problems in Engineering*. vol. 2012, Article ID 397637, 15 pages, 2012. doi:10.1155/2012/397637.

Motsa, S. S. and P. Sibanda (2012). A linearisation method for non-linear singular boundary value problems. *Computers & Mathematics with Applications 63*(7), 1197–1203.

Motsa, S. S. and P. Sibanda (2013). On extending the quasilinearization method to higher order convergent hybrid schemes using the spectral homotopy analysis method. *Journal of Applied Mathematics*. vol. 2013, Article ID 879195, 9 pages, 2013. doi:10.1155/2013/879195.

Motsa, S. S., P. Sibanda, J. M. Ngnotchouye, and G. T. Marewo (2014). A spectral relaxation approach for unsteady boundary-layer flow and heat transfer of a nanofluid over a permeable stretching/shrinking sheet. *Advances in Mathematical Physics*. vol. 2014, Article ID 564942, 10 pages, 2014. doi:10.1155/2014/564942.

Motsa, S. S., P. Sibanda, and S. Shateyi (2011). On a new quasi-linearization method for systems of nonlinear boundary value problems. *Mathematical Methods in the Applied Sciences 34*(11), 1406–1413.

Nazar, R., N. Amin, and I. Pop (2004a). Unsteady boundary layer flow due to a stretching surface in a rotating fluid. *Mechanics Research Communications 31*(1), 121–128.

Nazar, R., N. Amin, and I. Pop (2004b). Unsteady mixed convection boundary layer flow near the stagnation point on a vertical surface in a porous medium. *International Journal of Heat and Mass Transfer 47*(1213), 2681 – 2688.

Nazar, R., A. Ishak, and I. Pop (2008). Unsteady boundary layer flow over a stretching sheet in a micropolar fluid. *2*(2), 97 – 101.

Nieto, J. (1997). Generalized quasilinearization method for a second order ordinary differential equation with dirichlet boundary conditions. *Proceedings of the American Mathematical Society 125*(9), 2599–2604.

Ogundare, B. S. (2009). On the pseudo-spectral method of solving linear ordinary differential equations. *Journal of Mathematics and Statistics 5*(2), 136–140. DOI : 10.3844/jmssp.2009.136.140.

Pal, D. and H. Mondal (2011). Effects of soret dufour, chemical reaction and thermal radiation on mhd non-darcy unsteady mixed convective heat and mass transfer over a stretching sheet. *Communications in Nonlinear Science and Numerical Simulation 16*(4), 1942–1958.

Pop, I. and T. Na (1996). Unsteady flow past a stretching sheet. *Mechanics Research Communications 23*(4), 413 – 422.

Sakiadis, B. C. (1961). Boundary-layer behavior on continuous solid surfaces: I. boundary-layer equations for two-dimensional and axisymmetric flow. *AIChE Journal 7*(1), 26–28.

Seshadri, R., N. S. and G. Nath (2002). Unsteady mixed convection flow in the stagnation region of a heated vertical plate due to impulsive motion. *International Journal of Heat and Mass Transfer 45*, 1345 – 1352.

Sharidan, S., T. Mehmood, and I. Pop (2006). Similarity solutions for the unsteady boundary layer flow and heat transfer due to a stretching sheet. *APPLIED MECHANICS AND ENGINEERING 11*(3), 647.

Shateyi, S. and O. D. Makinde (2013). Hydromagnetic stagnation-point flow towards a radially stretching convectively heated disk. *Mathematical Problems in Engineering*. Volume 2013, Article ID 616947, 8 pages, 2013. doi:10.1155/2013/616947.

Shateyi, S. and G. Marewo (2013). A new numerical approach of MHD flow with heat and mass transfer for the UCM fluid over a stretching surface in the presence of thermal radiation. *Mathematical Problems in Engineering*. vol. 2013, Article ID 670205, 8 pages, 2013. doi:10.1155/2013/670205.

Shateyi, S. and S. S. Motsa (2011a). Boundary layer flow and double diffusion over an unsteady stretching surface with hall effect. *Chemical Engineering Communications 198*(12), 1545–1565.

Shateyi, S. and S. S. Motsa (2011b). Hydromagnetic non-darcy flow, heat and mass transfer over a stretching sheet in the presence of thermal radiation and ohmic dissipation. *The Canadian Journal of Chemical Engineering 89*(6), 1388–1400.

Shateyi, S. and J. Prakash (2014). A new numerical approach for MHD laminar boundary layer flow and heat transfer of nanofluids over a moving surface in the presence of thermal

radiation. *Boundary Value Problems*. vol. 2014, 2 pages, 2014. doi:10.1186/1687-2770-2014-2.

Shazad, N. and A. S. Vatsala (1995). Extension of the method of generalized quasilinearization for second order boundary value problems. *Applicable Analysis 58*(1-2), 77–83.

Sibanda, P., S. S. Motsa, and Z. G. Makukula (2012). A spectral-homotopy analysis method for heat transfer flow of a third grade fluid between parallel plates. *International Journal of Numerical Methods for Heat & Fluid Flow 22*(1), 4–23.

Simmonds, J. G. and J. E. Mann. *A first look at perturbation theory*. Robert E. Krieger Publishing Company, Inc.

Sun, G. and C. W. Trueman (2006). Efficient implementations of the crank-nicolson scheme for the finite-difference time-domain method. *Microwave Theory and Techniques, IEEE Transactions on 54*(5), 2275–2284.

Takhar, H. S. and G. Nath (1998). Unsteady flow over a stretching surface with a magnetic field in a rotating fluid. *Zeitschrift für angewandte Mathematik und Physik ZAMP 49*(6), 989–1001.

Trefethen, L. N. (1996). *Finite difference and spectral methods for ordinary and partial differential equations*. Cornell University [Department of Computer Science and Center for Applied Mathematics], New York, U.S.A.

Trefethen, L. N. (2000). *Spectral methods in MATLAB*, Volume 10. Society for Industrial and Applied Mathematics.

Trefethen, L. N. and M. R. Trummer (1987). An instability phenomenon in spectral methods. *SIAM journal on numerical analysis 24*(5), 1008–1023.

Tsou, F. K., E. M. Sparrow, and R. Goldstein (1967). Flow and heat transfer in the boundary layer on a continuous moving surface. *International Journal of Heat and Mass Transfer 10*(2), 219–235.

Van de Vosse, F. and P. Minev (1996). Spectral elements methods: Theory and applications. Technical report, EUT Report 96-W-001 ISBN 90-236-0318-5, Eindhoven University of Technology.

Wang, C. (1988). Stretching a surface in a rotating fluid. *Zeitschrift für angewandte Mathematik und Physik ZAMP 39*(2), 177–185.

Wang, C. Y. (1984). The three-dimensional flow due to a stretching flat surface. *Physics of Fluids (1958-1988) 27*(8), 1915–1917.

Wang, S. and Y. Lin (1989). A finite-difference solution to an inverse problem for determining a control function in a parabolic partial differential equation. *Inverse problems*. vol. 5, page 631, doi:10.1088/0266-5611/5/4/013.

Williams, III, J. C. and T. Rhyne (1980). Boundary layer development on a wedge impulsively set into motion. *SIAM Journal on Applied Mathematics 38*(2), 215–224.

Xu, H. and S. J. Liao (2005). Series solutions of unsteady magnetohydrodynamic flows of non-newtonian fluids caused by an impulsively stretching plate. *Journal of Non-Newtonian Fluid Mechanics 129*(1), 46 – 55.

Yüzbaşi, c., E. Gök, and M. Sezer (2014). Laguerre matrix method with the residual error estimation for solutions of a class of delay differential equations. *Mathematical Methods in the Applied Sciences 37*(4), 453–463.